Glutaminase Modulates T Cell Metabolism and Function in Inflammation and Cancer

by

Marc Owen Johnson

Department of Pharmacology and Cancer Biology
Duke University

Date: November 9th, 2018
Approved:

_____
Jeffrey C. Rathmell, Supervisor

_____
Donald McDonnell, Chair

_____
Christopher Newgard

_____
Jason Locasale

_____
Nancie MacIver

Dissertation submitted in partial fulfillment of
the requirements for the degree of Doctor
of Philosophy in the Department of
Pharmacology and Cancer Biology in the Graduate School
of Duke University

2018

ABSTRACT

Glutaminase modulates T cell metabolism and function in inflammation and cancer

by

Marc Owen Johnson

Department of Pharmacology and Cancer Biology
Duke University

Date: November 9th, 2018
Approved:

_____
Jeffrey C. Rathmell, Supervisor

_____
Donald McDonnell, Chair

_____
Christopher Newgard

_____
Jason Locasale

_____
Nancie MacIver

An abstract of a dissertation submitted in partial
fulfillment of the requirements for the degree of Doctor
of Philosophy in the Department of
Pharmacology and Cancer Biology in the Graduate School
of Duke University

2018

Abstract

During the immune response, helper T cells must proliferate and upregulate key metabolic programs including glucose and glutamine uptake. Metabolic reprogramming is imperative for appropriate T cell responses, as inhibition of glucose or glutamine uptake hinders T cell effector responses. Glutamine and glutaminolysis use in cancer cells has partially been explored. However, the role of glutamine and its downstream metabolites is incomplete and unclear in T cells. The first step of glutamine metabolism is conversion to glutamate via the hydrolase enzyme glutaminase (GLS). To target glutaminolysis, two different methods were employed: 1) genetic knockout of GLS using a CRE-recombinase system specific for CD4/CD8 T cells, and 2) pharmacological inhibition of GLS via the potent and specific small molecular CB839. These two models of glutaminase insufficiency were used as a tool to target glutamine metabolism during T cell activation and differentiation both *in vitro* and *in vivo*.

GLS-deficient T cells had decreased activation at early time points compared to control. Over several days, these GLS-deficient T cells differentiated preferentially to Th1-like effector cells. This was reliant on increased glucose carbons incorporating into Tri-Carboxylic Acid (TCA) metabolites. This increased effector response *in* vitro occurred in both CD4+ T helper cells and CD8+ cells (Cytotoxic lymphocytes, or CTLs). Differentiation of CD4+ T cells to Th1 or Th17 subsets showed decreased Th17 differentiation and

cytokine production, while Th1 effector responses were increased. This increased Th1 function was dependent on IL-2 signaling and mTORC1, as reducing IL-2 or inhibiting mTORC1 with rapamycin prevented GLS inhibition-induced Th1 effector function. Th17 cells, meanwhile, were inhibited by changes in reactive oxygen species, and recovery of Th17 function was achieved with n-acetylcysteine treatment.

T cells lacking GLS were unable to induce inflammation in a mouse model of Graft vs Host disease, an inflammatory bowel disease model, or in an airway inflammatory model. Importantly, Chimeric Antigen Receptor (CAR) T cells made from GLS knockout cells were unable to maintain B cell aplasia in recipient mice. Contrary to this, temporary inhibition of GLS via small-molecule inhibition increased B cell killing *in vitro* and enhanced T cell persistence in both the B cell aplasia and in a vaccinia virus recall response. These results indicate a balance, where permanent deficiency of GLS is detrimental to T cell responses, but acute inhibition can actually promote T effector responses and survival. Overall, this work aims to understand how perturbations in glutamine metabolism in T cells affects differentiation and function and the role of glutaminolysis and improve therapies for inflammatory disease and cancer.

Contents

List of Figures

List of Tables

List of Abbreviations

2DG – 2-deoxyglucose

AMPK – AMP-activated protein kinase

AMP – adenosine monophosphate

APC – antigen presenting cell

ATP – adenosine triphosphate

α-KG – alpha ketoglutarate

CB839 – GLS1 inhibitor from Calithera Biosciences

CPT1α – carnitine palmitoyltransferase 1 alpha

CTLA-4 – cytotoxic T-lymphocyte antigen 4

DN – double negative

DP – double positive

EAE – experimental autoimmune encephalomyelitis

FAD/H_2 – flavin adenine dinucleotide / $FADH_2$ dinucleotide form

FoxP3 – forkhead box P3

GAPDH – glyceraldehyde 3-phosphate dehydrogenase

Gata3 – GATA binding protein 3

Gclc – glutamate-cysteine ligase

Glut – glucose transporter

GLUD1 – glutamate dehydrogenase 1

GLS – Glutaminase 1

GOT – glutamic oxaloacetic transaminase 1/2

GPT – Glutamic-pyruvic transaminase 1/2 (aka Alanine Transaminase)

GS – glutathione sythetase

GSH – glutathione

GSHR – glutathione reductase

GSSG – oxidized glutathione

GTP – guanosine triphosphate

GvHD – graft-vs-host disease

HIF1α – hypoxia-inducible factor 1 alpha

HKII – hexokinase 2

IBD – inflammatory bowel disease

IFNγ – interferon gamma

iTreg – inducible regulatory T cell

LAT – Linker of activated T cells

LDH – lactate dehydrogenase

MAPK – mitogen-activated protein kinase

MHC – major histocompatibility complex

mTOR – mammalian target of rapamycin

NADH – nicotinamide adenine dinucleotide

NADPH – nicotinamide adenine dinucleotide phosphate

NFKB - nuclear factor kappa-light-chain-enhancer of activated B cells

nTreg – natural regulatory T cell

OAA – oxaloacetate

OXPHOS – oxidative phosphorylation

PDH – pyruvate dehydrogenase complex

PDHK – pyruvate dehydrogenase kinase 1

PI3K – phosphatidyl-inositol-3-kinase

PIK3IP1 – PI3K-interacting protein 1

PKC – protein kinase C

PLCγ1 – phospholipase C gamma 1

PPP – pentose phosphate pathway

PTEN – phosphatase and tensin homolog

RORγt – RAR-related orphan receptor gamma

SAM – S-adenosyl methionine

SP – single positive

SRC – spare respiratory capacity

STAT – signal transducer and activator of transcription

Tbet – T-box expressed in T cells

TCA – tricarboxylic acid cycle

TCR – T cell receptor

Teff – effector T cell

TET – Ten-Eleven Translocation

TIL – tumor infiltrating lymphocytes

TGFβ – transforming growth factor beta

Treg – regulatory T cell

TSC1 / TSC2 – tuberous sclerosis 1 or 2

Acknowledgements

This work is a culmination of so much support and mentorship from a variety of people. First, my success in graduate school would not have been possible without the support of my mentor, Dr. Jeffrey Rathmell. His mentorship in navigating the world of academia was invaluable to me and his style of research and analysis is something I can only hope to emulate.

They say that your work is only as good as the people around you, and in that regard, I think I had a lot of luck in the students, scientists, and mentors that I had in my life. Starting early in my career, Vipin Suri was my mentor at Sirtris Pharmaceuticals who helped stoke my love of scientific pursuit by being accessible, knowledgeable, and kind. He pushed me to apply to graduate school despite my fear of feeling inadequate. In the Rathmell Lab at Duke, I would like to acknowledge the other graduate students Valerie and Rigel who were welcoming and enthusiastic. Special thanks to Val for really taking me under her wing during a time when she was so busy with everything else in her life. I learned a lot in the year or so that you mentored me about T cell metabolism and putting up with my ten thousand questions. Huge thanks to Amanda, you are a good friend and were a big reason I survived the transition to flying solo in the lab. Amy and Colby, y'all were the most welcoming people in the world when I first moved down to North Carolina and I'll never forget how wonderful you were to me. Parties, board games, and just lazy

evening beer drinking to discuss life and grad school were invaluable. Nick and Felix, you guys helped me relax and be a real human being when the a-sociality of grad school would get to me. Thank you all!

I only spent two years at Duke University before the lab moved to Vanderbilt in Nashville. I can't imagine what life would have been like had I stayed in Duke because of all the people I met at Vanderbilt. Melissa you are the mini-me in the lab and you were so helpful and sociable, I wish you all the luck in the world as you transition from a tech to a fellow graduate student. Diana you were the first graduate student I met when I arrived in Nashville who I actually felt a connection with, and you ended up joining our lab, making me feel at home, and a fellow confidant. Katy (aka Big Red), I loved your positive attitude and loved that you would arrange social stuff to do with lab mates, including game nights and lunches and all sorts of things. Dr. Boothby helped me understand the world of immunology more than I thought I could and offered sage advice not just scientifically but also in navigating good vs bad science.

Another group of people that somehow dealt with me during my graduate work are my friends and family up in Boston. I loved being able to come back to Massachusetts for special occasions like weddings, birthdays, and holiday breaks and keep our friendships as if I had barely even left. Mom, you were absolutely essential to me surviving the move down south. I can't thank you enough for all the help you have given

me over the years, both emotional support and helping me organize my life whenever you visited. Dad, you have given me more prescient advice about navigating life than I can explain. Bobby, I've known you since we were 3 years old and love every second more that we get to be friends. Congrats on the new baby! Here's to another 30 years of friendship.

1. Introduction

Immunity in animals has two main arms: the innate and the adaptive immune system. The adaptive immune system in mammals evolved millions of years ago to fight infections with significantly enhanced recognition for non-'self'. This includes helper T cells, which provide and enhance cell-mediated responses, and B cells, which provide humoral immunity and can act as Antigen Presenting Cells (APCs) (Cooper and Alder, 2006). The innate immune system, including natural killer cells, macrophages, dendritic cells, among others, reacts to pathogens quickly. As its name suggests, the innate immune cells do this via pre-programmed Pattern Recognition Receptors (PRRs). PRRs are engaged by structurally conserved antigens termed Pathogen-associated Molecular Patterns (PAMPs) or Damage-associated Molecular Patterns (DAMPs). PAMPs are present in various microbes and many things not considered 'self', such as bacterial cell wall components or viral peptides, whereas DAMPs are components of the host system released during cell death or apoptosis. These PRR proteins are cell-surface receptors that initiate inflammatory programs to help promote innate and adaptive immune responses. PRRs are, by their nature, less sensitive to variations in pathogens (Medzhitov and Janeway, 1997). Adaptive immune responses are slow at first but become quick to respond after the initial insult, separating into the primary (slow) and secondary (fast) adaptive immune responses. The primary response takes several days to a week and is enacted by

effector T cells, but the secondary response can be much faster, stronger, and enacted by memory T cells in coordination with other immune cells upon a later exposure to the pathogen or antigen. In disease states, these responses can be enhanced, leading to uncontrolled inflammation in autoinflammatory disease, or attenuated, as in tumor infiltrating lymphocyte exhaustion.

1.1 T cells enact the adaptive immune response necessary for pathogen elimination and protective immunity.

The primary response is formed when naïve T cells first encounter antigens that have been processed and presented on Major Histone Compatibility (MHC)-I and MHC-II proteins by innate immune cells known as Antigen Presenting Cells. T cells that enact the effector response (generally referred to as Teff cells) activate after recognition of antigen epitopes on MHCI and MHCII proteins as a primary signal through the T Cell Receptor (TCR) (Smith-Garvin et al., 2009). These signals require a secondary signal, co-stimulation, to activate well. Activation of T cells is a metabolically demanding process that requires cells to generate biosynthetic precursors, balance redox reactions, enact host defense, and maintain pools of memory cells. Without the secondary signal, typically CD28, Teff cells become anergic, fail to activate, and can promote immune tolerance (Fathman and Lineberry, 2007). Activation of effector responses includes production of cytokines to promote inflammation and spur innate cell responses.

Activation of T cells is imperative to clearing immune insults. The signaling cascades and levels of modulation are complex, but initial studies probing at the lymphocyte response to antigen in the mid 1980s led to the isolation and discovery of the TCR (Allison et al., 1982; Haskins et al., 1983) and eventually the signaling co-receptors and complexes required for T cell activation in the 1980s and 90s (Smith-Garvin et al., 2009; Zhang et al., 1998). After antigen recognition presented on MHC proteins through the TCR, a cascade of signaling proteins are recruited. Initial signaling events through protein kinases Lck and Fyn bind and phosphorylate ZAP-70. A series of phosphorylation events mediated by LAT, PLCy1, the p85 subunit of phosphoinositide 3-kinase (PI3K), converts phosphatidylinositol(4,5)P_2 (PIP_2) to second messengers IP_3 and diacylglycerol (DAG). PI3K has many pleiotropic effects on T cell activation, including signaling through mTOR complex 1 (mTORC1) (Martini et al., 2014). Importantly, co-stimulation of T cells (required to prevent T cell anergy) is also thought to signal through PI3K via its p110 subunit and promotes Akt activation (Acuto and Michel, 2003). IP_3 and DAG are second messengers that result in activation of downstream mitogen-associated protein kinases known as ERKs, signal transducer proteins known as STATs, and protein kinase C (PKC). This cascade, along with tightly controlled release of calcium from the ER, induces downstream activation of immediate-early genes such as NFkB, c-myc, and c-jun (Bahrami and Drabløs, 2016). These early-

activation proteins then enhance T cell function and survival responsible for effector function and inflammatory responses.

Before activation of the TCR in response to antigen in the periphery, CD4 and CD8+ T cells are matured in the thymus. Through both positive selection and negative selection, mature naïve T cells migrate from the thymus to important sites of immunological surveillance such as the spleen and lymph nodes. While T cells are found throughout the body, concentrations of T helper cells are found where antigen presentation is accessible – such as by B cells and dendritic cells in the T cell zones of lymph nodes. Depending on the surrounding environment, naïve CD4+ T cells can be differentiated into effector T cells (Teff: such as Th1, Th2, Th17) or regulatory T cells (Treg) that have distinct gene expression signatures that are mediated by subset-specific STATs and transcription factors (MacIver et al., 2013). Type I and Type II interferons are produced by helper T cells and promote innate and adaptive immunity. The archetypical Type II interferon, IFNγ, promotes anti-viral immunity (Chesler and Reiss, 2002). IL-4 and IL-13-producing Th2 cells respond to parasitic infections such as helminths (Finkelman et al., 1997), while IL-17 production in Th17 cells is responsible for mucosal immunity, especially in the intestines, and a major contributor to autoimmune disease (Yang et al., 2014). Many effector responses rely on signaling through mTORC1 pathways (Delgoffe et al., 2011) and Myc upregulation. Metabolic reprogramming by

Myc induces glutaminolysis and glycolysis, as deletion of Myc prevents proliferation and activation-induced cytokine production (Wang et al., 2011). Combined, T cell receptor signaling and metabolic reprogramming leads to robust ribosomal activation, protein synthesis, and anabolic cell growth.

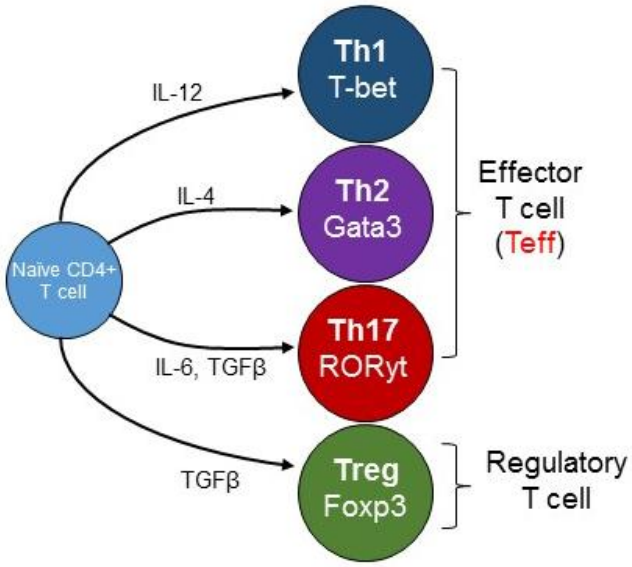

Figure 1: CD4+ T cell differentiation of naïve cells to effector (Teff) and regulatory (Treg) cells and their essential cytokines.

1.2 Th1 cells

Intracellular and viral immunity is promoted by the interferons. Effector cells responsible for viral immunity and initiating the anti-viral response are known as Th1 cells. Th1 cell programming is driven by the transcription factor Tbet (Szabo et al., 2000), which is induced by the cytokine IL-12 and STAT1 signaling (Afkarian et al., 2002).

Derived from dendritic cells and macrophages, IL-12 promotes B cell, T cell and Natural Killer T (NKT) cell activation and differentiation (Hsieh et al., 1993; Ling et al., 1995). Specifically, IL-12 does this in T cells through transactivation of Tbet target proteins such as IFNγ while suppressing Th2-specific production of GATA3 and IL-4 (Szabo et al., 2000; Zhou and Ouyang, 2003). Both STAT1 and STAT4 are required for Th1 differentiation and IFNγ production (Nishikomori et al., 2002).

Beyond signaling, metabolic flux has direct effects on T cell function. Glucose depletion prevented T cell effector responses, including IFNγ production. Trafficking of the glucose transporter, Glut1, was dependent on CD28 co-stimulation and induced Glut1 protein expression prevented T cell anergy when co-stimulation was removed (Jacobs et al., 2008). Recently, the glycolytic enzyme GAPDH has been shown to regulate IFNγ production. When glycolytic flux is low, GAPDH 'moonlights' and translocates to the nucleus to inhibit transcription of Th1-specific gene programming like at the IFNγ locus (Chang et al., 2013). However, the mechanism behind this is a little controversial, as Peng et al. show that the levels of acetyl-CoA resulting from glycolysis regulate histone acetylation and IFNγ translation (Peng et al., 2016). While these two mechanisms are not mutually exclusive, they do highlight the role of metabolism affecting T cell programming.

Whereas Th1 CD4+ T cells were only thought to be important in viral immunity, it has been discovered recently that Th1 cells and IFNγ production can improve anti-tumor effects in cancer therapy via enhancement of cytotoxic lymphocyte (CTL) activation (Kennedy et al., 2018). Additionally, Th1 and IFNγ+ cells have been implicated in regulating human colitis and inflammatory bowel disease (Brand, 2009). Regulation of Th1 cells could have wide-ranging immunomodulatory effects beyond just adaptive immunity to pathogens and could be a target for anti-tumor and anti-inflammatory immunity.

1.3 Th17 Cells

Immunity of the intestine and lung is regulated primarily by Th17 cells. Th17 cells produce the cytokines IL-17 and IL-23, and are driven by the transcription factor Retinoid Orphan Receptor gamma (RORγt) and STAT3 signaling (Harris et al., 2007). STAT3 and RORγt are induced through Transforming Growth Factor Beta (TGFβ)- and IL-6 receptor signaling, leading to upregulation of Th17-specific gene programming and via autocrine mechanisms increase IL-23 receptor and IL-23 production (Waite and Skokos, 2012). While inappropriate immune responses (autoimmunity and inflammation) can be driven by all effector T cell subsets, Th17 cells are implicated in the development of many autoimmune and inflammatory disorders in humans and in mice (Weaver et al., 2007). RORγt-knockout mice have reduced IL-17-producing Th17 cells, in addition to being resistant to

the inflammatory induced Experimental Autoimmune Encephalomyelitis (EAE) (Ouyang et al., 2008), showing that transcriptional regulation of these T cell programs has disease-specific impacts.

While the 'master' transcription factor in T cell subsets are known (Th1: Tbet, Th2: Gata3, Th17: RORγt, Treg: Foxp3), Th17 cells also rely on Hypoxia-Inducible Factor 1 alpha (HIF1α) for proper differentiation. Though HIF1α is induced in low oxygen tension environments across many cell types (Semenza, 2007), the activity of HIF1α is not entirely dependent on hypoxia as it is induced during Th17 differentiation even in the presence of oxygen. Upregulation of HIF1α promotes Th17 differentiation and inhibits regulatory T cell development. Foxp3, the transcription factor responsible for Treg programming, is targeted to proteasomal degradation via ubiquitination by HIF1α (Dang et al., 2011) thus providing important co-regulatory transcriptional tuning between effector and regulatory cell responses. This is further confused by studies showing Myc reprogramming initiates HIF1α activity, but HIF1α is not required for the upregulation of glycolytic and glutaminolytic reprogramming in all T cells (Wang et al., 2011). Contrary to this, Myc and HIF1α signaling can induce glycolytic and glutaminolytic pathways in cancer cells (Miller et al., 2012). The role of Th17 cells in human autoinflammatory disease is unclear, however, despite many current therapies involve targeting inflammatory auto-reactive T cells. In multiple sclerosis (MS), for example, mRNA expression is upregulated and up to

a seven-fold increase in Th17 cells is noted in MS patients versus control (Lock et al., 2002; Matusevicius et al., 1999). However, IFNy seems to be a key inflammatory cytokine for autoimmune gut diseases (Strober and Fuss, 2011) and IL-17/IFNγ double-producers could be the target (Galvez, 2014). Modulation of Th17 responses could be protective against autoimmune and gut inflammatory disorders.

1.4 Treg Cells

Contrary to the effector T cell subsets, Foxp3+ regulatory T cells (Treg) are required to help diminish the immune response. Treg inhibitory signaling helps prevent inappropriate immune responses in the periphery. Foxp3 was discovered as a result of genotyping human Immune dysregulation, Polyendocrinopathy, Enteropathy, X-linked syndrome (IPEX) patients who have severe, uncontrolled autoimmune reactions. Foxp3 was found to be required for Treg development (Bennett et al., 2001). Induced Treg (iTreg) and natural Treg (nTreg) are two functionally distinct subclasses of Foxp3+ regulatory T cells, in which iTreg are generated from naïve CD4+ T cell exposure to antigen, and nTreg are CD25+ Foxp3+ cells developed in the thymus to help prevent auto-reactive CD4+ inflammation (Wing and Sakaguchi, 2010). Inflammatory animal models can be rescued by adoptive transfer of Foxp3+ Treg cells (Mottet et al., 2003). Epigenetic regulation of the Foxp3 protein can strongly affect differentiation of Treg, as inhibition of methylation of

the Foxp3 locus leads to increased Treg differentiation (Xu et al., 2017), however stabilization of the Foxp3 locus via methylation of acetylation can promote Treg stability (Floess et al., 2007; van Loosdregt et al., 2010).

The metabolic differences between Treg and Teff are striking. Treg rely on the TCA and beta-oxidation of fatty acids, as opposed to Teff, which are thought to be more glycolytic (Michalek et al., 2011). They use CPT1a for transport of long-chain fatty acids into the mitochondria (Howie et al.; Michalek et al., 2011). Though the details of regulatory action on activated T cell responses are still being explored, one method of inhibition is through PD-1 (aka CD279) and its ligand, PDL-1, termed the immune check-point. During activation, effector T cells upregulate PD-1 receptor expression, and regulatory T cells express the PDL-1 ligand. PD-1 and PDL-1 interaction inhibits effector T cells through reduced TCR signaling via Zap70, which prevents mTORC1 activity and cytokine production and proliferation (Sheppard et al., 2004). Interestingly, evasion of the PD-1/PDL-1 axis is also thought to be how tumor cells evade elimination by the immune system. Cytotoxic lymphocytes within certain tumors, like melanoma, express high levels of PD-1 and reduced markers of activation (Ahmadzadeh et al., 2009). Thus, alteration in inhibitory check-point signaling can have profound physiological outcomes on the adaptive immune system.

1.5 CD8+ Cytotoxic Lymphocytes

The adaptive T cell subset responsible for cancer surveillance and elimination are CD8+ cytotoxic lymphocytes (CTLs). Driven primarily by the transcription factors Tbet, like in Th1 cells, and Eomes, which is implicated in promoting T cell memory (Banerjee et al., 2010), CD8+ T cells are MHCI class-restricted and enact host defense against intracellular pathogens (Harty et al., 2000). CTLs navigate to sites of inflammation and produce IFNγ, granzyme A and B, and perforin. Binding of the CTL and tight junction formation allows perforin to form holes in cell membranes, promoting granzymes to enter target cells via degranulation or direct fusion with the plasma membrane. They can be cytotoxic to tumor cells and infected cells, but their activity is not limited to cytolysis; Fas ligand (CD95L) protein on the CD8 T cell surface interacts with Fas (CD95) on target cells and induces apoptosis (Harty et al., 2000; Shresta et al., 1998). Clonal expansion of CD8+ cells in response to antigen stimulation parallels CD4+ T cells. Just like CD4+ T cells, naïve CD8+ T cells and memory T cells primarily rely on oxidative metabolism but induce high levels of glycolytic and glutaminolytic machinery upon antigen stimulation (Zhang and Romero, 2018). Tissue-resident memory CD8+ T cells enact similar oxidative phosphorylation programming that relies on autophagy for survival, as inhibition of autophagy prevented memory formation and response to LCMV (lymphocytic choriomeningitis virus) infection (Xu et al., 2014).

Similar to CD4+ T cells, engagement of the checkpoint receptors PD-1 and CTLA-4 are an escape mechanism CTL cytotoxicity. PDL-1 or CD80 for PD-1 and CTLA-4, respectively, on the surface of a cancer can inhibit the activation and killing properties of Tumor Infiltrating Lymphocytes (TILs) (Ahmadzadeh et al., 2009; Tumeh et al., 2014). Human TILs within renal cell tumors exhibit low glycolysis, high PD-1 expression, and a chronic inability to respond to activation (Siska et al., 2017), indicating an exhausted phenotype. Development of new drugs to hit these immune checkpoints have shown promising results in patients that are resistant to standard chemotherapy (Ott et al., 2013). Enhancing the cytotoxic properties of CD8+ TILs could increase response to chemotherapy or other immune therapies and reduce tumor persistence.

1.6 T cell metabolism as a therapeutic target

Rather than being merely an outcome of other signaling or genetic profile changes, metabolism is now known to have significant effects on cellular processes itself. T cells need to upregulate metabolic pathways in order to survive and enact host defense. Two of the primary pathways used by proliferating cells are glycolysis and glutaminolysis. Regulation of these pathways have been crucial in mediating T cell effector responses. Metabolism could therefore be harnessed to target specific T cells to either prevent autoimmune disease or enhance T cell killing.

Standard of care for some inflammatory disease such as graft versus host disease include metabolic targets. Rapamycin, an mTORC1 inhibitor, prevents immune cell activation and proliferation. In organ transplant, rapamycin has been effective at preventing graft versus host disease and organ rejection (Augustine et al., 2007). Metformin, an AMPK-promoting drug used to treat type II diabetes, was also found to prevent lethality in a mouse model of Graft vs Host Disease. This was due to inhibition of mTOR targets and a shift in the balance of Th1 and Th17 cells to Treg (Park et al., 2016). Unfortunately, responses to rapamycin-like drugs (known as rapalogs) in most cancers have been less successful (Hidalgo et al., 2006; Wang and Sun, 2009). Particularly good response to rapalogs are seen in proliferative disease that have mutations in directly-targeted mTOR signaling proteins, such as TSC1 and TSC2 (Franz et al., 2006; Herry et al., 2007). Despite this, being able to predict which patients or cancer types would respond has been elusive. The mTOR/PI3K/Akt pathways have significant overlap and feedback circuits, which leads to inconsistent responses in mTOR- or PTEN mutation-driven cancers that, at the outset, seemed to be good candidates for rapamycin treatment (Wander et al., 2011).

Front-line treatments for autoimmune disease include the anti-folates, such as methotrexate, which inhibit dihydrofolate reductase (DHFR). DHFR is required to synthesize thymidine, a key nucleoside for DNA synthesis. Anti-folate drugs act by

inhibiting cell proliferation, which have use in autoimmune treatment and cancer chemotherapy (Neurath et al., 1999). Anti-folates and rapalogs have been in use for over 50 years but have been successful as front line anti-metabolite treatments. Unfortunately, they have significant side effects and are global in effect: anti-proliferative drugs given systemically hit all the cells of the body, including in the gut and brain. Lymphomas and lymphoproliferative diseases are a concern with anti-metabolite treatments such as methotrexate, thought to be related to the global immunosuppression. Resolution of these lymphoproliferative diseases could be related specifically to drug treatment (Mariette et al., 2002). Additionally, anti-metabolite drugs are solely responsible for this increase in cancer, as anti-TNFα biologic etanercept is also associated with increased incidences of lymphoma (Wolfe and Michaud, 2004). Investment in more targeted therapies that spare or promote certain aspects of the immune system could yield significant inroads in preventing additional disease burden during treatment.

A more recent success story of T cell metabolic therapy is the recent use of checkpoint inhibitors against PD-1 and CTLA4 in cancer. Checkpoint proteins such as PD-1 are known to be metabolic inhibitors, as they suppress PI3K and mTORC1 signaling and inhibit T effector responses (Parry et al., 2005; Patsoukis et al., 2015). Immune escape is one of the mechanisms whereby cancer cells continue to proliferate and survive. While there are many potential models for why this occurs, one

predominant mechanism in relapse or refractory tumors is inhibition of innate and adaptive immune cells. Cancer cells can upregulate surface markers of inhibitory receptors such as PD-L1 and CTLA4, which are collectively known as checkpoint inhibitors. These downregulate T cell activation and cytokine production and lead to a so-called exhausted or anergic state. Through biologics such as nivolumab, signaling through PD1 and CTLA4 can be restored, leading to induction of durable CD4 and CD8+ T cell responses in tumors. This is, in effect, a metabolic control of T cell responses which provides enhanced tumor cytotoxicity and remission that are specifically inhibited by tumor cells and the tumor environment.

1.6.1 T cell subsets and differential metabolism

During the development and activation of naïve T cells the surrounding environment plays a significant role in differentiating T cells. Naïve T cells can become Th1, Th2, Th17 (collectively known as Teff cells) or induced regulatory T cells (Treg) (MacIver et al., 2013). Teff cells utilize both glycolysis and glutaminolysis and are pro-inflammatory (Shi et al., 2011). Treg, in contrast, rely on oxidative metabolism and are anti-inflammatory, preventing autoimmunity by suppressing Teff cells (Beier et al., 2015). The timing of activation and metabolic requirements is also important: initially, T cells rely on mitochondrial metabolism but switch to the aerobic glycolysis during the strong proliferative response (van der Windt et al., 2012). The environment surrounding

the T cell can also drive T cell differentiation and function: cytokines and growth factors signal through disparate pathways to affect STAT signaling, Th1 and Th2 cells rely almost exclusively on glycolytic metabolism but Th17 cells have a mix of both glycolytic and mitochondrial oxidative metabolism (Michalek et al., 2011). Disruption of glucose uptake via the glucose transporter Glut1 receptor prevents Teff activation and their ability to enact inflammatory response *in vivo* (Macintyre et al., 2014). This was true despite partial compensation by other glucose transporters such as Glut3. However, regulatory T cells lacking Glut1 were still able to suppress Teff responses, indicating that glucose use is not tied directly to all T cell function.

1.6.2 mTOR/AMPK and nutrient sensing

Upregulation of glucose and amino acid uptake machinery to support T cell proliferation and function is controlled by the mammalian target of rapamycin (mTOR) pathway (Wang et al., 2011). Growth signals via surface receptors and stimulation of the TCR activate PI3K and MAPK pathways downstream to promote mTOR, a serine/threonine kinase, which drives protein synthesis, inhibits autophagy, and increases nutrient uptake (Laplante and Sabatini, 2012). mTOR was named because its activity was modified by the antiproliferative compound rapamycin. mTOR acts to integrate growth signals, nutrient sensing, energy status, and oxygen availability which allows cells to grow (Chi, 2012). These signals are balanced between two similar but

opposing units: the mTOR complex 1 (mTORC1) complex 2 (mTORC2). Among them are several shared proteins - mTOR kinase catalytic unit, along with DEPTOR, mLST8, and Tti1/Tel2 proteins. mTORC1 uniquely contains Raptor and PRAS40, while mTORC2 has the three exclusive associated proteins Rictor, mSin1, and protor (Locasale and Cantley, 2011). Upstream regulation of mTORC activation converges on TSC1 and TSC2, tumor suppressor proteins with kinase activity (Tee et al., 2003). Downstream activation of mTORC1 includes phosphorylation of ribosomal subunit 6 (S6) and eukaryotic initiation factor 4E-binding protein (4-EBP1). These and other proteins coordinate cell cycle advancement, anabolic metabolism, RNA transcription, and glutamine and glucose uptake. mTORC2 downstream signaling promotes cell survival and cytoskeleton dynamics. Signaling within the mTOR axis is complex, with feedback and feedforward mechanisms to allow fine-tuning of anabolic growth (Laplante and Sabatini, 2012). In the past decade, the role of mTOR regulation in T cells has been fruitful. Specific deletion of the mTORC1 GTPase Rheb (preventing mTORC1 activation) permitted Th2 differentiation but inhibited Th1 and Th17, whereas deletion of mTORC2 protein Rictor prevented Th2 differentiation but retained Th1 and Th17 (Delgoffe et al., 2011). Interestingly, genetic deletion of the mTOR catalytic unit prevented Teff generation but promoted regulatory T cells (Delgoffe et al., 2009) yet deletion of Raptor (mTORC1 protein) in vivo lead to disadvantaged Treg suppressor cells in a competitive

environment (Zeng et al., 2013). The balance of mTORC1 and mTORC2 seems to be important in Treg function, as specific deletion of mTORC1 can enhance mTORC2 activity and Treg function (Zeng et al., 2013). Further, the timing of mTORC1 and mTORC2 activation may be extremely important in T cell biology, as temporary inhibition of mTOR with rapamycin promoted Treg proliferation and suppression (Procaccini et al., 2010). While the role of mTOR in subset activation is somewhat convoluted, much research points to mTORC1 as a requirement for Teff cells function and growth.

Because the directive "grow or don't grow" is such an important question for T cells, energy status is tightly monitored. Availability of energy in the form of amino acids can modify mTOR signaling. mTOR is sensitive to levels of glutamine, leucine, and arginine. Arf1 signals glutamine availability to mTOR (Jewell et al., 2015), Sestrin2 senses leucine (Saxton et al., 2016), while Castor1 senses arginine (Chantranupong et al., 2016). Nutrient levels sensed by mTOR is handled primarily by recently discovered proteins RagA/B and RagC/D. The presence of amino acids allow these lysosomal-associated Rag proteins, along with a scaffold protein, Ragulator, to coordinate translocation of the mTOR complex to the lysosome surface, where Rheb is activated to initiate mTOR signaling (Zoncu et al., 2011). Thus, there is an intimate connection between nutrient availability and metabolic programming. The lysosome and

coordinating proteins like mTOR appear to integrate cell nutrient status and growth signaling.

AMPK, which is sensitive to AMP levels in the cell, acts as a rheostat switch to mTOR regulation. During energy stress, AMPK is phosphorylated and prevents the growth pathways such as mTOR from activating. It does this by phosphorylating the mTOR inhibiting units TSC1/2, which prevent their kinase activity and inhibition of mTORC pathways (Laplante and Sabatini, 2012). AMPK induces cell cycle arrest and induction of autophagy in addition to promoting oxidative phosphorylation and fatty acid beta oxidation (Kim et al., 2011). AMPK activity is specifically required for appropriate T cell function in Th1 and Th17 cells (Blagih et al., 2015). Interestingly, Treg are known to have increased levels of phosphorylated AMPK, a marker of AMPK activation, and inhibition of mTOR with rapamycin induces Foxp3+ Treg *in vitro*. The AMPK-activating drug metformin also induces Treg generation *in vivo* (Michalek et al., 2011).

1.6.3 Metabolic demands of T cells

Naïve T cells have very low rates of glucose uptake and rely on oxidative metabolism for survival (MacIver et al., 2013). In response to activation through the TCR, T cells begin to grow and proliferate rapidly. T cells must maintain appropriate levels of biosynthetic molecules for RNA, DNA, protein, and fatty acid synthesis.

Glycolytic machinery is driven by mTORC1 signaling, as discussed above. Teff subsets are known to be highly glycolytic and primarily switch to glycolytic metabolism in the presence of oxygen, called aerobic glycolysis (aka the Warburg Metabolism). Aerobic glycolysis eschews oxidative phosphorylation for production of lactate from glucose. Many proliferative cells, such as T cells and cancer cells, have this peculiar Warburg metabolism in common (Wang et al., 1976). However, the reasons for this upregulation of glycolytic metabolism in the presence of oxygen are somewhat unknown. Several theories persist, including that glucose uptake would tend to push more carbons into the pentose phosphate pathway (PPP), which is necessary for nucleotide synthesis (Jones and Bianchi, 2015). This metabolic program could also be imperative to maintain ATP and redox molecules NAD+ (Nicotinamide Adenine Dinucleotide) and its reduced form NADH in rapidly dividing T cells.

Glycolysis occurs in the cytoplasm, generates 2 ATP per glucose molecule, and 2 molecules of NADH, a reducing coenzyme important in redox reactions. Oxidative phosphorylation of glucose occurs in the mitochondria, generates approximately 24 ATP per glucose molecule, but also generates 8 NADH and 2 $FADH_2$. NADH and $FADH_2$ can then be used in the electron transport chain reactions in complex I and II, respectively, to push hydrogen ions into the mitochondrial space. These hydrogen ions generate a positive electrochemical gradient in the mitochondria to drive generation of ATP via

ATP synthase, or complex V in the electron transport chain. Glycolysis is less efficient per mole of glucose than oxidative phosphorylation, but glycolytic intermediates can be used for anabolic processes such as fueling the Pentose Phosphate Pathway (PPP) and purine synthesis for DNA and reducing equivalents NAD+ and NADH. Redox reactions are important for eliminating harmful reactive oxygen species and for continuation of TCA (Belikov et al., 2015; Locasale and Cantley, 2011). Glucose is first taken into the cell via several different glucose transporters (GLUTs). Glut1 is the primary transporter in Teff cells, though Glut3 and Glut5 have some function as well. Importantly, T cells deficient for the glucose transporter Glut1 failed to proliferate well and could not produce effector cytokines nor induce inflammatory disease (Macintyre et al., 2014). The initial commitment step of glycolysis is performed by the hexokinases (HK). HKII is the predominant isoform that converts glucose to phospho-6-glucose and locking it within the cell. Further downstream, pyruvate dehydrogenase 1 (PDH1) complex forms an important bifurcation point in glycolysis: commitment to push pyruvate oxidation in the mitochondria or convert pyruvate into lactate via lactate dehydrogenase (LDH). Pyruvate dehydrogenase kinase (PDHK1) phosphorylates PDH1, preventing conversion of pyruvate to acetyl-CoA thus promoting pyruvate conversion to lactate. Lactate is then exported out of the cell and regenerates NAD+ (Gerriets et al., 2015). Treg have been shown to use lactate as a fuel source, unlike Teff cells, providing one method in which

the lactate-rich tumor microenvironment can promote T cell exhaustion via inhibition by fueled-up Treg (Angelin et al., 2017).

T cells increase their anabolic metabolism and dampen catabolism strongly during the immune response. However, after clearance of pathogens, TCR stimulation is reduced and Teff enact apoptotic mechanisms. Some small number of T cells that 'remember' the antigen response need to remain viable and survive long term to maintain host defense. These memory T cells are estimated to have lifespans of months to years in humans (Umeki et al., 1998). In order to survive after ramping up mTORC1 and effector programming, T cells must downregulate anabolic metabolism and enact oxidative metabolism, driven by AMPK-dependent survival. Just as the AMPK-activating drug metformin could promote Treg cells in vitro, which rely on oxidative phosphorylation (OXPHOS), metformin also increased CD8+ T cell memory formation by controlling fatty acid metabolism and OXPHOS (Pearce et al., 2009). Almost simultaneously, Araki et al. showed that memory CD8+ cells could also be enhanced by addition of the mTOR inhibitor rapamycin (Araki et al., 2009). Memory CD8+ T cells require the cytokine IL-15 for survival. IL-15-induced expression of CPT1α, the primary mitochondrial transporter of long-chain fatty acids (LCFA), promoted memory T cell formation and longevity (van der Windt et al., 2012). The interplay between AMPK and

mTOR, two opposing forces in the metabolic landscape, can regulate T cell effector and memory responses.

1.6.4 Glutaminase

The first step of glutamine metabolism is conversion to glutamate. Glutamine is converted to glutamate via the hydrolase enzyme glutaminase (GLS), the first step in glutamine metabolism pathway (Aledo et al., 2000):

$$\text{L-glutamine} + H_2O \longrightarrow \text{L-glutamate}^- + NH_4^+$$

There are two isozymes of glutaminase: GLS1 (GLS; Kidney-type, human chromosome 2, two active splice variants) and GLS2 (Liver-type, human chromosome 12, two splice variants). GLS1 and GLS2 were both named for their high expression in kidney tissue or liver tissue, respectively. Though GLS2 (also known as LGA, GAB) expression is low in T cells, it is induced during activation (Wang et al., 2011). GLS1 (also known as KGA, CAG) requires phosphate for activity, is product inhibited by glutamate, and is generally present in the mitochondria, though localization of GLS is debated (Katt et al., 2017; Yu et al., 2015). Active GLS exists as a large homo-tetramer but is inactive as a homo-dimer, and BPTES, a GLS-specific inhibitor, disrupts the homo-tetramer conformation (Curthoys and Watford, 1995; Thangavelu et al., 2014). Regulation of glutaminase is mixed across many cell types, though transcriptional

regulation of GLS by Myc and c-JUN has been shown (Gao et al., 2009; Lukey et al., 2016) and linked to progression of cancer (Katt et al., 2017; Wise and Thompson, 2010). Inhibition of GLS by compound 968 showed reduced tumor transformation (Wang et al., 2010).

1.6.5 Glutamine metabolism

Many proliferative cells, including cancers, require glutamine for protein synthesis and elimination of reactive oxygen species. The role of glutamine in cancer cells has been well studied. Glutaminolysis supports both anaplerotic and catabolic metabolism but is upregulated during proliferation in T cells. Glutaminolysis is generally upregulated in cancers and drives TCA cycle intermediates, however, dependency on glutamine varies among cancer subtypes (Yang et al., 2017). Glutamine is not an essential amino acid, but rapidly proliferating cells can become dependent on glutamine uptake to maintain a sufficient glutamine pool (Wang et al., 2011). Glutamate is converted to α-KG via glutamate dehydrogenase (GLUD1) by removal of NH_4^+. Ammonia ions are toxic, and so cells remove excess NH_4^+ via the urea cycle (Yang et al., 2017). Metabolically, glutamate feeds into the Tricarboxylic Acid (TCA) cycle via glutamate dehydrogenase, which converts glutamate to α-ketoglutarate. Conversion of glutamate to alpha-ketoglutarate via GLUD1 also produces the redox coenzyme NADPH from NADP+. These redox molecules resolve oxidative stress resulting from

electron transport chain metabolism (Belikov et al., 2015) and are used as cofactors for enzymatic activity and fatty acid beta-oxidation.

Glutamate can also be converted to α-KG via Glutamine Oxaloacetate Transferase (GOT), which uses oxaloacetate to produce α-KG and aspartate. This is a primary driver of the malate/aspartate shuttle in mitochondria (Birsoy et al., 2015). Another enzyme that converts glutamate to α-KG, alanine aminotransferase (GPT1 / GPT2, or ALAT1), uses pyruvate as substrate to form alanine and α-KG. Additionally, the NH_4^+ (ammonia) removed from glutamine and glutamate are shuttled into the urea cycle to be disposed of (Kovacevic and McGivan, 1983). While glutaminolysis is important for proliferating cells, cancer cells are known to be both sensitive (van Geldermalsen et al., 2015) or insensitive (Cheng et al., 2011) to glutaminolysis inhibition, showing that not all proliferative cells require glutaminolysis. There are several mechanisms in which cancers could be insensitive to glutaminolysis inhibition. First, Pyruvate Carboxylase (PC) can directly convert pyruvate into oxaloacetate and consuming ATP and bicarbonate. PC allows for replenishment of oxaloacetate and promotion of the electron transport for anaplerotic reactions. Further, because glutamate can be formed by multiple different transaminases including GPT and GOT, levels of glutamate and α-KG could be restored by upregulating amino acids such as alanine and aspartate, respectively. In one setting, upregulation of aspartate transporters and

aspartate conversion to glutamate provided a significant source of glutamate during glutamine starvation, promoting survival in a p53-dependent process (Tajan et al., 2018). The complex interactions of metabolic fuels and enzymes in a context- and cell-dependent way opens new avenues for exploration.

Glutamine transporters and downstream glutaminolysis proteins are upregulated during T cell activation in an mTOR-dependent process, similar to glycolytic machinery (Wang et al., 2011). Teff cells activated in glutamine depleted media cannot activate properly, indicating that glutamine uptake is important in T cell function. However, the product of this reaction, glutamate, does not rectify glutamine depletion (Carr et al., 2010). This may be because glutamine is a nitrogen donor in some reactions and another requirement of T cell activation is import of cysteine via the xCT transporter, which is dependent on anti-port transport of glutamate outside of the cell (Siska et al., 2016). Thus, T cells may be unable to import glutamate to maintain glutamate or glutamine pools at suitable levels. T cells required the glutamine transporter ASCT2 (SLC1A5) for appropriate Th1 and Th17 effector function, but was unnecessary for proliferation, counter to expected results from glutamine deprivation experiments (Nakaya et al., 2014). This may imply that ASCT2 is not the only transporter for glutamine uptake. Additionally, CD8+ T cells dosed with an SLC1A5-specifc inhibitor, V-9302, showed slightly increased viability and activation markers seven days

after activation. This selective glutamine transport inhibitor also showed in vivo efficacy in reducing cancer growth in hepatocellular carcinoma HCC-1806 xenografts (Schulte et al., 2018). Finally, inhibition of Glutamate Oxaloacetate Transaminase 1 (GOT1) promoted Treg while inhibiting differentiation of Th17 cells (Xu et al., 2017). Thus, modification of different steps of the glutaminolysis pathway can have a variety of biology activity in T cell function in addition to the role of glutaminolysis in various cancers.

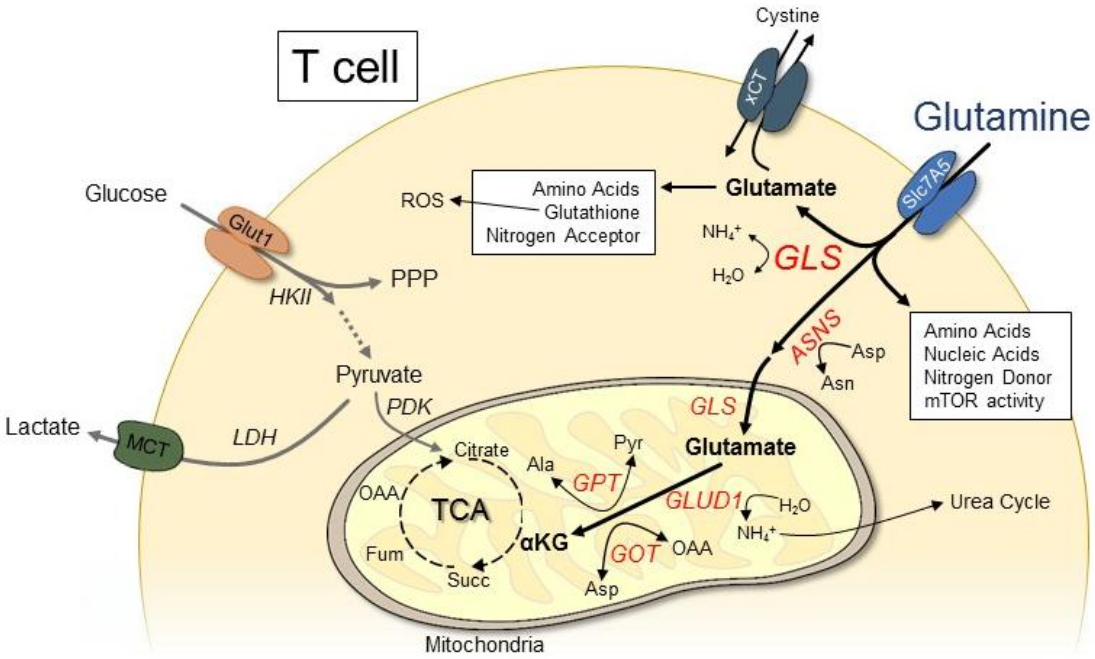

Figure 2: Glutaminolysis pathways important in T effector cell function.

Pyr – Pyruvate. OAA – oxaloacetate. Fum – Fumarate. Succ – Succinate. ROS – reactive oxygen species. PPP – pentose phosphate pathway. Italicized items are enzymes. Red italicized are glutaminolysis-specific enzymes.

1.6.6 Reactive Oxygen Species

Mitochondria are the powerhouse of the cell and a major site of metabolism and signaling integration. Reactive oxygen species (ROS) are generated primarily as a result of oxidative phosphorylation in the mitochondria but can also be formed by the NOX NADPH oxidases) family of transmembrane proteins in the cytosol (Bedard and Krause, 2007; Murphy, 2009). ROS are small oxygen-bound molecules that readily oxidize cellular components. NOX proteins have pleiotropic functions in cells, but primarily transport electrons across membranes and generate significant amounts of superoxides (O_2-). Superoxides ($O_2^{\bullet -}$) and other ROS (hydroxyl •OH, alkoxyl RO_2•) are dangerous to nucleic acids, proteins, and lipids, as they can irreversibly destroy or modify their function. These ROS are quickly converted to less hazardous species such as hydrogen peroxide (H_2O_2), which can freely disperse throughout the cell. Innate immune defense actually relies on generation of ROS species, though the mechanisms are still unclear. Deletion of NOX2 protein on the human X chromosome results in chronic granulomatous disease patients who have severe, uncontrolled infections(Bedard and Krause, 2007). Actively proliferating cells rely on several mechanisms to attenuate toxic ROS levels.

Glutathione (GSH) is one of the most abundant regulators of cellular ROS. GSH is derived from ligation reactions of glutamate, cysteine, and glycine by glutamate

cysteine ligase (Gclc) and glutathione synthetase (GS). Levels of GSH are dependent on availability of these amino acids and modulate T cell biology. GSH can also be regenerated in a recycling pathway primarily driven by glutathione-disulfide reductase (GSR). Oxidized glutathione can directly reduce ROS but it also rejuvenates other ROS detoxification species. In T cells, control of ROS is imperative for appropriate activation and function (Sena et al., 2013). Oxidative stress from ROS can include DNA damage, programmed cell death, lipid peroxidation, and protein damage (Espinosa-Diez et al., 2015). Because mitochondrial ROS are primarily produced by complex I and III of the electron transport chain, mitochondria generate ROS levels to a high degree and require ROS detoxification programs. Superoxide dismutases (SODs) catalyze the detoxification of superoxides in the mitochondria into H_2O_2.

T cells specifically are sensitive to a reducing environment, can be influenced by extracellular ROS, and addition of a GSH mimetic, N-acetylcysteine, can prevent T cell activation (Cemerski et al., 2002). Homeostatic mechanisms likely drive sensitivity to ROS, as both too much and too little ROS can be deleterious to cell survival (Rashida Gnanaprakasam et al., 2018). Glutamine availability and *de novo* GSH synthesis was required for Th17 differentiation as knockout of glutamate-cysteine ligase (the first step in *de novo* synthesis of glutathione) prevented Th17 function and was protective against

induction of a mouse model of multiple sclerosis (Lian et al., 2018; Mak et al., 2017). Changes in ROS signaling could have profound impacts on T cell function.

While ROS are generally considered deleterious in high levels (termed oxidative stress), ROS are also important signaling molecules within the cell and are used by some cells of the immune system, such as phagocytes, to enact immune defense, as discussed above (Bedard and Krause, 2007). The best-studied signaling effects of reactive oxygen species are the protein tyrosine phosphatases (PTP), which regulate phosphorylation states of many different signaling proteins. Cysteine moieties on are very susceptible to oxidization by ROS, and catalytic sites in PTPs contain these oxidization-sensitive cysteines, affecting signal transduction globally. Additionally, ROS can enhance kinase activation, calcium influx and efflux, and modulate cellular apoptosis. Indeed, the activity and signaling of PKC, NFkB, and MYC is altered in T cells by ROS levels, where ablation of GSH synthesis increased ROS generation and prevented T cell activation (Rashida Gnanaprakasam et al., 2018). Apoptotic proteins such as Bcl-2 and FasL and expression of cleaved caspases are also induced by excessive ROS levels in T cells, indicating an important role of ROS in survival and T cell function (Hildeman et al., 1999). GLS inhibition by the small molecule inhibitors BPTES or CB839 enhance ROS in cancer cells and induced tumor cell death (Abu Aboud et al., 2017; Elgogary et al., 2016).

Therefore, it will be important to identify mechanisms of ROS signaling and function in GLS inhibited T cells.

1.7 Epigenetic modifications in T cells

Cell metabolic state and substrate availability can significantly alter the epigenetic landscape (Reid et al., 2017). Regulation of methylation and acetylation of histones inhibit or enhance transcription of biologically relevant genes, which are durable and heritable (Kohli and Zhang, 2013). Genetic regulation is imperative for survival, so it is no surprise that a suite of enzymes are responsible for methylation, demethylation, acetylation, and deacetylation of DNA to control these modifications. Histone acetyltransferases (HATs) and de-acetylases (HDACs) rely on acetyl-CoA and nicotinamide dinucleotide (NAD+) levels for activation. While mechanistic outcomes are diverse, HDAC inhibitors are FDA approved and are currently being explored for cancer treatments alone and in combination with standard of care chemotherapies (Li and Seto, 2016; Ropero and Esteller, 2007).

Another layer of DNA modification is handled by methyltransferases and demethylases. EZH2 is a methyltransferase which relies on s-adenosylmethionine (SAM), a member of one-carbon metabolism, for methyl substrate, add methyl marks, whereas demethylases, such as KDM6B (aka JMJD3, a member of the jumonji-demethylases/oxygenases) remove methyl marks from histones and requires α-KG for

co-substrate (Wang et al., 2013). KDM6 family members are inhibited by succinate, one of the products of the reaction (Rose et al., 2011). Thus, key epigenetic regulators are sensitive to metabolic perturbations and metabolite levels.

The polycomb repressor complex (PRC2) contains EZH2 and has been shown to trimethylate H3K27, leading to silenced DNA regions (Jiao and Liu, 2015). H3K4 trimethylation functionally opposes the H3K27 trimethylation mark by promoting gene transcription, and is present primarily at transcription start sites (Eissenberg and Shilatifard, 2010). Inhibition of KDM6B reduced epithelial-mesenchymal transition in mammary cells, a crucial event in the development of metastases (Ramadoss et al., 2012). Recently it was reported that methyl modifications to the KDM6 family genes in non-small cell lung cancer and squamous cell carcinomas yielded associations to patient survival. Additionally, KDM6B inhibition by small-molecule GSKJ1 reduced inflammatory responses in macrophages exposed to lipopolysaccharide (Kruidenier et al., 2012). In T cells, 2-hydroxyglutarate-derived methylation of the Foxp3 locus promoted Th17 even in Treg skewing conditions by decreasing transcription of Foxp3 (Xu et al., 2017). While the interplay of differing methyl marks, acetylation marks, and gene expression is complicated, analyzing epigenetic modifications at specific gene loci could uncover new targets for small molecule intervention. Methyltransferases and

demethylases as a potential target for therapeutics both in cancer and inflammation (Wei et al., 2018).

Availability of substrate and co-factors involved in these DNA and protein-modifying enzymes can exquisitely fine-tune gene transcription. Moreover, while kinases and other signaling molecules do rely on metabolic intermediates, epigenetic enzymes are much more sensitive to levels of relevant metabolites (Reid et al., 2017). Small metabolic perturbations could thus impact specific and sensitive proliferating cells such as T cells in context-dependent ways. While the field of epigenetic regulation is enormous, this dissertation will focus on the jumonji-members because they are sensitive to the availability of metabolically relevant substrates such as s-adenosylmethionine, α-KG, and succinate, key metabolites of glutaminolysis and the TCA.

1.8 In vivo models of T cell function

Mouse models of inflammation and cancer have been used extensively in research in lieu of human testing. The significance of rodent models compared to human responses is mixed (Webb, 2014), however they represent a consistent, available source of *in vivo* evidence for mammalian biology. Inflammatory models induced by adoptive transfer of CD4 and CD8 cells or immune insult drive pre-clinical development of new

inflammatory drugs, and tumor-bearing mice offer avenues for testing anti-cancer drugs. Whether the role of GLS in T cells *in vitro* have *in vivo* consequences will ultimately decide the biological validity of GLS inhibition as a potential method for pre-clinical application and treatment of inflammatory or cancer disease.

Th17 inflammation is especially controlled in the gut. In mice, Th17 cells are implicated in development of colitis and inflammatory bowel disease and lupus (Y et al., 2012). IL-17 knockout mice are protected from colitis (O'Connor et al., 2009) and addition of functional regulatory T cells attenuates colitis , indicating that Th17 cells drive inflammatory responses. In humans, both Th1 and Th17 cells are linked to different gut inflammatory settings, Crohn's disease and ulcerative colitis, respectively. The relative contribution of IFNγ from Th1 and IL-17 from Th17 is debated, as Th17 cells have also been shown to produce IFNγ, however it is clear that pro-inflammatory signaling from helper T cells plays a significant role (Galvez, 2014; Lee et al., 2009). Several mouse models of colitis induction are tractable: dextran sulfate sodium (DSS) model requires addition of DSS to drinking water to induce gut damage. However, DSS does not require the adaptive immune system for development of inflammatory responses (Chassaing et al., 2014). A more useful approach to colitis *in vivo* is the piroxicam model of colitis. Piroxicam is a non-steroidal anti-inflammatory drug that can be mixed into food to induce gut damage in mice to allow subsequent inflammation

caused by immune recognition of microbiome constituents. Mechanistically, the regulation of inflammatory responses in the gut by NSAIDs is unknown, however, inhibition of cyclooxygenase enzymes by piroxicam leads to changes in prostaglandins, which have immunomodulatory effects (Berg et al., 2002).

A major consequence of organ transplant is dysregulation of inflammatory effector cells leading to graft versus host disease (GvHD). Graft survival and overall success rate in humans in abysmal and requires strong immunosuppressive medication, especially in lung transplants. One of the main consequences of lung transplant is bronchiolitis obliterans (BO). BO is a significant lesion of lung airway epithelium promoted by CD8 and CD4+ T cells. This accounts for almost 30% of all deaths in lung grafts after three years and does not respond to enhanced immunosuppression (Estenne and Hertz, 2002). A mouse model of BO (and GvHD) was developed by Blazar et al, in which lethally irradiated mice received donor bone marrow and CD4/CD8+ T cells. Mice receiving bone marrow alone do not develop BO-like lesions. Induction of lung injury like BO is reliant on IL-6, TGFβ, IL-17, TNFα, and IFNγ (MacDonald et al., 2017) and like many other inflammatory diseases is a balance of effector cell and regulatory cell responses.

So far, the mouse models discussed focus on reducing T cell inflammatory responses. However, in cancer, promoting T cell activation and cytotoxicity would

beneficial to improve responses. Chimeric Antigen Receptor T (CAR T) cells have emerged recently as transformative in treating human B cell leukemia (Davila et al., 2013). In this model, T cells are removed from mice and transduced retrovirally to express a combination construct of a CD19 specific TCR (to target B cells) plus co-activation molecules CD3 and CD28z. This promotes T cell proliferation and cytotoxicity against CD19+ leukemic B cells. In 2017, the Federal Drug Association (FDA) approved CAR T cell therapy in humans. CAR T cell therapy is attractive because autologous transplant of the patient's own T cells has far fewer autoinflammatory problems than allogeneic transplant. Metabolic modification was effective in promoting T cells responses via inhibition of Akt, a key mTOR regulator. Inhibition performed *ex vivo* before transfer to recipient mice led to robust increases in effector T cell-mediated killing of leukemic B cells compared to controls (Urak et al., 2017). Control of leukemic B cells is dependent on CAR T cell cytotoxicity and survival. Problems arise in cure rates when leukemias either lose the CD19+ antigen (Ruella et al., 2018) or survive the initial killing phase of CAR T transfer. Because CAR T cells die off quickly after transfer, improving the fitness and survival of CAR T cells through metabolic modification could boost T cell performance in CAR T cell cancer models.

Despite the plethora of mouse models available for pre-clinical analysis of inflammatory and cancer disease, there are potential liabilities. In some inflammatory

model settings, mouse inflammatory responses and humans simply aren't recapitulated well. Asthma, for instance, is not a naturally occurring disease in any animal tested as yet (Webb, 2014). Sepsis treatments have also had significant setbacks from the perspective of pre-clinical mouse models, as mouse and human responses were found to be similar in response to certain immune insults, but were dependent mouse strain, microbiota of the gut, and timing of readouts (Webb, 2014; Wiersinga, 2011).

Beyond the somewhat poor recapitulation of disease initiation, many animal models deliberately chosen for the speed at which disease progresses. For example, in inflammatory bowel disease (IBD) and colitis, induction usually takes place over just a few weeks or months and treatment, even shorter. In humans, colitis can be present for years and treatment can go for a lifetime. Mouse models of Unfortunately, these types of problems are inherent in any animal model, as expediency and cost-savings are imperative in pre-clinical exploration.

1.9 Questions to be addressed

Metabolic reprogramming from a quiescent, naïve status to actively proliferating and functional T effector cells has been well described (Macintyre et al., 2014; Wang et al., 2011). However, despite elucidating metabolic differences between Treg and Teff (Th1, Th2, Th17) cells, little is known about how metabolic reprogramming differs between the effector subsets. All are driven by different cytokine and growth signals,

despite having common activation through kinases and the TCR. Glucose use in Teff and Treg has been explored (Macintyre et al., 2014), though other major sources of biosynthesis, such as amino acids and fatty acids, are currently being researched (Carr et al., 2010; Tajan et al., 2018; Xu et al., 2017).

Much work has been performed in cancer and cancer cell lines, yielding new insights into glutaminolysis in highly proliferative cells. For example, a significant portion of glutaminolysis carbons enter the TCA cycle via alpha-ketoglutarate. During mitochondrial stress, or in an environment of mitochondrial disfunction, α-KG is used via reductive carboxylation to generate citrate (Mullen et al., 2014). Citrate is then exported to the cytosol and used for biosynthesis of lipids. The glutamine pathway is strongly upregulated during T effector cell activation, yet we know little about how this pathway modulates T cell responses. Deletion of the primary glutamine transporter, ASCT2, prevented Teff function but didn't affect proliferation (Nakaya et al., 2014). Glutamine withdrawal, meanwhile, promoted Treg development (Klysz et al., 2015). Glutamine has many uses in a cell, including incorporation into protein and co-transport of other required amino acids. These previous studies targeted glutamine availability for T cell function, which could have a variety of effects on T cells, including preventing activation of the glutamine-sensitive mTORC1 pathway. We endeavored in this work to explore the first step in glutamine catabolism: conversion to glutamate by the enzyme

GLS. In this way, glutamine levels are maintained (or increased) while availability of glutamate is potentially reduced. We use both genetic and pharmacological approaches to affect GLS activity, which together allow us to eliminate off-target pharmacological effects.

Targeted approaches to affect one subset of T cells while sparing, or even promoting, other subsets could be clinically useful. Standard of care for autoimmune disorders results in strong immunosuppression across all immune cell types. For improved patient outcomes, a targeted approach could allow the immune system to continue operating normally while suppressing unwanted inflammatory responses. We approach the inflammatory setting in several Th1 and Th17-mediated viral and inflammatory murine models. Specifically, response to vaccinia (Th1) and models of graft versus host disease and colitis (Th17).

GLS inhibition could be successful in cancer treatments as well, because maintaining CD4 and CD8+ effector responses while dampening Treg function could promote cancer killing. Tumor infiltrating lymphocytes (TILs) have been shown to upregulate PD-1, an inhibitory marker of T cell function. Restoring T cell function or boosting T cell responses can improve cancer therapies (Norde et al., 2011). To get at this, we use genetic and pharmacological approaches to generate GLS-deficient effector

T cells in the Chimeric Antigen Receptor (CAR) T cell murine model, which models the human CAR patients with B cell leukemias.

Taken together, the work presented here aims at modifying T cell responses at the level of glutaminase, which may yield a new target for both cancer therapy and autoimmune disease.

2. Materials and Methods

2.1 Mice

Mice were obtained from the Jackson laboratory or described previously. GLS1fl/fl animals were obtained as Glstm1a(KOMP)Mbp embryonic stem cells (Project ID: CSD29307) from the KOMP that were blastocyst microinjected to generate mice (Duke University Transgenic and Knockout Shared Resource) and crossed to FLP transgenic animals. Progeny were then crossed with CD4-CRE transgenic mice to develop the GLS1fl/fl CD4-CRE (GLS KO). In all cases comparing wild type to GLS KO, healthy, sex-matched and age-matched littermates were used (male and female, 8 to 14 weeks of age unless otherwise stated). No sex differences in phenotype were noted in WT and GLS KO CD4 T cells. Animals were genotyped for floxed alleles and CRE allele. Male C57BL/6J mice aged 8-16 weeks were used for in vitro CB839 experiments (RRID: IMSR_JAX:000664). Mice were not involved in previous procedures or tests before use and co-housed under the same husbandry conditions. All mouse procedures were performed under IACUC-approved protocols from Duke University, Vanderbilt University (2W tetramer, IBD, homeostatic proliferation, and asthma models), the National Cancer Institute (Vaccinia model), the Moffitt Cancer Center and Research Institute (CAR T cell in vivo model), and the University of Minnesota (Graft vs. Host Disease model).

2.2 T cell in vitro activation and skew experiments

T cell in vitro experiments were carried out using primary mouse T cell cultures from male and female mice at 37° C with 5% CO2 in RPMI media (CAT#10-40-CV) supplemented with HEPES, β-mercaptoethanol, Pen/Strep, and glutamine, unless otherwise stated. Generation of viral particles was performed in PLAT-E retroviral packing cell lines (Cell Biolabs). T cell killing assays were performed on CD19 expressing Emu cell lines (Generous gift from Dr. Davila Lab).

CB839 was dosed at 1 μM (activation) or 500 nM (differentiation), GSKJ4 (Cat#:S7070) at 1 μM, dimethyl-2-oxoglutarate (DMaKG) (Cat#: 349631) at 1.5 mM and/or rapamycin (Cat#: 553210) at 5 nM. Briefly, CD4+ T cells were isolated (Cat#130-104-454) from wild type animals (WT) and GLS1fl/fl CD4-CRE+ mice (GLS KO) and activated over various time points via 5 ug/mL anti-CD3/anti-CD28 antibodies plate bound (CD3: Cat # 16-0031-85, CD28: Cat # 16-0281-85). Non-stimulated CD4 samples were maintained using 10 ng/mL IL-7 (Cat#: 217-17). For skewing experiments, naïve CD4 T cells from WT or KO animals were plated with αCD3 (2.5 ug/mL) and subset-specific cytokines and antibodies (Th1: IL-12p70 (10 ng/mL), αIFNy (1 uL/mL), αIL4 (10 uL/mL); Th17: IL6 (40 ng/mL), αIFNy (10 uL/mL), TGFβ (1 ng/mL), Treg: TGFβ (2 ng/mL) and stimulated with feeder layer of irradiated splenocytes. Th0 experiments were run in skewing condition (+αCD3 antibody 2.5 ug/mL) without additional

cytokines. After 3 days, cells were split with fresh media and stimulated with or without 10 ng/mL IL-2 (Cat#:14-8021-64) for a further 2 days. For intracellular cytokine stains, cells were re-stimulated using PMA/ionomycin in the presence of GolgiPlug (Cat#: 555029) for 4 hours, then fixed and stained for intracellular subset-specific cytokines using fix/perm kit (Cat#: 554714). For all other intracellular or intranuclear stains such as transcription factor, pS6, C-MYC, H3K4me3, H3K27me3, and total H3 protein, cells were removed from media, stained for surface markers (See Key Resources antibodies table), fixed, then stained for intracellular proteins using fix/perm kit (Cat# 00-5223-56, 00-5123-43). Cell proliferation was assessed by staining naïve CD4+ cells with Cell Trace Violet proliferative dye at 5 μM (Cat#: c34557).

2.3 Homeostatic Proliferation

Homeostatic proliferation was measured as previously described(Jacobs et al., 2010). Briefly, naïve $CD4^+$ and $CD8^+$ T cells were isolated from $GLS^{fl/fl}$CD4-Cre and wild-type $Thy1.1^+$ mice. Cells were mixed in a 1:1 ratio and stained with proliferative dye CellTrace Violet (Cat#: c34557). Cells were transplanted by i.v. injection into recipient RAG knockout mice 8 weeks of age. Five days after injection, spleen and mesenteric lymph node were collected, homogenized, and stained with antibodies against CD4, CD8, and Thy1.1 for flow cytometry analysis.

2.4 ATAC-Sequencing Experiments

Crude nuclei pellets for ATAC-seq were isolated according to Buenrostro et. al (Buenrostro et al., 2013) with modifications. Briefly, naïve CD4 T cells were skewed to Th1 and Th17 subsets in vitro with vehicle or in the presence of 0.5 μM CB839. At Day 5, T cells were re-isolated for CD4+ cells using CD4+ negative selection kit (Cat#: 130-104-454). $1x10^5$ cells were removed for nuclei extraction for 30 minutes in ATAC-Seq lysing buffer. Cells were exposed to Tn5+adaptor proteins from Nextera DNA for 30 min at 37°C and immediately placed on ice. Transposed eluate was amplified via PCR using Nextera DNA preparation kit (Cat #: FC-121-1030), NEBNext High-fidelity 2x PCR mix (Cat#: M0541) and multiplexed (Cat#: FC-121-1011). Samples were purified using Zymo DNA cleanup kit (Cat#: D4011). Initial verification of library generation was performed by ethidium bromide agarose gel, looking for repeating bands of DNA. QC of samples was run on bioanalyzer before being sent for sequencing.

ATAC-seq libraries were sequenced on a Hiseq 4000 paired-end sequencing (100 bp read length). All reads for each library were aligned to UCSC mm9 genome assembly with bowtie2 [18] using pair-end settings (--local, -X 2000, --no-mixed, --no-discordant). Greater than 50 million reads were obtained for each library and reads mapping to mitochondrial DNA were excluded from the analysis together with low quality reads (MAPQ < 10). Peaks were called for each sample using HOMER (Heinz et al., 2010) with

parameters -style factor -fdr 0.01 -F 0 -L 0 -C 0", and differential peaks were identified using the HOMER-style factor module comparing different cell types. Peak annotation was performed using HOMER. Overlapping open chromatin regions with in replicate cell types, and between cell types and other genomic features (within 1 bp) were identified using HOMER.

2.5 RNA Sequencing Experiments

Naive CD4+ T cells from C57BL/6J mice were skewed to Th1 and Th17 subsets with or without CB839 over 5 days and total RNA extracted for RNAseq (Cat#: 74104). RNA was sent to VANderbilt Technologies for Advanced GEnomics (VANTAGE) core at Vanderbilt University. Libraries were prepared using 50ng of total RNA using the NEBNext Ultra RNA Library Kit for Illumina (Cat# E7530) and sequenced on HiSeq3000 at 75bp paired-end. Each sample was analyzed in triplicate. Sequencing reads were aligned against the Mouse GENCODE genome, Version M14 (January 2017 freeze, GRCm38, Ensembl 89) using the Spliced Transcripts Alignment to a Reference (STAR) software (Mudge and Harrow, 2015). Reads were preprocessed and index using SAMtools (Li et al., 2009). Mapped reads were assigned to gene features and quantified using featureCounts (Liao et al., 2014). Normalization and differential expression was performed using DESeq2 (Love et al., 2014). Skewed lymphocytes with and without CB839 were compared in both Th1 and Th17 groups. The top most significantly

differentially expressed genes (FDR<0.01 and Log2 difference greater than 0.5 in magnitude) were considered for subsequent functional enrichment using Geneset Enrichment Analysis. The top 200 most differentially expressed genes were used for unsupervised hierarchical cluster analysis and visualized using heatmap representations.

2.6 PCR

Pan T cells (CD4+ and CD8+) were isolated and purified using Miltenyi isolation kit (Cat#: 130-095-130). Genomic DNA was generated using Kapa express Extract kit (Cat#: KR0370) in 50 uL total volume. Primers targeted over exon 10 and exon 11 were generated for wild type band with a melting temperature of 54°C:

Forward: ACGAGAAAGTGGAGATCG

Reverse: GCCTTCTGGAAAACA

10 uL PCR product was then run on a 1% agarose gel with ethidium bromide and visualized by GelDoc XR (Cat#: 1708195).

2.7 Glucose Uptake

Glucose uptake assays were performed as previously described (Macintyre et al., 2014). Naïve CD4+ T cells were differentiated into Th1 and Th17 cells, in triplicate, in the presence or absence of CB839 over five days and spun down after reisolation using CD4 kit as previously described. At day 3 and 5, cells were removed, washed twice in PBS,

counted, then rested in 1 mL Kreb's Ringers HEPES (KRH) for at least 10 minutes. Cells were spun and resuspended to $5x10^5$ cells/50 μL KRH for glucose uptake assay. Briefly, 3H-2-deoxyglucose was suspended in KRH bubble layered in oil, and cells were added to this bubble. Cells were incubated for 10 minutes at 37°C. Immediately after incubation, reaction was quenched with 200 μM phloretin (Calbiochem, Cat#: 524488). Cells were spun, washed, and then resuspended in scintilation fluid for counting on Beckman-Coulter scintillation counter (3H, 1 min/sample read).

2.8 Extracellular Flux Analyses (Seahorse)

Experiments were carried out on Agilent Seahorse XF96 bioanalyzer (Agilent). Briefly, wild type CD4+ cells were isolated as previous and activated for 3 days on αCD3/CD28 coated plates as previously described, or skewed to Th1 and Th17 subsets as described above. T cells were isolated and spun onto XF96 Cell-Tak (BD Bioscience, Cat#: 354240) coated plates and rested in Seahorse XF RPMI 1640 media supplemented with glutamine, sodium pyruvate, and glucose. For immediate metabolic response, 1 μM CB839 and 5 μM UK5099 (Cat#: PZ0160-5MG) were injected separately or in combination, and OCR and ECAR measured. For activation response, 1 μM CB839 was injected into IL-7 maintained naïve CD4+ T cells in seahorse medium and allowed to incubate for 20 minutes, followed by soluble αCD3/CD28 injection.

2.9 Mass Spectrometry

13C Tracing. To measure 13C-Glucose tracing in T cell activation, CD4 cells were stimulated on 5 μg/mL anti-CD3/CD28 for 3 days. At day 3, cells were pooled, washed 3x in PBS, and re-stimulated in presence of 1 μM CB839 or Vehicle (DMSO) and 11 mM 13C glucose (Cambridge Isotope Labs, Cat#: CLM-1396-1). Cells were incubated for 24 hours at 37oC, then scraped and combined in triplicate. Cells were rinsed with 0.9% saline and metabolites were extracted in methanol. Metabolites measured by LC-High-Resolution Mass Spectrometer (LC-HRMS) using a Q-Exactive machine as previously described (Liberti et al., 2017). The time-dependent glucose labeling pattern was modeled as with the following equation:

$$\frac{[X^*]}{X^T} = 1 - e^{-\frac{f_X}{X^T}t}$$

In which $[X^*]$ is the concentration of labeled glucose, X^T is the total concentration (both labeled and unlabeled) of glucose, f_X is the glucose production flux. This model was fit to glucose MIDs using the fit() function in MATLAB to determine relative glucose production fluxes. Relative glucose pool sizes were estimated from MS signal intensities.

Differentiation. CD4 cells were isolated as previously described and differentiated in subset-specific medium in the presence of vehicle or CB839 (in

triplicate) for 3 days, split at day 3 with new media and IL-2, then allowed to incubate a further 2 days. At day 5, wells were combined, cells washed 1x in MACS buffer and re-isolated for CD4 via AutoMACS Pro automated magnetic separator (Miltenyi, Cat#: 130-092-545). Metabolites from Th1 and Th17 cells were extracted and analyzed by LC-High-Resolution Mass Spectrometer (LC-HRMS) using a Q-Exactive as described previously (Gerriets et al., 2015). Data were range scaled and analyzed using Metaboanalyst 3.5(Xia and Wishart, 2002) (http://www.metaboanalyst.ca/faces/home.xhtml) to generate heat maps and for principle component analyses.

2.10 Nuclear Magnetic Resonance (NMR) metabolite analysis

For cellular metabolite analysis, water-soluble and lipid metabolites were extracted using a dual phase extraction protocol (Tyagi et al., 1996). Cells were grown in 24-well culture plates, scraped into a centrifuge tube, centrifuged at 4C and the culture medium was removed for NMR analysis. The cells were washed with sterile ice-cold saline, which was removed by centrifugation and the cell samples flash-frozen in dry-ice/MeOH bath. The samples were stored in -80C.

For metabolite extraction, frozen cell pellets were placed on dry ice and immediately resuspended in 1 ml of ice-cold methanol. The cell suspension was vortexed vigorously for 30 s and 1 ml of ice-cold chloroform was added. The vortexing was repeated and 1 ml of ice-cold de-ionised water was added before repeating the

vortexing again. The cell suspension was then centrifuged at 2200 g for 1 h at 4 °C to separate the phases. Chelex 100 (Sigma-Aldrich, USA) was added to the top methanol-water phase (containing water-soluble metabolites) to remove metal ions. After the Chelex 100 was removed by centrifugation at 1000 g 4C 5 min, the water-soluble extracts were evaporated at 4C on vacuum evaporator. The dried samples were reconstituted in 167 µl D2O and 13 µl of 0.75% sodium 3-trimethylsilyl- 2,2,3,3- tetradeuteropropionate (TSP) in D2O (Sigma-Aldrich) for chemical shift calibration and quantification. 170 µl of the sample was placed in a 3 mm NMR tube and the pH adjusted to pH 7 using 0.6% perchloric acid.

Media from cultured cells following various treatments was also collected. 50µl D2O and 50 µl of 0.75% TSP was added to 500 µl media in 5 mm NMR tube.

Deuterated solvents were used to minimise the solvent signal in the proton NMR spectra since the resonance frequency ranges for a proton and a deuteron differ due to the different spin properties of these two nuclei. Additionally, the spectrometer used utilises deuteron frequency monitoring to compensate for any temporal drifts in the magnetic field strength by keeping the deuteron resonant frequency in D2O constant.

All spectra were acquired on a 600 MHz spectrometer equipped with a 5mm Z-gradient TCI cryo-probe and 14.1 Tesla Bruker Magnet (Bruker, Germany) at 298 K. The spectra were acquired with 7,500 Hz spectral width, 32,768 time domain points and

relaxation delay of 2.7 s. The water resonance from media and soluble cell extract samples was suppressed by a gated irradiation centered on the water frequency. 32 and 256 scans were performed on medium, and water-soluble cells extracts, respectively. The spectra were phased and manually baseline corrected using Bruker TopSpin-3.1 software package. Media and soluble cell extracts were referenced to TSP. Spectral assignments were based on literature values (Sitter et al. 2002).

For 1H-MRS of soluble cell extracts and media samples, metabolite amounts in the sample were calculated by adjusting the peak integrals, corresponding to individual metabolite resonances, to the peak integrals of TSP, corrected for the number of protons. Metabolite levels were standardized to cell number.

2.11 Immunoblotting

Immunoblots were performed as previously described (Jacobs et al., 2008) with the following modifications. Cells lysed with RIPA buffer and Halt protease/phosphatase cocktail inhibitors (Life Tech, Cat#: 78443). Protein was quantified by Pierce BCA kit II (Cat#: 23227). Actin blots were visualized by near infrared fluorescence via Licorr Odyssey imager. GLS blots were visualized by chemiluminescence using anti-rabbit conjugated horseradish peroxidase. The antibodies used for westerns were: GLS (Cat#: GTX81012, 1:1000), β-Actin (Cat#: 8226, 1:10,000).

2.12 Viral Infection with PIK3IP1

Naïve $CD4^+$ T cells were isolated from wild type C57BL6 mice. T cells were stimulated in Th1 and Th17 skewing conditions plus vehicle of CB839 as previously described. These were incubated for 16 hours with a feeder layer of irradiated splenocytes. Plasmid constructs MSCV-PIK3IP-IRES-Thy1.1 ("PIK3IP1") and control vector MSCV-IRES-Thy1.1 ("Control") were used to transfect Plat-E cells. T cells were then infected with cell supernatant containing retrovirus and polybrene and rested for 48 hours. Cells were split at Day 3 in new media containing IL-2 (10 ng/mL) and then incubated for 48 hours before removing for intracellular cytokine and transcription factor staining by flow cytometry as described above.

2.13 CRISPR/CAS9 PIK3IP1

Naïve CD4+ T cells were isolated from Cas9 transgenic mice (RRID:IMSR_JAX:024858)) aged 10-12 weeks old. T cells were plated on an αCD3/CD28 coated 24-well plate and one day after activation, cells were transduced with viral supernatant prepared from PLAT-E cells (Cat#: RV-101) transfected with a solution of 2000μg DNA (empty vector pMx-U6-empty-GFP or two different PIK3IP1 targeting guide RNA containing vectors pMx-U6-PIK3IP1-GFP). T cells with the viral particles were centrifuged at 2000rpm for 2 hours at 37°C, followed by incubation for 2 hours at 37°C and 5% CO2. The media was then replaced with 1mL fresh Th1 skewing media and

incubated overnight. This was repeated a second time on day 2 of T cell activation. Cells were collected ten days post activation for pS6, intracellular cytokine production, and transcription factor staining by flow cytometry as described.

2.14 PIK3IP1 Antibody in vitro

Naïve CD4+ T cells were isolated from C57BL6 mice and activated on aCD3/CD28-coated 24 well plates at $1x10^6$ cells/well with either control antibody (Cat#bs-0295P) or PIK3IP1 antibody (Cat#16826-1-AP) at 0.5 μg/mL. Cells were incubated at 37° C for 72 hours and cells removed at 24, 48, and 72 hours for flow cytometry analysis of activation.

2.15 In vivo Graft Versus Host Disease

Induction of Graft vs Host Disease (cGVHD) was performed as previously described (Panoskaltsis-Mortari et al., 2007). Briefly, mice were lethally irradiated the day before bone marrow transplant. Mice were dosed with cyclophosphamide (Cytoxan, Bristol Myers Squibb, Seattle WA) at 120 mg/kg/day on days -3 and -2. Recipient irradiated mice were transplanted via caudal vein with 15×10^6 T-cell depleted allogeneic marrow with 1 x 106 cells splenic CD4+ cells from WT or GLS KO mice, or control (no CD4+ T cells). Mice were assessed for lung elasticity, resistance, and compliance at Day 28 by whole body plethysmography using the Flexivent system

(Scireq, Montreal, PQ, Canada). Histological assessment of GVHD was assessed as previously described (Blazar et al., 1998).

2.16 Asthma & Acute Lung Inflammation Model

Female mice were administered intranasal sensitization of either PBS alone or a combination of 100 μg house dust mite extract (Greer, Lenoir, NC) and 0.1 ug LPS from Escherichia coli 0111:B4 (Sigma, St. Louis, MO) in 50 ul of PBS. Sensitizations were performed on Day 0, 7, and 14. Mice were harvested 24 hours post-challenge, and lung homogenates were digested to single cells using the following protocol:

Euthanize mice and harvest lungs into C Tubes containing 3 mL of complete RPMI on ice. Add 2 mLs of complete RPMI containing digestion solution (25 ul of Collagenase IA [0.5 mg/mL] and 100 ul of DNAse I [0.19 mg/mL] stocks) into the C Tubes. Run *m_lung_02.01* twice

Place tubes on a rocker at 37°C for 30 min. Use the tissue culture incubator and a rocker for constant agitation. Stop digestion by adding 5 μL of 0.5 M EDTA to each tube and mixing well. Transfer into 15 mL conicals through a 70 μm filter and centrifuge at 2,000RPM for 5 min at 4°C to pellet cells. Remove supernatant, resuspend lung homogenate in 1 mL of ACK lysis buffer, and let sit for 1 minute. Add 10 mLs of RPMI to stop the reaction. Centrifuge at 2,000RPM for 5 min at 4°C to pellet cells and remove

supernatant. Cells were restimulated on PMA/Ionomycin for 4 hours, then stained and analyzed for cytokine production and transcription factors by flow cytometry.

2.17 In vivo Vaccinia Viral Response

Spleens from pmel-1 Ly5.1 (B6.Cg-Thy-1a/Cy Tg [TcraTcrb] 8Rest/J) mice were used to generate a single cell suspension and treated with ACK buffer to lyse red blood cells. Splenocytes were stimulated in vitro with 1 μM human glycoprotein 100 nine-mer peptide ($hgp100_{25–33}$) and expanded in culture medium containing IL-2 for 7 days along with 1 μM CB839 or DMSO vehicle. Subsequently, one million $CD8^+$ cells from each condition were transferred by IV injection into recipient Ly5.2 C57BL/6 mice. Immediately following transfer, mice were infected with rhgp100 vaccinina virus (1×10^7 plaque-forming units (PFU)). At the indicated time points following transfer, recipient mouse blood or tissues were collected for analysis.

2.18 Immunization with 2W peptide

10-14 week old GLS WT and KO animals were injected with 10 μg 2W peptide (Genscript, Peptide EAWGALANWAVDSA) emulsified with Complete Freunds Adjuvant or PBS control and injected subcutaneously in the rear flank as previously described (Moon et al., 2007) and rested for 8 days. At day 8, inguinal lymph nodes and spleens were removed and isolated. MHCII-specific CD4 cells were isolated and purified with APC-conjugated tetramers (generously provided by Dr. Marc Jenkins laboratory,

Minneapolis, MN) using Miltenyi LS magnetic columns (Cat#: 130-042-401) and stained for extracellular and intracellular targets. Intracellular IFNγ was measured in a separate experiment on day 15 after immunization.

2.19 In vitro CAR T cell co-culture with target Eμ B ALL cells

T cells were isolated from wild type C57BL6 spleens using the Pan T Cell isolation kit (Cat#: 130-095-130) and were activated on anti-CD3 anti-CD28 coated plates with IL2 for four days with or without CB839. On days 1 and 2, T cells were transduced with retrovirus produced by Plat-E cells carrying the CAR 28-ζ construct targeting CD19 with GFP reporter. On day 4, CAR T cells were washed three times to remove any drug remnants and plated to equal concentrations on a 96 well plate at $5x10^5$ cells per well and serial dilutions thereof. $5x10^5$ Emu cells, a CD19+ B cell acute lymphoblastic leukemia cell line (Generously provided by Dr. Davila Lab) were then added to every well to assay cell numbers. CD19+ and GFP+ events were stained and counted by flow for each well after 72 hours.

2.20 In vivo CAR T cells

CAR T cells were produced as previously described (Li et al., 2017). Briefly, spleen T cells were isolated from wild-type B6, Thy1.1, or GLS KO mice at day 0. Cells were then activated with mouse CD3/CD28 Dynabeads and 30 IU/mL recombinant human IL2. At day 1 and 2, cells were spin transduced twice with retrovirus carrying

CARs. At day 3, cells were fed with fresh medium. At day 4, transduced T cells were harvested, beads removed, evaluated for viability, transduction efficiency, immune phenotype and ready for use. For CB839 treated CAR T cells, compound was added to the culture at day 1, 2 and 3. For in vivo study, C57B6 mice (n = 25) were i.p. injected with cyclophosphamide (CTX) at 300 mg/kg. Mice were i.v. injected with $3x10^5$ CAR T cells one day after CTX injection. Peripheral blood (PB) samples were collected after CAR T injection, stained with B cell and T cell antibodies and subjected to flow cytometry. CountBright beads were added to measure B and T cell numbers.

2.21 Colitis/IBD Induction

Colitis was induced by adoptive transfer of $0.4x10^6$ purified (>99% purity) CD4+CD25-CD45RBhi true naïve T cells i.p. in 200 ul of PBS. Spleen and lymph node suspensions were used first to purify CD4+ cells using magnetic bead cell separation with a StemCell Kit and these cells were stained with anti-CD4, anti-CD25 and anti-CD45RB for further flow sorting using a FACS Diva flow cytometer (Becton-Dickinson) with purities over 95% of the indicated populations. Mice that received adoptive transfers of different cell genotypes were always cohoused in the same cages to avoid differences due to microbiota composition divergence during colitis development. Mice were treated with the NSAID Piroxicam to induce gut damage and initiate disease and animals were weighed over time. Mice that reached humane endpoints and were

euthanized were maintained in the analysis at the final weight. At the end of the experiment, mesenteric lymph nodes were isolated and single cell suspensions were analyzed for cytokine production. To initiate IBD, you will i.p. inject naïve effector T cells (CD4+CD25-CD45RBhi) into C57BL/6 RAG1-/- recipients. Treg (CD4+CD25+CD45RBlo) can either by co-injected to prevent disease or injected later as a rescue when the mice start to lose weight. You can also use Thy1.1 Teff or Treg if want to look specifically at a certain population.

We typically get 3-5 million Teff and 0.2-0.4 million Treg after they are sorted so plan accordingly with mouse numbers.

IBD setup

Day of exp setup

1. Isolate CD4 T cells from each group using standard isolation protocol Also save ~1 mil splenocytes for comp controls for the sorter. Label the T cells with CD4 FITC, CD25 PE and CD45RB APC in the presence of Fc-Block (buy new fluor-abs and keep sterile for sorting) – 30 mins 4C in 1-2mL of 2% FBS/PBS + abs depending on the number of cells. Also divide splenocytes into 4 groups for comp controls: unstained, CD4-FITC, CD4-PE, and CD4-APC (ALL CD4, don't use CD25 PE/CD45rb APC)
    a. Sort naïve effector T cells (CD4+CD25-CD45RBhi)
    b. Recount the cells after the sort. Spin down the cells and resuspend in 1-2mL PBS and recount. Resuspend cells in appropriate amount of PBS. 400,000 Teff per 200ul injection or 200,000 Treg per 200ul injection per mouse.
2. Dose mice via i.p. injections.
3. Weigh the mice for their starting weight

2 weeks later:

Weigh the mice 3x per week until end of experiment.

Piroxicam treatment: piroxicam is very toxic to the mice so monitor carefully. Make sure to remove ALL traces of non-piroxicam food. Mice will begin to stop eating as the piroxicam makes them sick. Treat for 5 days if possible. If they are really not looking good and lost a lot of weight, err on the side of ~4 days.

2.22 Statistical Analysis

Statistical analyses were performed with Prism software version 7.01 (GraphPad Software, La Jolla California, USA, www.graphpad.com) using the student T-test, one-way ANOVA, or one-sample T-test. Longitudinal data was analyzed by two-way ANOVA followed by Tukey's test and followed up with one-way ANOVA or T-test at one specific time point as specified. Statistically significant results are indicated (* $p < 0.05$, ** $p < 0.01$, *** $p < 0.001$) and ns indicates select non-significant data. Error bars show mean ± Standard Deviation unless otherwise indicated. RNA-Seq data were analyzed by DESeq2 (Love et al., 2014) in R (Team, 2017).

2.23 DATA AND SOFTWARE AVAILABILITY

RNASeq data have been deposited in the GEO database under ID code GSE112244.

ATACSeq data have been deposited in the ArrayExpress database under ID code E-MTAB-6648.

3. Glutaminase promotes Th1- and CTL-effector function but inhibits Th17

3.1 Introduction

Stimulated T cells exit quiescence to proliferate and develop effector functions that are essential for immunity. To support the bioenergetic and biosynthetic demands of an immune response, antigen receptor signals and co-stimulation activate the Phosphatidtyl-inositide-3 kinase (PI3K)/Akt/mTORC1 signaling pathway to induce Myc and metabolic flux through glycolysis and mitochondrial oxidative phosphorylation (Ho et al., 2015; Sena et al., 2013). Elevated glycolysis and mitochondrial production of reactive oxygen species also promote T cell calcium signaling (Ho et al., 2015; Sena et al., 2013) and specific effector functions, including transcription and translation of Interferon-γ (IFNγ) (Cham and Gajewski, 2005; Chang et al., 2013; Jacobs et al., 2008; Peng et al., 2016) in activated Th1 CD4 T cells and CD8 T cells. Importantly, each T cell subset utilizes and requires a distinct metabolic program (Michalek et al., 2011; Nakaya et al., 2014). If activated T cells fail to induce appropriate metabolic pathways, effector function and ability to induce inflammatory disease *in vivo* are impaired (Lee et al., 2015; Macintyre et al., 2014; Yin et al., 2015). How specific metabolic programs establish and promote the function of T cell subsets remain poorly understood but may allow selective modulation of immunity in inflammation and cancer.

In addition to increased use of glucose in activated effector T cells, glutamine uptake and glutaminolysis are also upregulated (Carr et al., 2010; Wang et al., 2011). Glutamine is a conditionally-essential amino acid in rapidly-proliferating cells (Curthoys and Watford, 1995) and is a target in cancer treatment (Cheng, 2009; Cheng et al., 2011; Wise and Thompson, 2010). Activated T cells upregulate amino acid transporters (Sinclair et al., 2013) and multiple enzymes that metabolize glutamine (Nakaya et al., 2014; Wang et al., 2011). Deletion of the glutamine transporter, ASCT2, prevented both Th1 and Th17 effector responses (Nakaya et al., 2014). Inhibition of ASCT2 by small-molecule inhibitor V-9302 promoted CD8+ cell viability and activation (Schulte et al., 2018). Glutamine is initially hydrolyzed via the enzyme Glutaminase (GLS) (Wang et al., 2010) to produce glutamate. Glutamate is used in protein synthesis, to generate glutathione to regulate reactive oxygen species (ROS), and is exchanged to promote cystine uptake (Siska et al., 2016). Glutamate is further metabolized to α-ketoglutarate (α-KG), which provides anaplerotic support of the TCA cycle in growing cells (Yuan et al., 2014). α-KG is also a substrate for histone and DNA demethylases which regulate chromatin accessibility (Nakajima and Kunimoto, 2014).

In addition to effector T cell activation, glutamine metabolism has been implicated in the establishment of specific CD4 T cell subsets. Glutamine deprivation or deletion of ASCT2 were shown to promote Foxp3 expression, the transcription factor of

regulatory T cells (Treg) (Klysz et al., 2015; Nakaya et al., 2014). Inhibition or silencing of the Glutamic-oxaloacetate transaminase 1 (GOT1) enzyme that mediates conversion of glutamate to α-KG using oxaloacetate led to a shift in the balance of Th17 to Treg via methylation of the Foxp3 locus (Xu et al., 2017). Further, direct treatment of T cells with α-KG altered gene expression and chromatin methylation, in part through the CCCTC-binding factor (CTCF) (Chisolm et al., 2017). Glutamine metabolism thus provides multiple metabolites that mediate important effects on T cell epigenetics and differentiation.

Conversion of glutamine to glutamate by GLS may play a critical role in T cell function and fate. Although under investigation as a target to inhibit the metabolism of cancer cells (Cerione and Richard, 2010; DeBerardinis et al., 2008; Lobo et al., 2000), the role of GLS in T cells has been unclear. Here we show that unlike glutamine deprivation, GLS-deficiency did not affect Treg. It did, however, lead to increased ROS that impaired Th17 and reduced α-KG that promoted effector differentiation of Th1 and CD8 cytotoxic cells. These differential responses appear to be mediated by changes in chromatin accessibility and gene expression that sensitize Th1 cells to PI3K/Akt/mTOR signaling via IL-2. Importantly, GLS-deficiency suppressed Th17-mediated inflammatory diseases and led to increased *in vivo* effector differentiation of Th1 and CTL. Transient GLS inhibition, however, enhanced Th1 and CTL accumulation in viral and chimeric antigen

receptor (CAR) T cell studies. These results demonstrate a key role for GLS to both promote Th17 and suppress Th1 and CD8 CTL differentiation.

3.2 Results

3.2.1 GLS and Glutaminolysis Contribute to T Cell Metabolism Upon Activation

Activated T cells have significant metabolic requirements to support proliferation and differentiation. To determine the relative roles of glucose and glutamine in these processes, intracellular metabolites were measured following activation of CD4 T cells. In addition to increased pyruvate and lactate, glutamate and α-KG levels increased, suggesting elevated glutamine metabolism (Figure 3A). To determine the relative roles of glutaminolysis and glycolysis as fuels for mitochondrial metabolism, we measured oxygen consumption of stimulated T cells treated with mitochondrial pyruvate carrier (UK5099) or GLS (CB839) inhibitors. While neither UK5099 nor CB839 were sufficient to reduce T cell respiration alone, the combination led to a significant decrease in oxygen consumption (Figure 3B). These data demonstrate that stimulated T cells utilize glycolysis and GLS-dependent glutaminolysis. Intracellular glutamate is primarily generated from glutamine by GLS or from α-KG and aspartate by GOT1 and GOT2 and is converted to α-KG by Glutamate Dehydrogenase 1 (GLUD1), which are each expressed in CD4 and CD8 T cells (Figure 3C). The increased

levels of both α-KG, glutamate, and high relative ratio of glutamine to glutamate (Figure 3D), suggested GLS as a key source of glutamate and α-KG.

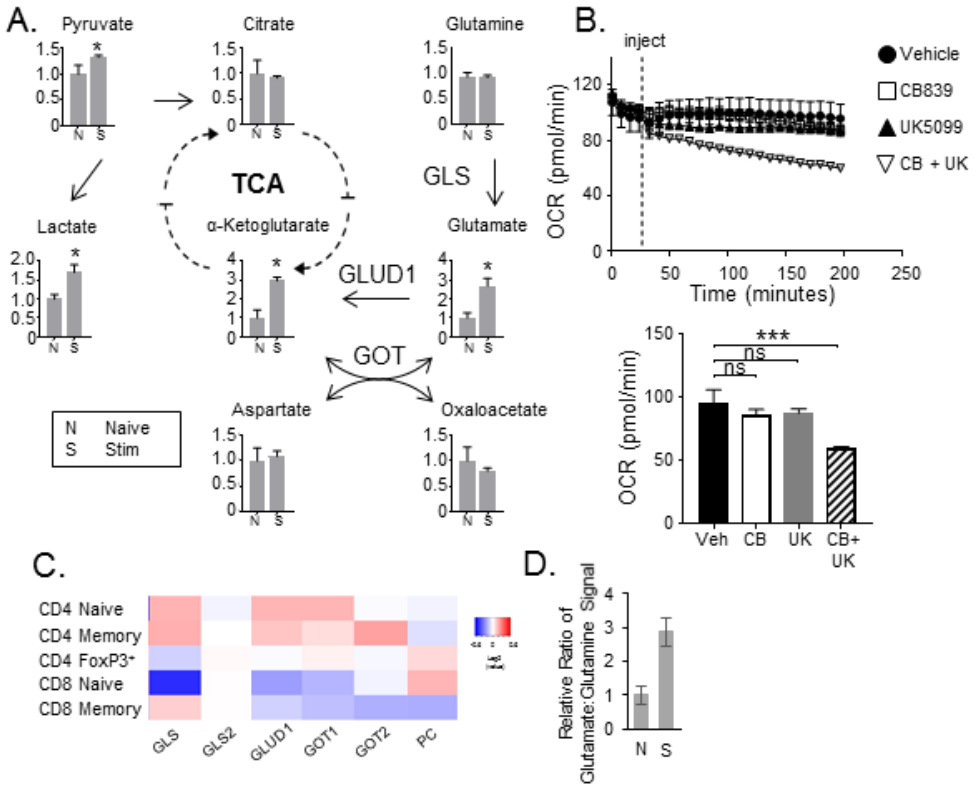

Figure 3: Activated T cells rely on glutaminolysis and glycolysis to fuel metabolism.

(A) Metabolites extracted for mass spectrometry and presented as fold change from naïve in T cells stimulated for 16 hours (S) or naïve (N) conditions. (B) Oxygen Consumption Rate (OCR) assayed from naïve CD4 cells from WT mice stimulated for 3 days on αCD3/CD28, injected with drug described (top). OCR at timepoint 200 min (bottom). (C) Relative expression of glutamine pathway genes, data from Immgen (immgen.org) (D) Relative ratio of glutamate:glutamine metabolite levels normalized to IL-7 (naïve, N) αCD3/CD28 (stimulated, S) normalized to naive in wild type CD4+ T cells.

To directly determine how inhibition of GLS affects glucose metabolism, CD4 T cells were stimulated in uniformly labeled ^{13}C-glucose with or without CB839 and

glucose derived carbons were traced. As expected, inhibition of GLS led to increased intracellular glutamine and decreased glutamate (Figure 4A). Aspartate levels also decreased significantly. Glucose-derived ^{13}C was increased in both glutamate and aspartate, indicating a greater fraction of glucose contribution to synthesis of these amino acids. Serine and alanine overall abundance also decreased, while glycine was unchanged and each showed a decreased portion derived from glucose (Figure 4B). Overall levels of TCA intermediates were also reduced, yet with increased fractional labeling from glucose-derived ^{13}C (Figure 5A). Glycolytic intermediates were more abundant upon GLS-inhibition, suggesting elevated glycolysis (Figure 5B). However, lactate levels and ^{13}C-labeling were unchanged and pyruvate levels decreased (Figure 5C). Anabolic pathways were also affected, and total levels of the nucleotide precursor N-carbamoyl-aspartate decreased (Figure 5D). Thus, glucose metabolism increased and a greater fraction of glucose carbon entered the TCA cycle when GLS was impaired.

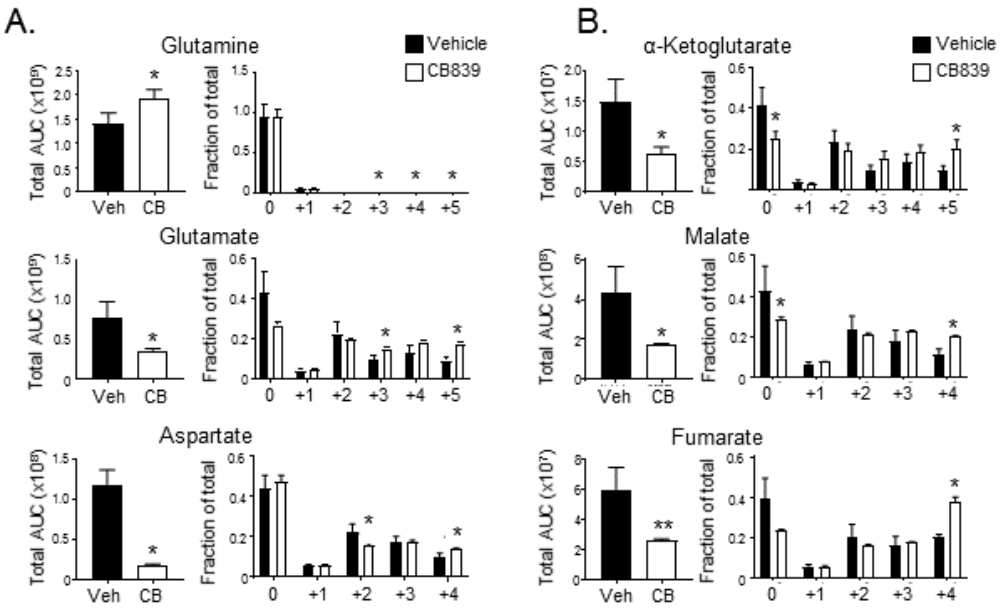

Figure 4: GLS inhibition by CB839 reduces intracellular glutamate and downstream TCA cycle intermediates

(A and B) Abundance of metabolites (left, ** $p < 0.01$, unpaired t-test) and fractional labeling (right) of stimulated CD4+ T cells in the presence of CB839 and 13C-glucose for glutaminolytic intermediates (A) and TCA intermediates (B). Means +/- Std dev, (total abundance, left, *** $p<0.001$, student's t test; fractional labeling, right, *** $p < 0.001$, one way ANOVA).

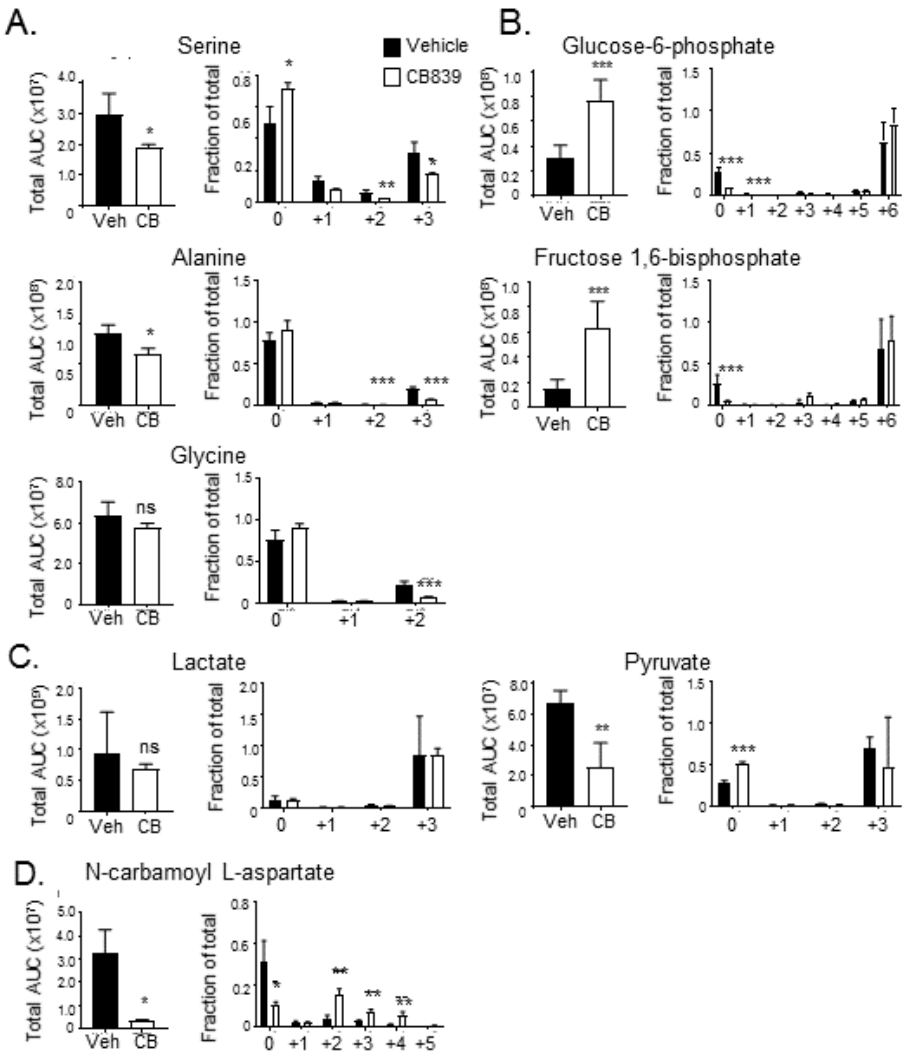

Figure 5: GLS inhibition by CB839 reduces some intracellular amino acids, promotes glycolytic intermediates.

(A-D) Additional intracellular metabolite abundance (left) and fraction labeled from 13C-glucose (right). (A) Amino acids Serine, alanine, and glycine. (B) Glycolytic intermediates G6P, F16BP. (C) Lactate and Pyruvate. (D) Nucleotide precursor N-carbamoyl L-aspartate (average of n = 3 replicates/group). Means +/- Std dev, (total abundance, left, *** $p<0.001$, student's t test; fractional labeling, right, *** $p < 0.001$, one way ANOVA).

3.2.2 CD4 T Cell Subsets Have Distinct Programs of Glutamine Metabolism

Distinct cytokines lead activated T cells to induce specific metabolic programs. Th1, Th17, and Treg cells (Gerriets et al., 2015) were examined to assess if CD4 T cell subsets had different patterns and reliance on glutamine metabolism. T cells activated and differentiated into each subset showed increased glutamate and α-KG levels relative to naïve T cells. This was most pronounced in Th17 cells (Figure 6A), which also had the highest relative ratio of glutamate to glutamine (Figure 6B). To test the role of glutamine and GLS in Th1, Th17, and Treg T cell subsets, CD4 T cells were differentiated with or without glutamine, or with GLS inhibitor.

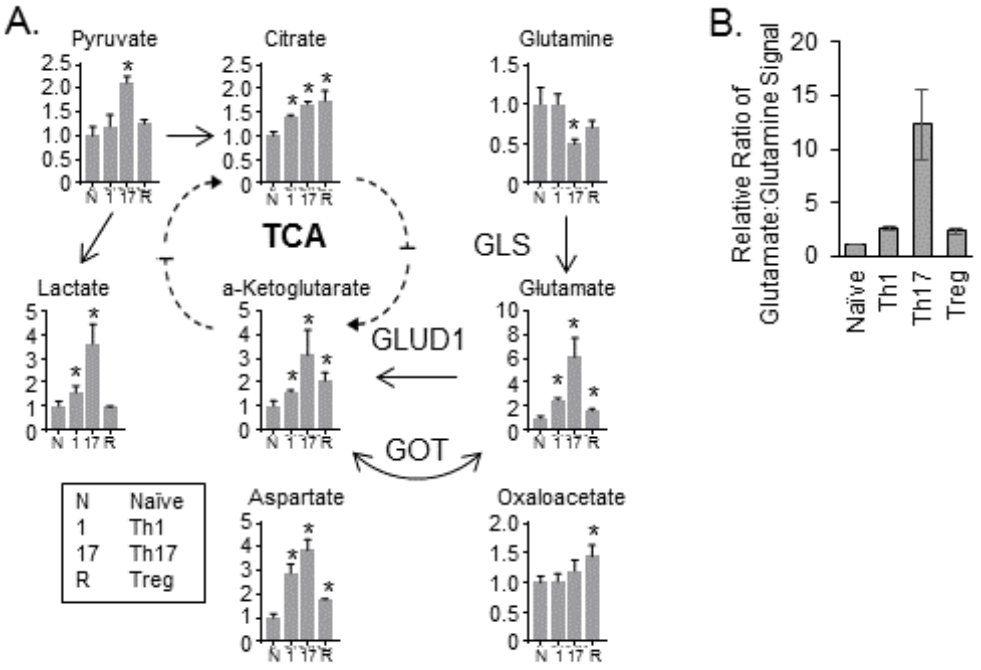

Figure 6: Th1 and Th17 cells differ in their use of glutaminolysis and glutamine deficiency is distinct from GLS inhibition.

(A) Metabolite fold change from naïve in wild type CD4+ cells maintained in IL-7 (N), or differentiated for 5 days into Th1 (1), Th17 (17), or Treg (R) cells (* $p < 0.05$, one-way ANOVA). (B) Relative ratio of intracellular metabolites glutamate:glutamine from CD4+ T cells in Th1, Th17, and Treg skewing conditions normalized to naïve (average n = 3 replicates/group).

Both Th1 and Th17 required glutamine, as glutamine-deficient media markedly reduced Th1 production of IFNγ and Th17 production of IL-17, yet GLS-inhibition decreased cytokine production and proliferation only from Th17 cells and appeared to increase Th1 cytokine secretion (Figure 7A). Glutamine deficiency reduced proliferation

at day three and five in both Th1 and Th17 cells. GLS-inhibition impaired proliferation of both Th1 and Th17 cells after three days in culture (Figure 7B, C). Importantly, however, CB839-treated Th1 cells partially recovered proliferation by day five. Glutamine deprivation also induced Treg even under Th1 and Th17 conditions, yet GLS inhibition failed to do so (Figure 7D). GLS-deficiency, therefore, has distinct effects on T cell subsets from glutamine deprivation.

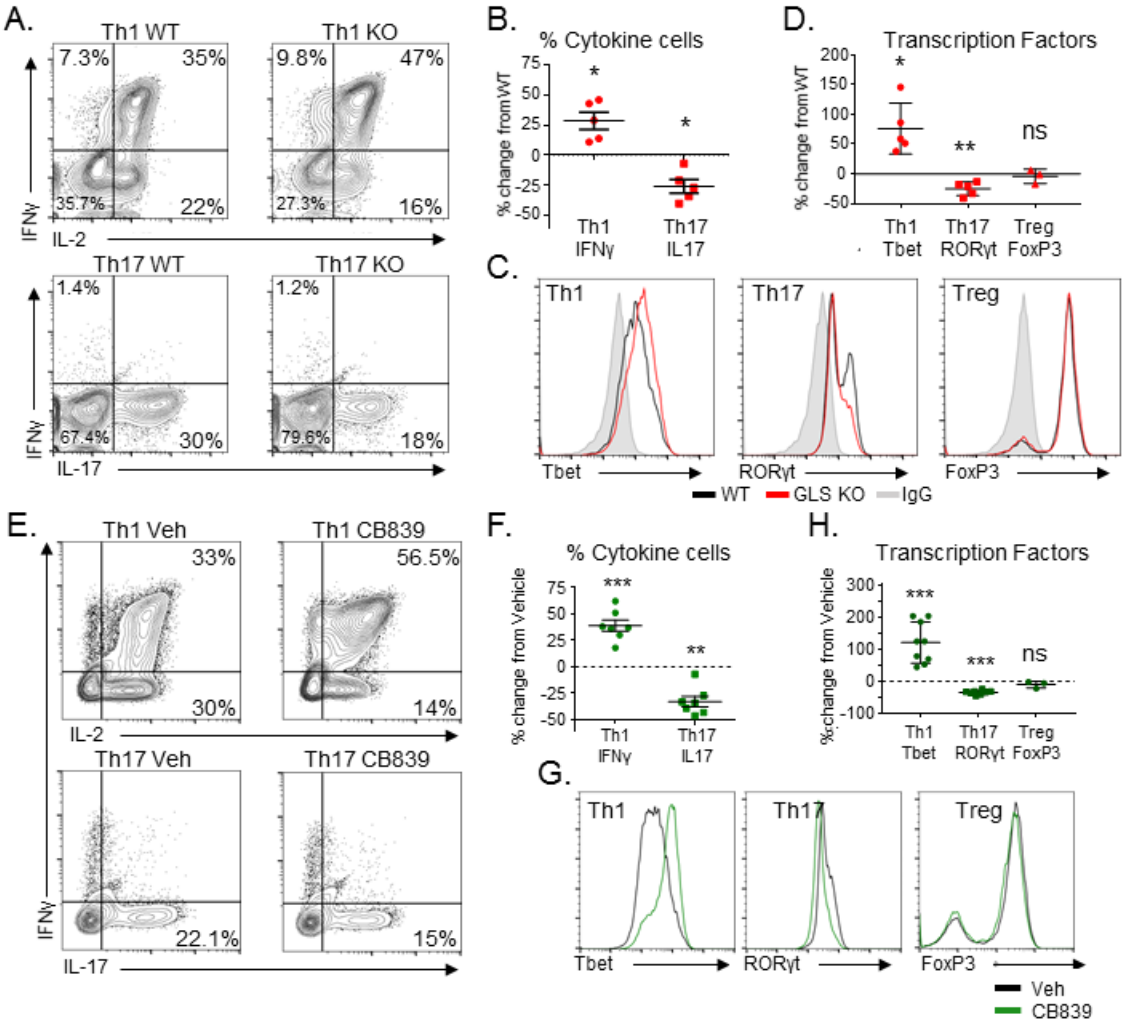

Figure 7: Glutamine and the role of GLS in Th1 and Th17 cell metabolism

(A) Cytokine production from Th1 (top) and Th17 (bottom) differentiated T cells in the presence of glutamine (left), absence of glutamine (middle), or presence of GLS1 inhibitor CB839 (right) (representative of n = 3 replicates). (B) Proliferation of Cell Trace Violet (CTV) labeled T cells stimulated and differentiated in Th1 or Th17 conditions with (black lines) or without (red lines) glutamine after 3 and 5 days of culture. (C) Same as in (B), but with vehicle (black lines) or CB839 (green lines) (representative of n = 3 replicates). (D) Foxp3 expression in CD4 T cells activated in Th1 or Th17 skewing conditions in glutamine deficient (red, left) conditions or in the presence of CB839 (green, right).

Several enzymes contribute to regulation of glutaminolysis in T cells. Th17 cells had greater expression of GLS protein than Th1 at protein and RNA levels (Figure 8A, B). Th1 and Th17 cells expressed low levels of *Gls2* mRNA and expressed similar levels of other glutamine and anaplerotic metabolic enzymes (Figures 8C and 8D). Th1 and Th17 cells had distinct metabolic profiles and intracellular metabolites shifted in both Th1 and Th17 cells upon GLS-inhibition, including alanine, aspartate, and glutamate metabolism pathways (Figure 8E and Table 1). Nutrient uptake and secretion also differed between Th1 and Th17 cells and were modified by GLS inhibition. Glutamine uptake and glutamate, pyruvate, and lactate secretion were higher in Th17 but reduced upon GLS inhibition (Figure 9A). GLS may contribute to cellular redox regulation through generation of glutamate for glutathione synthesis and ROS increased in both Th1 and Th17 cells when treated with CB839 (Figure 9B).

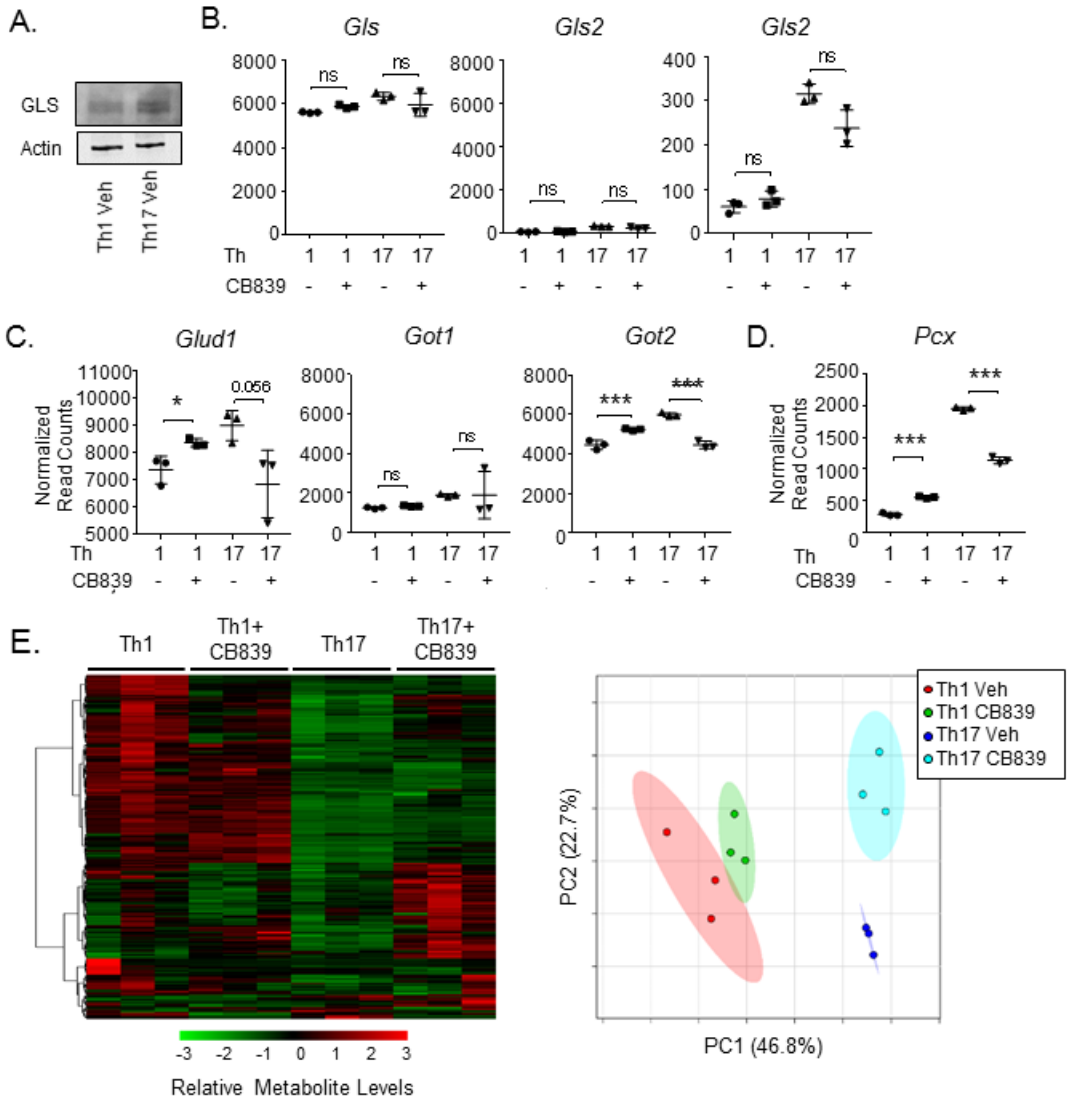

Figure 8: Expression of GLS and glutaminolysis enzymes varies by T cell subset and with CB839 treatment.

(A) Immunoblot of GLS protein (top) and actin control (bottom) in T cells after five days in Th1 and Th17 skewing conditions. (B-D) Normalized counts of message from RNA-Seq. (B) Gls RNA expression from RNA-Seq from Figure 2D. Gls2 expression from RNA-Seq from Figure 2D on the same scale as Gls expression (left) and in smaller scale (right). For all RNA-Seq expression data, P values are determined from RNA-Seq analysis, all groups run in triplicate. (C) Glud1, Got1, and Got2 expression as in (B). (D) Pcx RNA

expression as in (B) (All p values from defSeq2 program, n = 3 replicates/group). (E) Heat map (left) and principle component analysis (right) of metabolites from Th1 and Th17 cells with or without CB839 (n = 3 replicates/group).

Table 1: Metabolic pathways altered following CB839 treatment

Th1 Pathway	Total	Hits	Raw p	Hits Discovered
Alanine, aspartate and glutamate metabolism	24	8	5.34E-08	Fumaric acid; Pyruvic acid; Ureidosuccinic acid; L-Aspartic Acid; Arginosuccinic acid; L-glutamic acid; L-glutamine; Oxoglutaric acid
Citrate cycle (TCA cycle)	20	5	0.0001074	Oxoglutaric acid; L-malic acid; Pyruvic Acid; Fumaric acid; Phosphoenolpyruvate
D-Glutamine and D-glutamate metabolism	5	3	0.00015834	L-Glutamic acid; L-glutamine; oxoglutaric acid
Pyrimidine metabolism	41	6	0.00048197	L-Glutamine; 4,5-Dihydroorotic acid; Dihydrouracil; Cytidine monophosphate; Cytidine; Ureidosuccinic acid
Arginine and proline metabolism	44	6	0.00071444	L-Glutamine; L-Aspartic acid; Argininosuccinic acid; L-Glutamic acid; L-4-Hydroxyglutamate semialdehyde; Fumaric acid
Histidine metabolism	15	3	0.0060105	L-Glutamic acid; Methylimidazoleacetic acid; L-Aspartic acid
Butanoate metabolism	22	3	0.017935	Oxoglutaric acid; Pyruvic acid; 2-Hydroxyglutarate
Pyruvate metabolism	23	3	0.020258	Phosphoenolpyruvic acid; Pyruvic acid; L-Malic acid;
Nitrogen metabolism	9	2	0.021285	L-Glutamic acid; L-Glutamine;
Cysteine and methionine metabolism	27	3	0.031146	5'-Methylthioadenosine; 2-Aminoacrylic acid; Pyruvic acid;

Th17 Pathway	Total	Hits	Raw p	Hits Discovered
Pentose phosphate pathway	19	5	0.00433	Deoxyribose 5-phosphate; D-Ribulose 5-phosphate; Sedoheptulose 7-phosphate; 6-Phosphogluconic acid; D-Erythrose 4-phosphate
Alanine, aspartate and glutamate metabolism	24	5	0.01245	Argininosuccinic acid; L-Alanine; Ureidosuccinic acid; Succinic acid; Glucosamine 6-phosphate
Phenylalanine, tyrosine and tryptophan biosynthesis	4	2	0.02017	L-Phenylalanine; L-Tyrosine
Purine metabolism	68	8	0.04882	Xanthine; D-Ribulose 5-phosphate; ADP; Deoxyinosine; Hypoxanthine; Guanosine triphosphate; Guanosine; Adenosine diphosphate ribose

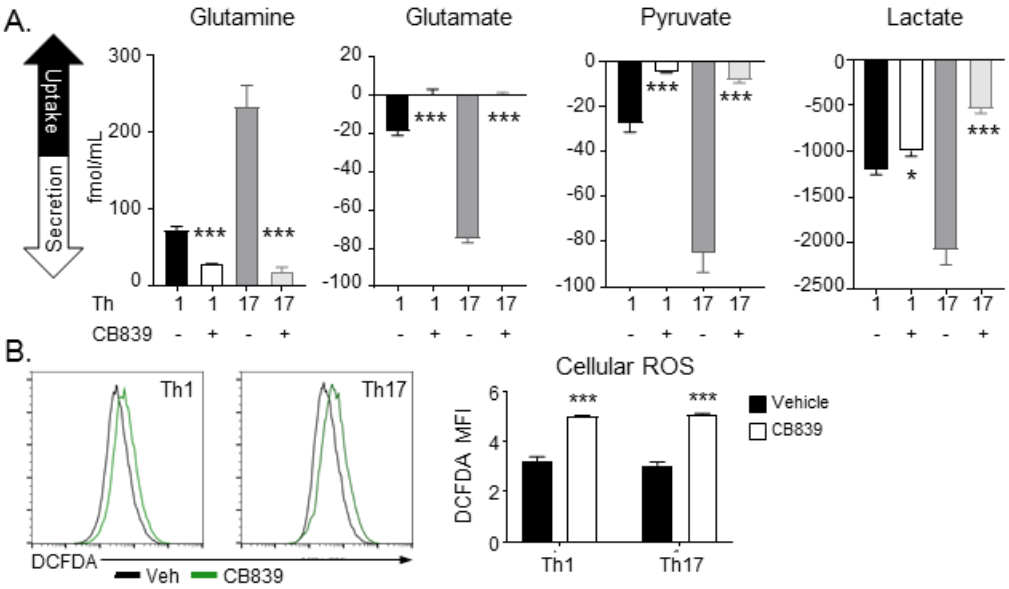

Figure 9: CB839 modifies amino acid, metabolite uptake, and ROS levels in Th1 and Th17 cells.

(A) Uptake (positive numbers) and secretion (negative numbers) of metabolites in CB839 treated wild type CD4+ T cells in Th1 and Th17 skewing conditions as measured by Nuclear Magnetic Resonance (NMR) (average of 3 replicates, *** P<0.001, unpaired t-test). (B) Fluorescence of DCFDA dye by flow cytometry, representative histograms (left) and average of n = 3 replicates (right, *** p < 0.001, student's t-test) of vehicle or CB839-treated T cells in Th1 and Th17 skewing conditions.

3.2.3 GLS-Deficiency has Little Effect on Resting T Cells But Modulates Activation

A GLS$^{fl/fl}$ model was generated and crossed o CD4-Cre to specifically delete GLS late in T cell thymic development to test the role of GLS in T cells. Although GLS$^{fl/fl}$CD4-Cre T cells efficiently deleted *Gls* compared to control GLS$^{fl/fl}$ T cells (Figure 10A),

lymphocyte frequencies and numbers were unaltered (Figure 10B). Treg cells have been previously shown to be increased by ASCT2 or GOT1 deficiency (Nakaya et al., 2014; Xu et al., 2017), but were unchanged with GLS-deficiency. Resting $GLS^{fl/fl}$CD4-Cre^{+} CD4 T cells also had normal cell size and phenotype (Figure 10C).

GLS-deficiency did, however, impact T cell activation. Measurement of immediate lactate secretion showed that acute GLS inhibition did not impair immediate events in T cell activation to rapidly induce glycolysis (Figure 10D). However, *in vitro* stimulated GLS-deficient T cells failed to efficiently undergo blastogenesis and increase in cell size in the first two days (Figure 10E). In addition, *in vitro* accumulation of viable stimulated T cells was reduced by GLS-deficiency (Figure 10F). GLS-deficient CD4 T cells had reduced induction of CD25 and CD44, and downregulation of CD62L (Figure 10G) at 48 hours.. By day five of stimulation in IL2 (Th0 conditions), however, GLS-deficient CD4 T cells had adapted and activation markers were similar to control (Figure 10H).

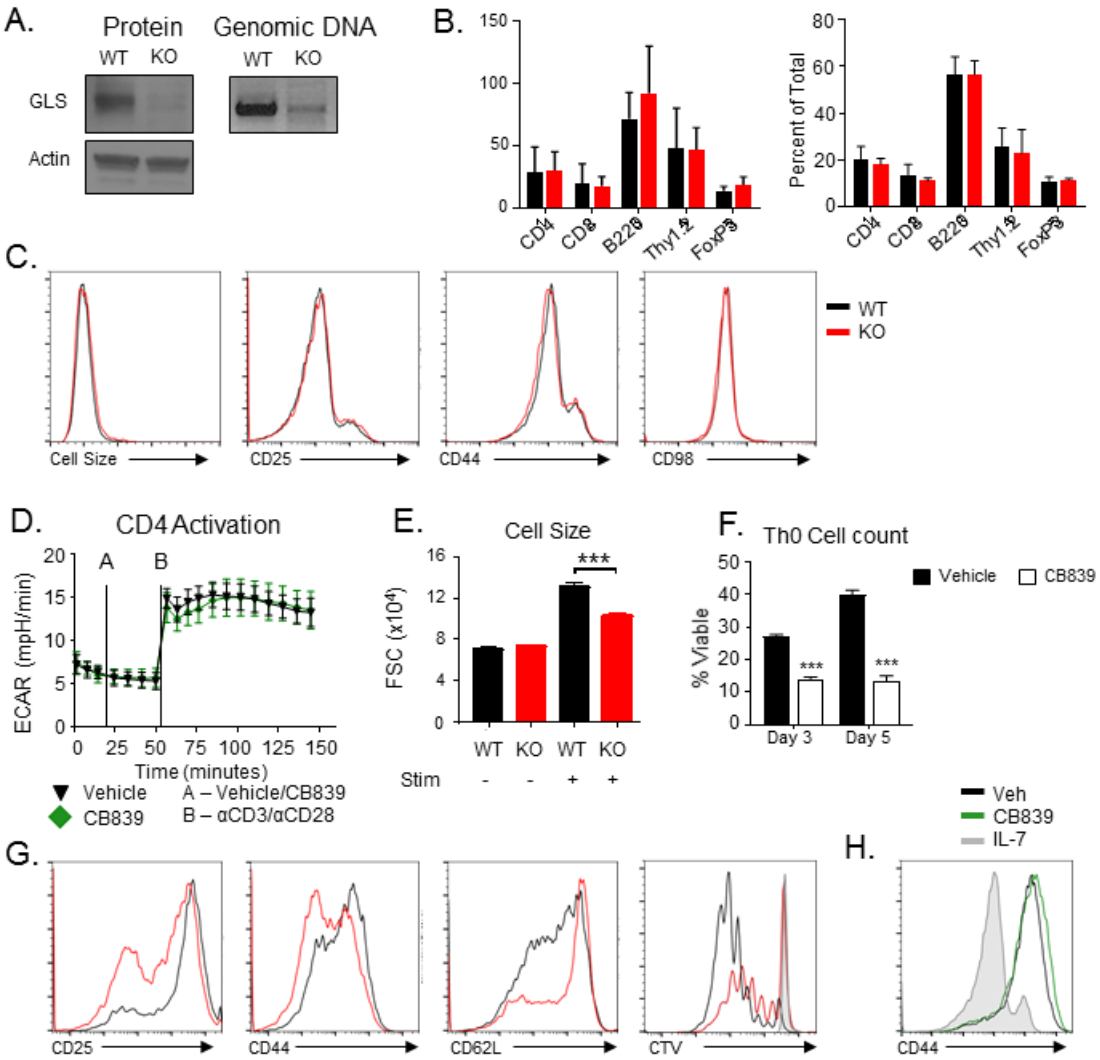

Figure 10: GLS is dispensable for maintenance but required for T cell short-term activation.

(A) Immunoblot (left) and genomic DNA (right) in isolated Pan T cells (CD4+ and CD8+) from GLSfl/fl CRE+ (GLS KO) and littermate wild type controls (WT). (B) Cell counts (left) and percent of total splenocytes (right) from WT and GLS KO animals. No significance vs wild type, one-way ANOVA. (C) Flow cytometry analysis of T cell activation markers and cell size of CD4+ T cells freshly isolated from WT and GLS KO T spleens. (D) Extracellular Acidification Rate (ECAR) of naïve CD4+ T cells treated with vehicle or CB839 as measured by Seahorse (n = 4 replicates/group). (E) Average MFI of

forward scatter (FSC) in activated CD8+ WT and GLS KO T cells (*** $p < 0.001$, student's t test, replicates of n = 3/group). (F) Viability by propidium iodide staining at day 3 and day 5 of WT T cells in activation condition with no cytokines (*** $p < 0.001$, student's t test, average of n = 3 replicates). (G) Activation markers and proliferation of WT and GLS KO CD4+ T cells activated on αCD3/CD28 over 48 hours. (H) Flow cytometry analysis of CD44 in CB839- or vehicle-treated T cells activated on αCD3/CD28 at day five.

Delayed activation marker expression and proliferation of GLS-deficient T cells suggested impaired function and differentiation. Surprisingly, a greater frequency of GLS$^{fl/fl}$CD4-Cre^{+} T cells produced IFNγ after five days in Th0 conditions than did control T cells (Figure 11A, B). In addition, GLS-deficient cells that expressed IFNγ did so to a higher level than IFNγ-producing control T cells. IFNγ expression is regulated in part by the transcription factor, Tbet, and Tbet levels were elevated in activated GLS$^{fl/fl}$CD4-Cre^{+} Th0 T cells (Figure 11C). Similarly, inhibition of GLS with CB839 also led to greater expression of IFNγ and Tbet (Figures 11D-F).

The ability of T cells to adapt to GLS-deficiency and display enhanced function *in vitro* suggested *in vivo* responses may be altered. Control and GLS$^{fl/fl}$CD4-Cre mice were immunized, therefore, with 2W peptide to measure proliferation and IFNγ secretion. At eight days after immunization, 2W-MHC tetramer positive CD4 T cells proliferated similarly regardless of GLS expression (Figure 12A, B). At day fifteen, IFNγ levels, however, were increased in GLS-deficient 2W-MHC tetramer positive T cells (Figure 12C). In contrast, proliferation to weaker homeostatic cues was reduced for GLS$^{fl/fl}$CD4-

Cre T cells in both spleen and lymph node compared to wild type T cells five days after transfer to recipient RAG1$^{-/-}$ mice (Figure 12D).

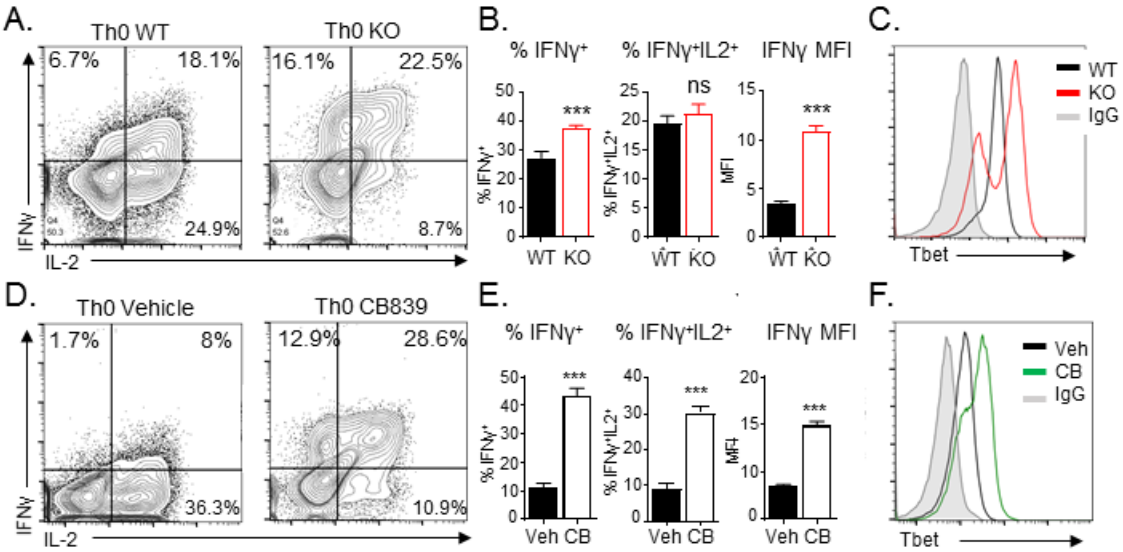

Figure 11: GLS inhibition enhances Th1 effector cell differentiation and cytokine production.

(A-F) Naïve CD4+ T cells activated without cytokines over three days, split with IL-2, then stimulated to measure cytokines on day five. (A) Cytokine production of wild type and GLS KO T cells. (B) Average percent total IFNγ+ producers (left), percent double positive IFNγ+IL2+ producers (middle), and the median fluorescence intensity (MFI) (right) of all IFNγ+ cells in (A) (unpaired t-test). (C) Tbet protein expression in WT, GLS KO, and isotype control T cells. Representative of n = 2 experiments. (D-F) Same as in (A-C), except with GLS inhibitor CB839 and vehicle.

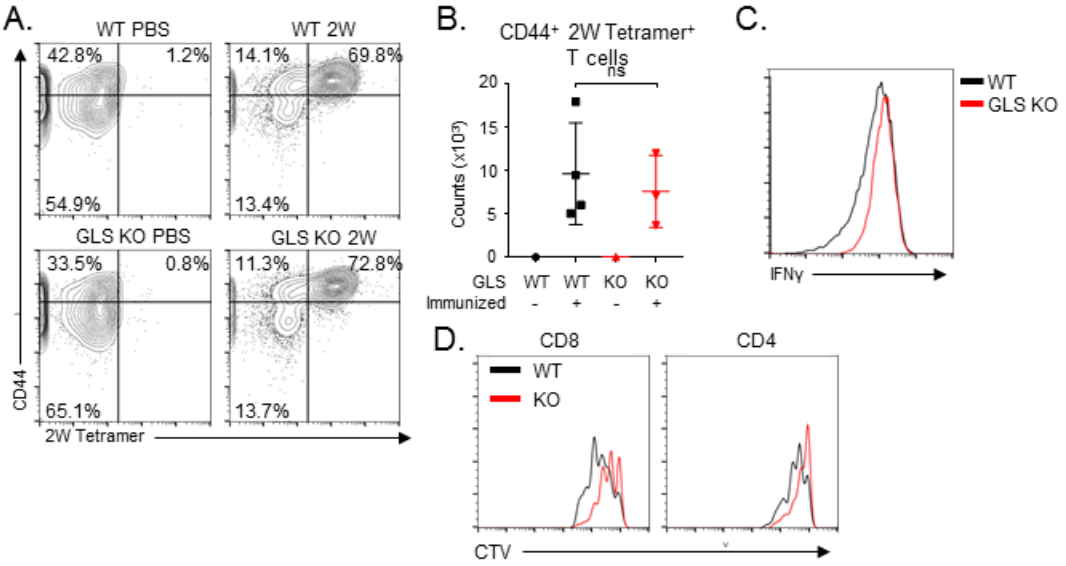

Figure 12: GLS deficient T cells *in vivo* have increased IFNγ and reduced proliferation.

(A-C) 2W peptide immunization of WT and GLS KO. (A) Percent 2W-MHC II tetramer+ and CD44+ T cells by flow cytometry in both spleen and inguinal lymph nodes eight days after immunization with 2W antigen + CFA (right) or PBS control (left) in WT and GLS KO animals. (B) Average count of CD44+ Tetramer+ T cells as in (A) ($p > 0.05$, student's t-test). (C) IFNγ protein expression by flow from CD44+ MHC II tetramer+ T cells isolated from WT and GLS KO spleen and lymph nodes. (D) Homeostatic proliferation of WT and GLS KO CD4/CD8+ T cells stained with cell trace violet (CTV) and injected into RAG1 KO recipient mice after five days (representative of n = 5 replicates/group).

Because cytotoxic CD8 T cells are also driven by Tbet (Knox et al., 2014), the dependence of CD8 T cells on GLS was assessed. Similar to CD4 cells, *in vitro* stimulated $GLS^{fl/fl}$CD4-Cre^{+} CD8 T cells survived and accumulated less efficiently than control T cells (Figure 13A). Importantly, $GLS^{fl/fl}$CD4-Cre^{+} CD8 T cells had increased expression of the effector protein Granzyme B (Figure 13B) and Tbet (Figure 13C). Acute inhibition of

GLS with CB839 led to increased Granzyme B and Perforin after five days stimulation (Figure 13D, E). In addition to increased effector proteins, CB839-treated CD8 T cells expressed increased levels of Tbet and Eomes and markers of proliferation (Figure 13F-H). However, GLS-inhibition also increased the portion of CD8 T cells that expressed the inhibitory receptors Lag3 and PD-1 (Figure 13I). GLS-deficiency thus can impair initial activation and proliferation of CD4 and CD8 cells, while promoting Th1-like and CTL effector programs that may ultimately sensitize to inhibition.

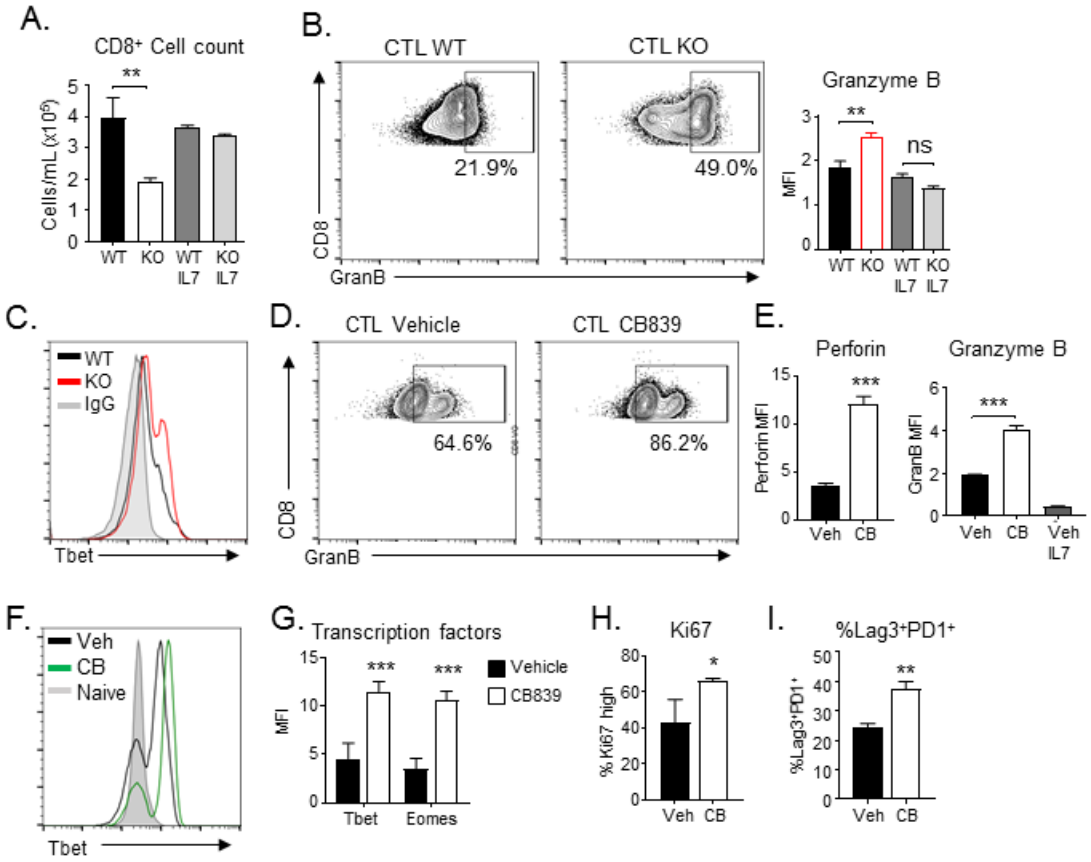

Figure 13: GLS inhibition promotes CD8+ effector differentiation and cytokine production while also inducing markers of T cell exhaustion.

(A) Cell counts of CD8+ T cells from WT and GLS KO animals activated on αCD3/CD28+IL2 for five days (** $p < 0.01$, student's t-test). (B and C) CD8+ T cells from WT or GLS KO animals activated on αCD3/CD28 + IL2 for five days. (B) Expression of CD8+ granzyme B protein at day 5, left, and average of granzyme B MFI signal, right (student's t test, n = 3 replicates/group). (C) Tbet protein expression in WT, GLS KO, and isotype control (representative of n = 2 experiments). (D-I) CD8+ T cells activated αCD3/CD28+IL2 for five days in the presence of CB839 or vehicle. (D) Representative FACs plots of granzyme B producing cells, (E) Perforin MFI (left) or granzyme B MFI (right) (*** $p < 0.001$, student's t-test). (F) Representative Tbet expression, (G) Average transcription factor expression (*** $p < 0.001$, student's t-test, n = 3 replicates), (H) Ki67 expression, (I) Percent LAG3+ and PD1+ T cells as in (I). (* $p < 0.01$, ** $p < 0.01$, student's t test, average of n = 3 replicates,).

-

3.2.4 GLS Plays Differential Roles in CD4 T Cell Effector Subsets

Given the differences in glutamine metabolism between Th1 and Th17 cells and spontaneous Th1-like differentiation with IL2 in Th0 conditions, we directly tested if GLS-deficiency differentially affected T cell subset specification and function. Control and GLS$^{fl/fl}$CD4-Cre^{+} or CB839-treated CD4 T cells were differentiated *in vitro* into Th1 and Th17 subsets. Similar to Th0 cells, a greater percentage of GLS$^{fl/fl}$CD4-Cre^{+} T cells expressed IFNγ when in Th1 skewing conditions (Figure 14A, B). Conversely, a decreased percentage of GLS-deficient T cells expressed IL17A when in Th17 skewing conditions. Expression of effector molecules and differentiation in Th1, Th17, and Treg are regulated by Tbet, RORγt, and FoxP3, respectively, and GLS-deficient T cells showed increased Tbet under Th1 conditions and decreased RORγt under Th17 conditions (Figure 14C, D). In contrast, FoxP3 expression was unchanged in the absence of GLS. Similar results were obtained when GLS was acutely inhibited using CB839, as Th1, Th17, and Treg cytokine production and differentiation were increased, decreased, or unchanged, respectively (Figure 14E-H).

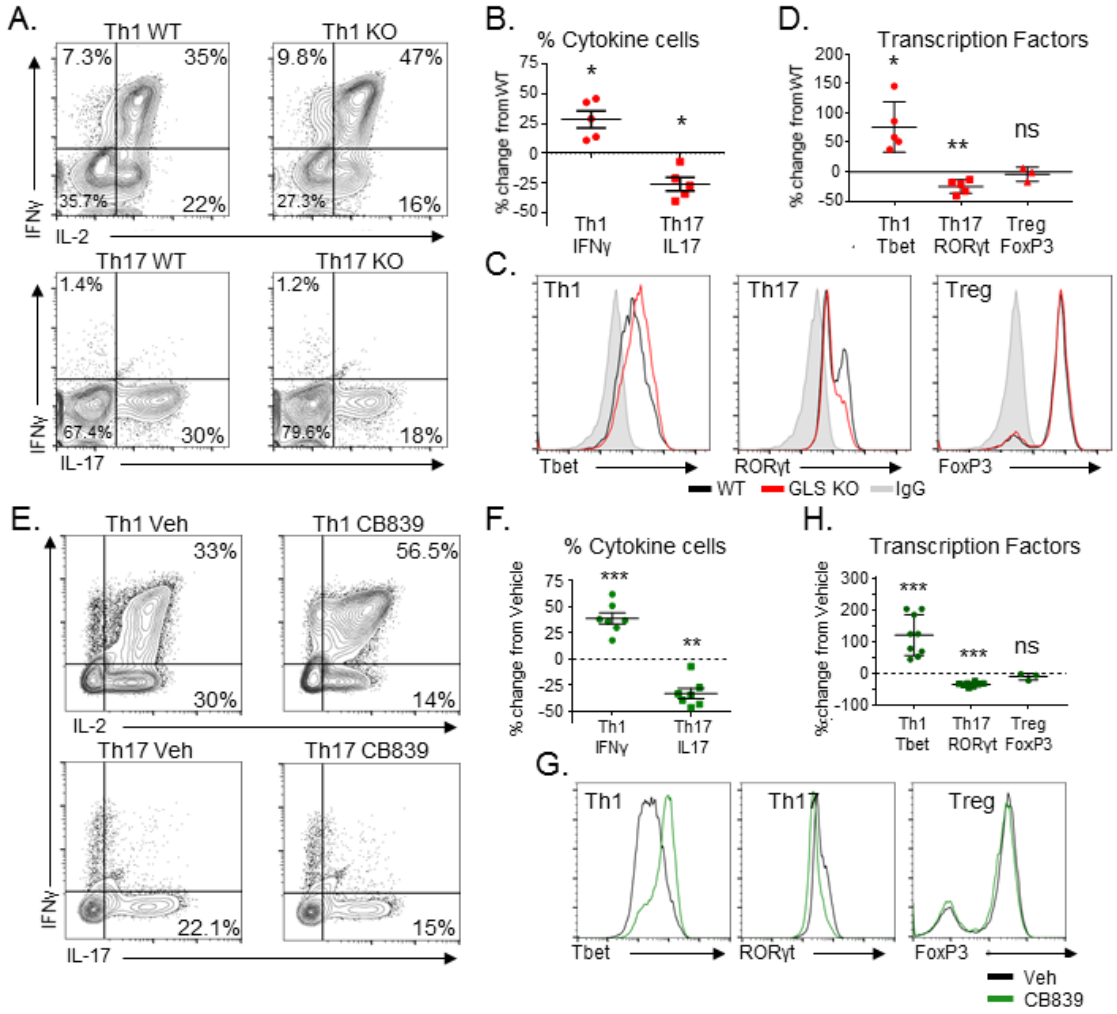

Figure 14: GLS specifies Th1 and Th17 differentiation and metabolism

(A-D) Naïve CD4+ T cells from WT and GLS KO T cells differentiated in Th1, Th17, or Treg skewing media over five days. (A) IFNγ and IL2 production in Th1 skewing conditions (top) and IL-17 production in Th17 skewing conditions (bottom). (B) Average percent change cytokine producers in Th1 and Th17 cells from WT (paired t-test). (C) Transcription factor expression of Th1, Th17, and Treg cells in WT (black) and GLS KO (red). (D) Average percent change from WT of transcription factors (one-sample t test) in GLS KO T cells. (E-H) Naïve CD4+ T cells from WT differentiated in Th1, Th17, or Treg skewing media over five days in the presence of CB839 or vehicle as in Figure 4A. (E) IFNγ and IL2 production in Th1 skewing conditions (top) and IL-17 production in Th17 skewing conditions (bottom) (representative of n = 3 replicates/group). (F) Percent

change cytokine producers in Th1 and Th17 cells from vehicle (Th1, Th17 n = 9 experiments, *** $p < 0.001$, student T test,). (G) Transcription factor expression in wild type cells treated with Vehicle or CB839 (Tbet and RORγt, n = 9 experiments, Foxp3 n = 3 experiments). (H) Average percent change from WT of transcription factor expression (Th1, Th17 n = 7 experiments, Treg n = 3 experiments, *** $p < 0.001$, one-sample T test).

GLS-deficiency promoted Th1 and suppressed Th17 differentiation and may affect plasticity and terminal fates. However, GLS-deficient T cells stimulated in Th17 conditions that failed to express RORγt and IL17 did not significantly elevate IFNγ or FoxP3 (Figure 7A, 7D, Figure 14E). In contrast, GLS-deficient T cells stimulated in Th1 conditions showed evidence of excessive effector differentiation as the proportion of multi-functional Th1 cells (Figure 15A) as well as expression of KLRG1 and inhibitory receptors, PD-1, Tim3, and Lag3 were elevated (Figure 15B-D).

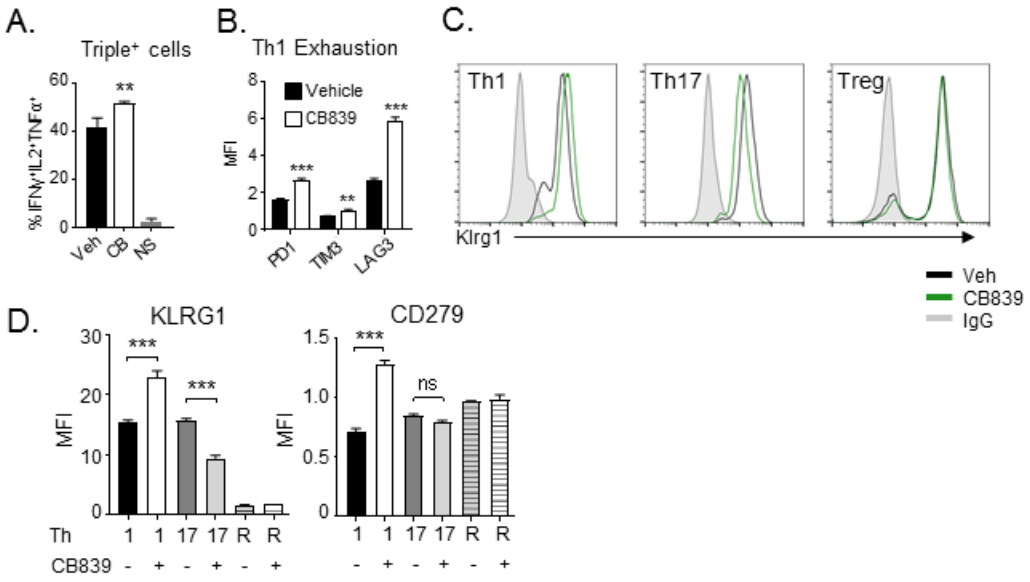

Figure 15: GLS inhibition promotes effector responses but also induces markers of exhaustion in Th1 cells.

(A-D) WT $CD4^+$ T cells differentiated in Th1 or Th17 conditions in the presence of vehicle or CB839 over five days. (A) Percent of Th1 cells producing IFNγ, IL2, and TNFα at day 5 (unpaired student T test, NS = no stim). (B) Median Fluorescence Intensity of inhibitory receptors (two-way ANOVA). (C) Representative Klrg1 protein expression and (D) average Klrg1 and CD279 expression (*** $p < 0.001$, student's t-test).

We next assessed how GLS inhibition affected Th1 and Th17 metabolism and differentiation over time. Steady state levels of glutamine rapidly increased while glutamate and aspartate rapidly decreased in both Th1 and Th17 cells upon GLS inhibition (Figure 16A). While levels of these metabolites partially recovered in GLS inhibitor-treated Th1 cells starting on day three, they remained low in treated Th17 cells. Likewise, oxidized glutathione (GSSG) recovered in Th1 but remained low in Th17. Similar trends of initial decrease followed by recovery in Th1 cells were observed in glycolytic and TCA cycle intermediates (Figure 16B, C). Consistent with impaired early metabolism, flux measurements showed glucose uptake was reduced in both Th1 and Th17 cells on day three (Figure 16D). By day five, however, Th1 cells had increased levels of glucose uptake and glycolytic flux relative to controls while Th17 remained impaired by GLS inhibition (Figures 16E).

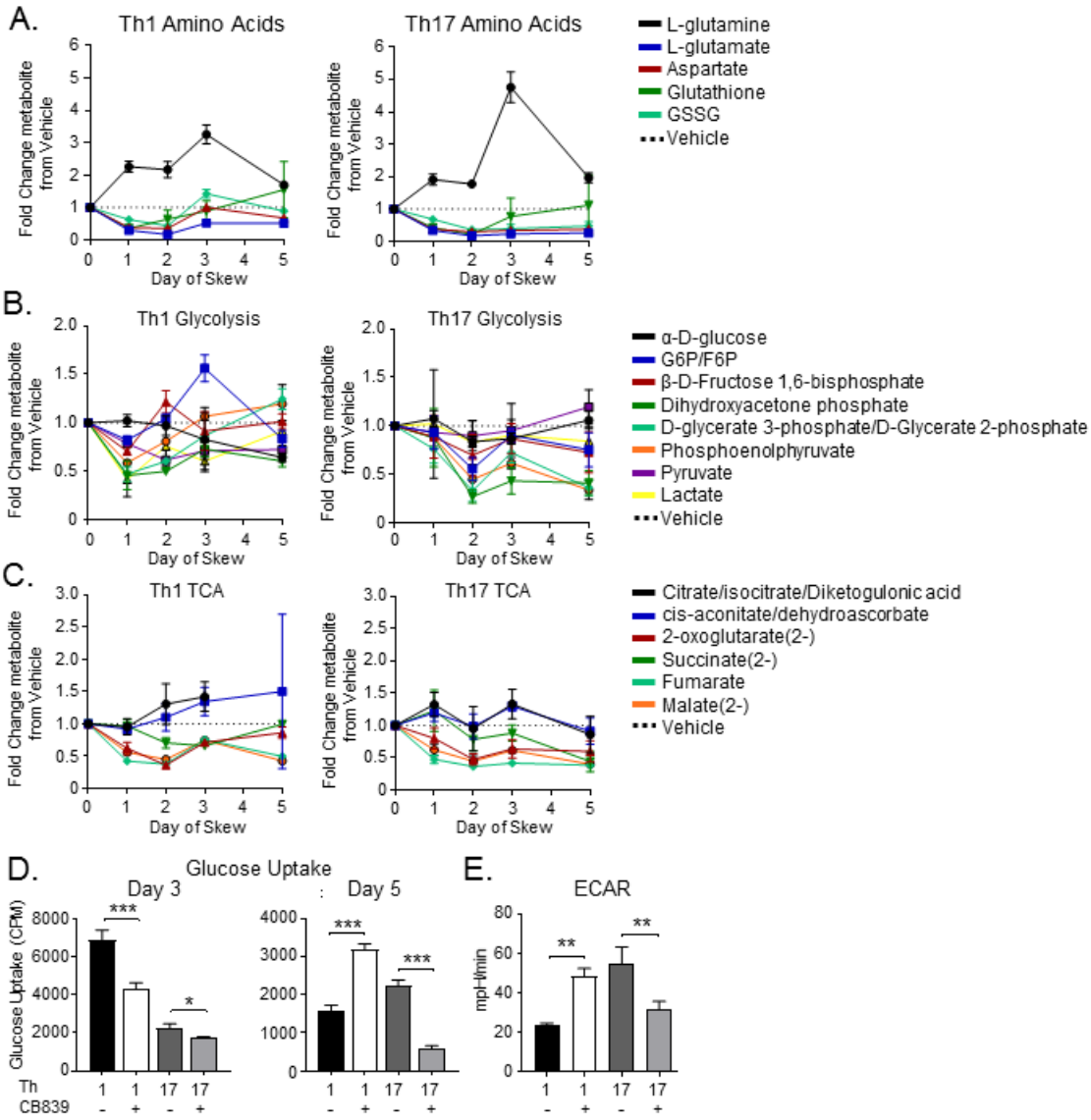

Figure 16: GLS inhibition reduces available metabolites downstream of glutamine but is recovered in Th1 cells

(A-D) Naïve WT CD4+ T cells differentiated to Th1 and Th17 cells in the presence of CB839 or vehicle. (A) Fold change of metabolites relative to vehicle by mass spectrometry over five days. (B and C) Metabolites in glycolysis (B) and Tricarboxylic Acid cycle (C) (average of 3 replicates/group fold change from vehicle). (D) 3H-2-deoxyglucose uptake in Th1 and Th17 skewed T cells at day 3 (left) and day 5 (right). (E)

Extracellular Acidification Rate (ECAR) of Th1 and Th17 skewed T cells at day 5 as in (D) (student's t test).

Changes in metabolism occurred rapidly upon GLS inhibition and preceded Th1 and Th17 differentiation. GLS inhibition led both Th1 and Th17 to have reduced levels of subset-specific transcription factors and prevented an increase in cell size relative to control cells on days one and two after activation (Figure 17A, B). By day five, however, Th1 cells had recovered and increased both cell size and Tbet expression. These data are consistent with overall changes in biomass, as total rRNA levels per cell were similar in GLS inhibitor or control treated T cells on day three, but Th1 had increased and Th17 had decreased rRNA levels by day five of GLS inhibition (Figure 17C).

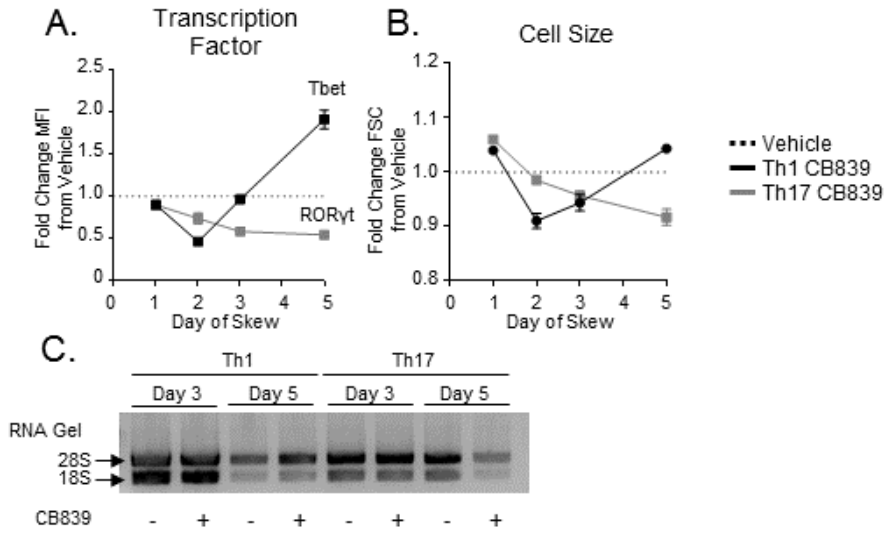

Figure 17: GLS inhibition metabolic changes precedes specification of Th1 or Th17 cells.

(A-C) Naïve WT CD4+ T cells differentiated to Th1 and Th17 cells with or without CB839 over five days. (A) Fold change of Tbet (Th1) or RORγt (Th17) protein levels and (B) cell size in CB839-treated cells normalized to vehicle. (C) Total RNA extracted from cells as in (A) at day 3 and day 5 (representative of n = 2 experiments).

3.2.5 GLS Affects Gene Expression and Chromatin Accessibility

Deficient GLS activity may alter differentiation through production of cofactors, including α-KG and 2-hydroxyglutarate (2-HG), for epigenetic marks and changes in chromatin status (Reid et al., 2017; Xu et al., 2017). Based on intracellular metabolite analysis by mass spectrometry, α-KG was reduced in CB839-treated Th1, but not Th17 cells, while 2-HG increased in both Th1 and Th17 (Figure 18A, B). The reduced α-KG in CB839-treated Th1 cells suggested that α-KG may become limiting to regulate Th1 differentiation and function. A cell-permeable α-KG analog, dimethyl 2-ketoglutarate (DMaKG), was tested to determine if provision of α-KG could restore normal Th1 specification of CB839-treated T cells. DMaKG did not reduce cytokine production in Th1 cells by itself. However, DMaKG rectified IFNγ production and Tbet expression of CB839-treated Th1 cells to control levels (Figure 18C, D). In contrast, Th17 cells were not rescued by DMaKG and IL17 production and RORγt were unchanged or further decreased (Figure 18E, F), suggesting a distinct mechanism of regulation for Th17 cells by GLS.

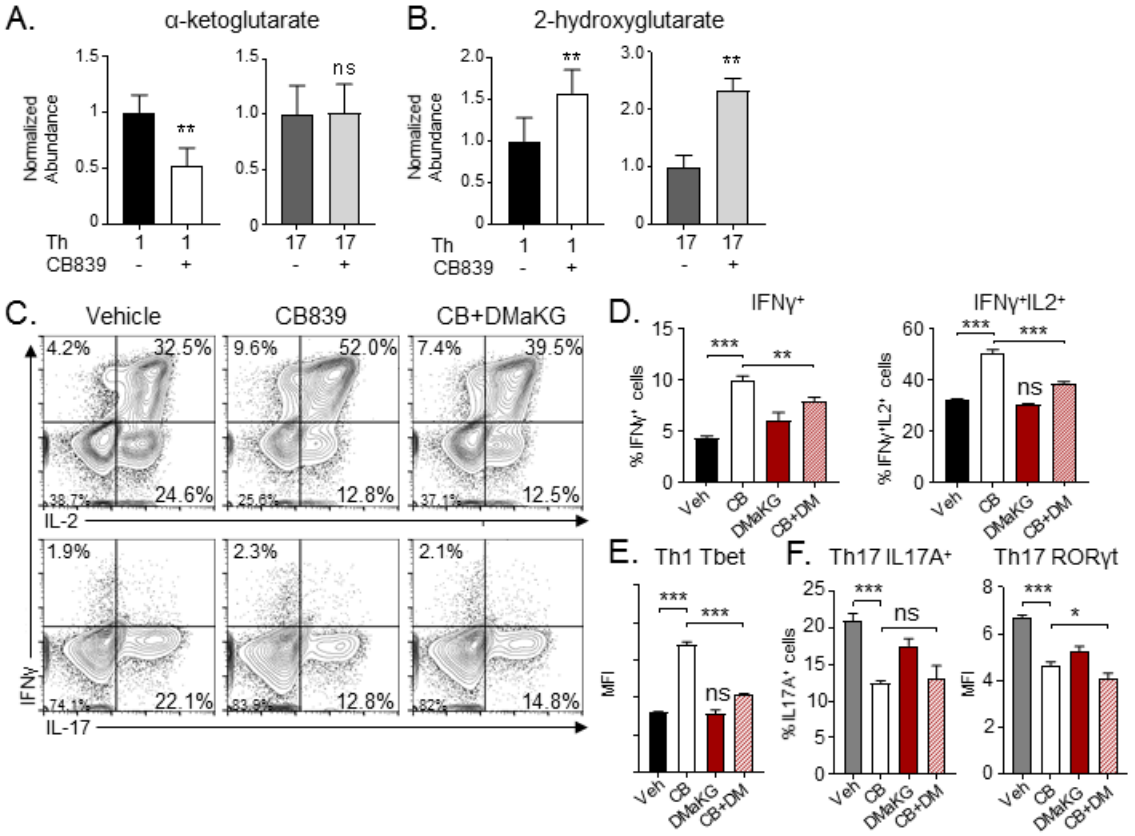

Figure 18: Dimethyl-alpha ketoglutarate (DMaKG) rectifies Th1 effector responses in the presence of GLS inhibition but has no effect on Th17.

(A-B) Metabolite levels normalized to vehicle of each subset (A) Intracellular α-ketoglutarate metabolite levels and (B) 2-Hydroxyglutarate metabolite levels as in A (** P<0.01, unpaired t-test). (C-E) WT CD4+ T cells differentiated in Th1 or Th17 conditions in the presence of vehicle or CB839 over five days with or without DMaKG. (C) Cytokine production in Th1 (top) and Th17 (bottom) skewing conditions dosed as indicated. (D) Average IFNγ+ only producers (left) and average IFNγ+IL2+ producers (right) as in (C). () Average protein expression of Tbet as in (A). (D) Average IL-17A producers in Th17 skewing media (left) and average RORγt expression (right) (one-way ANOVA).

Changes in α-KG and 2-HG may alter histone methylation and chromatin accessibility that influence T cell differentiation (Xu et al., 2017). Histone tri-methylation

was globally assessed by flow cytometry. Initially, GLS inhibition led to increased H3K27 tri-methylation (Figure 19A). At later time points when Th1 differentiation was enhanced, however, CB839-treated Th1 and Th17 cells were found to have decreased or increased global H3K27 trimethylation, respectively (Figure 19B). H3K4 trimethylation was similarly reduced or increased in Th1 and Th17 cells, respectively, at day five (Figure 19C). Consistent with altered regulation of demethylation as a cause of Th1 differentiation upon GLS inhibition, treatment of T cells with an inhibitor of the histone demethylase JMJD3 also led to increased cytokine production in Th1 but not Th17 cells at day five (Figure 19D).

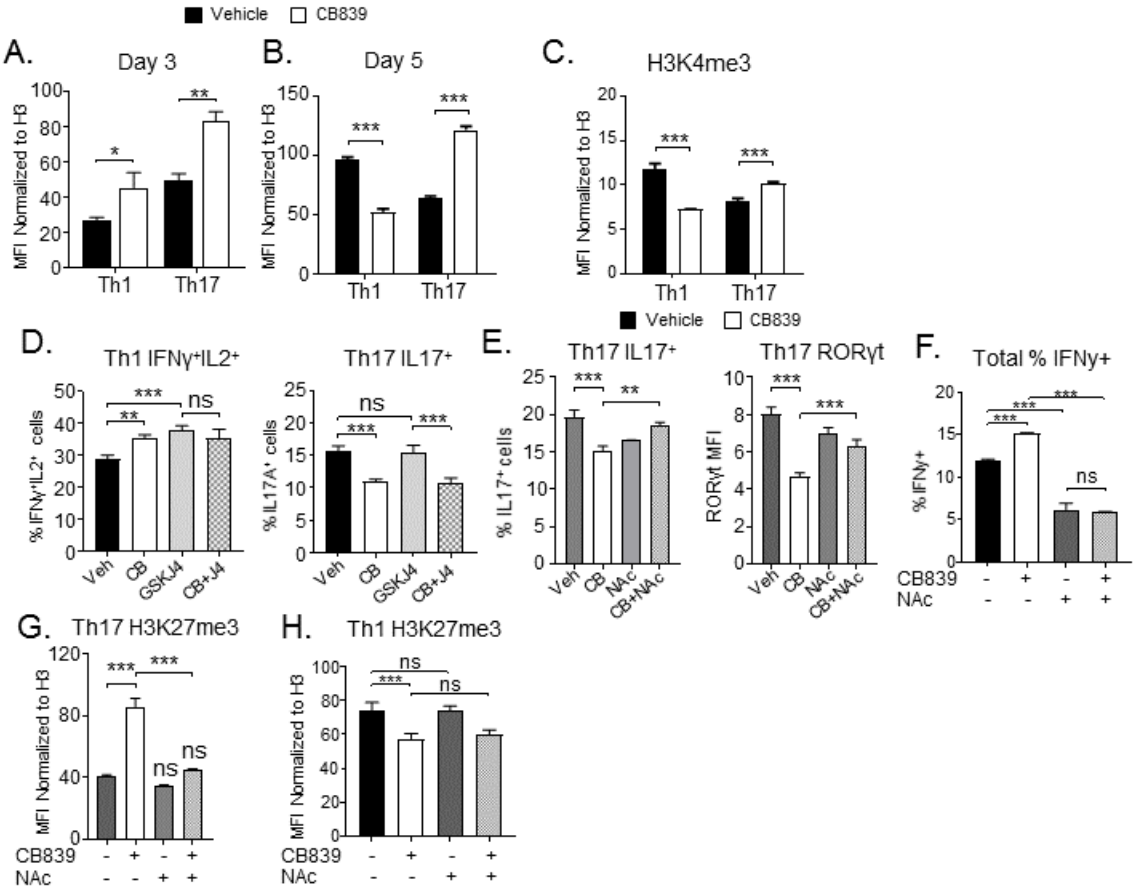

Figure 19: GLS inhibition exerts epigenetic changes in methylation of H3K4 and H3K27 trimethylation.

(A and B) Global H3K27 trimethylation normalized to total H3 by flow cytometry. (A) Average H3K27 trimethylation expression at Day 3. (B) Same as (A), but at Day 5 (*** $p < 0.001$, student's t test, n = 3 replicates/group). (D) Average cytokine producers of skewed CD4+ T cells in the presence of CB839, JMJD3 inhibitor GSKJ4, or CB839+GSKJ4 (CB+J4) at day 5 (** $p < 0.01$, one-way ANOVA, n = 3 replicates/group). (E) Percent IL17A+ producers (left) and protein expression of RORγt (right) in Th17-skewed cells with or without CB839 and NAc. (G and H) H3K27me3 by flow cytometry in Th17 (G) or Th1 (H) skewing conditions and NAc treatment as described.

The dependence of Th17 cells on GLS was not rescued by DMaKG, but Th17 cells can be highly sensitive to increased ROS (Gerriets et al., 2015). The glutathione mimic N-acetyl cysteine (NAc) was tested to rescue GLS-deficient Th17 cells. NAc treatment alone modestly reduced Th17 expression of IL17 and RORγt (Figure 19E) while decreasing IFNγ secretion by Th1 (Figure 19F). Th17 production of IL17 and expression of RORγt were partially restored to control levels when combined with CB839. The combination did not, however, increase Th1 production of IFNγ. Changes in Th17 inhibition by CB839 may be mediated through chromatin modifications as NAc also restored H3K27 trimethylation in GLS-deficient Th17 cells to control levels (Figure 19G) yet had no effect on H3K27 trimethylation in Th1 cells (Figure 19H).

Because multiple epigenetic marks may be altered, we performed the Assay for Transposase-Accessible Chromatin sequencing (ATAC-seq) to determine if GLS deficiency altered chromatin accessibility after five days of Th1 and Th17 differentiation. CB839-treated Th1 cells had more genes with regions of increased accessibility than genes with decreased accessibility (Figure 20A). Th17 cells however, had more genes with regions of reduced accessibility. While partially overlapping, affected genes were largely distinct for Th1 and Th17 cells (Figure 20B). Key Th1 and Th17 genes showed changes, including the *Ifng* and *Il17a/f* loci in Th1 and Th17 cells, respectively (Figure 20C). Further, Ingenuity Pathway analyses of genes with altered promoter accessibility

in Th1 cells showed changes in networks of cell survival and inflammation (Figure 20D). Analysis of promoter regions with altered accessibility identified recognition motifs for canonical T cell differentiation transcription factors, including AP-1, ETS, and IRF (Figure 21). These altered promoter regions were also enriched in CTCF recognition motifs, a DNA binding protein recently implicated to mediate the effects of glutamine on chromatin state (Chisolm et al., 2017).

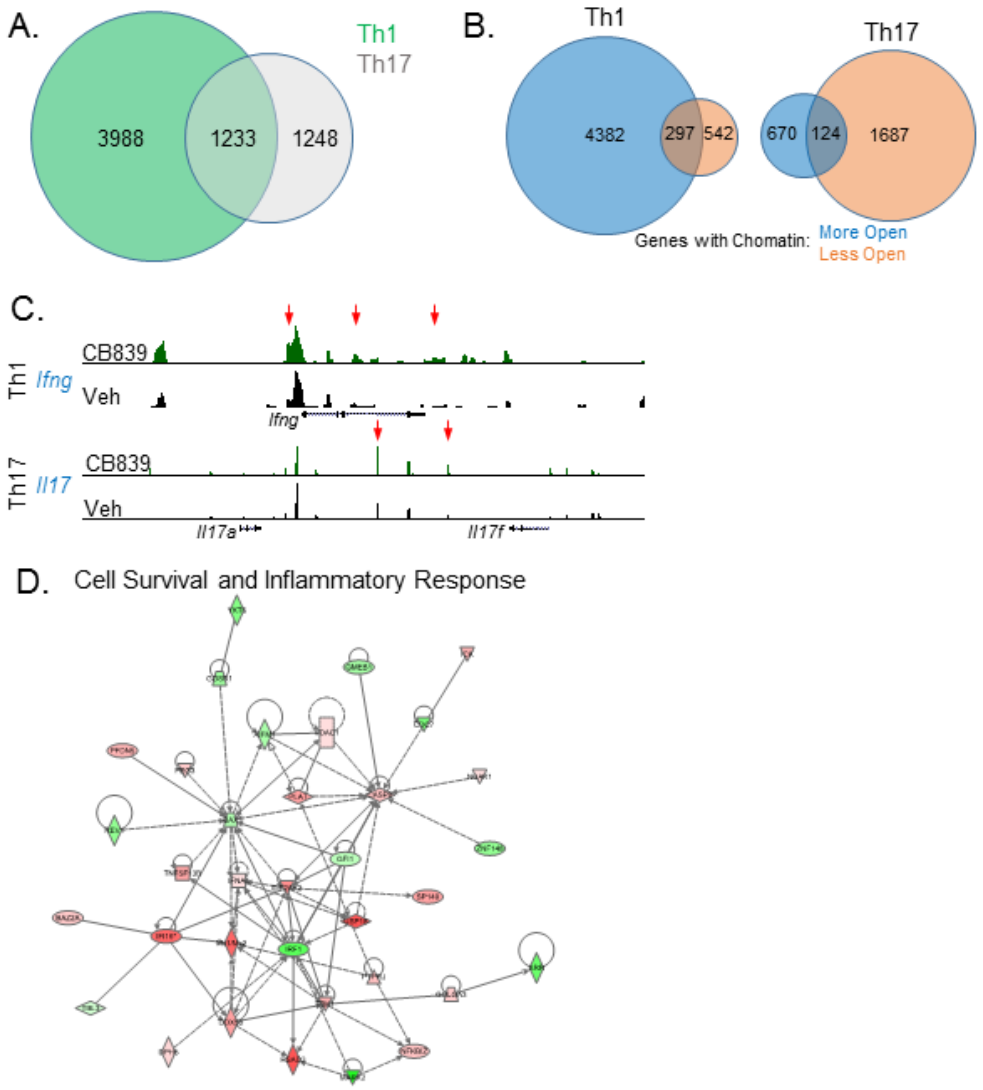

Figure 20: GLS inhibition affects global methylation of DNA to change accessible DNA.

(A-D) ATAC-Seq on skewed Th1 and Th17 cells in the presence or absence of CB839. (A) Venn diagram of ATAC-Seq total changed peaks (either open or closed). (B) Number of loci with more (blue circles) and less accessible (orange circles) chromatin peaks with CB839 as determined by ATAC-Seq in Th1 or Th17 cells. (C) Example ATAC-Seq traces of IFNγ in Th1 and IL17 gene locus in Th17 skewing conditions. (D) Ingenuity pathway analysis of altered ATAC-seq peaks from promoter regions in Th1 cells for Cell Survival

and Inflammatory response (green – downregulated, red, upregulated, relative to vehicle treated).

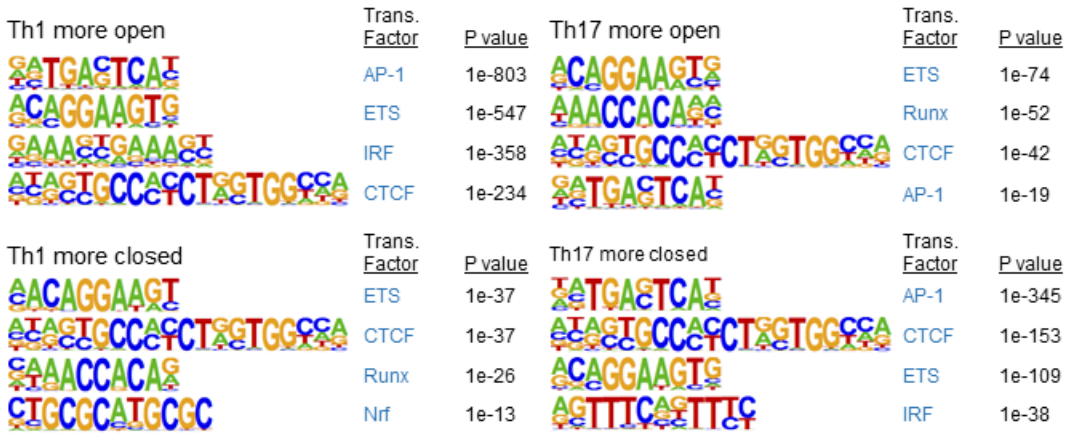

Figure 21: GLS inhibition differentially affects transcription factor consensus sequences in Th1 and Th17 cells.

Motif analysis of the promoter regions with significantly changed peaks in Th1 and Th17 cells, affecting canonical T cell promoter regions. AP-1, ETS, CTCF are all implicated in T cell function and differentiation.

Because altered chromatin accessibility can influence gene expression and T cell differentiation, T cells were cultured in Th1 or Th17 conditions with vehicle or CB839 and examined by RNA sequencing. Interestingly, of the 200 genes with the most significantly altered expression in CB839-treated Th1 cells, the majority showed increased expression (Figure 22A). Conversely, more of these genes were downregulated in Th17 cells.

IL2 signaling activates mTORC1 to promote Myc signaling, glycolysis, and Th1 effector differentiation (Boyman and Sprent, 2012; Chisolm et al., 2017). Given

enrichment in these pathways by RNA-seq, the contribution of IL2/mTORC1 signaling was tested to increased effector function of GLS-deficient Th1 cells. Levels of the mTORC1 downstream target phospho-S6 were measured in Th1 and Th17 cells differentiated in IL2 and the presence or absence of CB839. GLS-inhibition led to increased phospho-S6 in Th1 and decreased phospho-S6 in Th17 cells (Figure 22B). IL2 played a key role to promote phospho-S6, as increased phospho-S6, IFNγ, and Tbet in CB839-treated Th1 were dependent on IL2 (Figure 22C, D). Consistent with mTOR

regulation of Myc protein, GLS-inhibition modestly increased Myc in Th1 but not Th17 cells (Figure 22E).

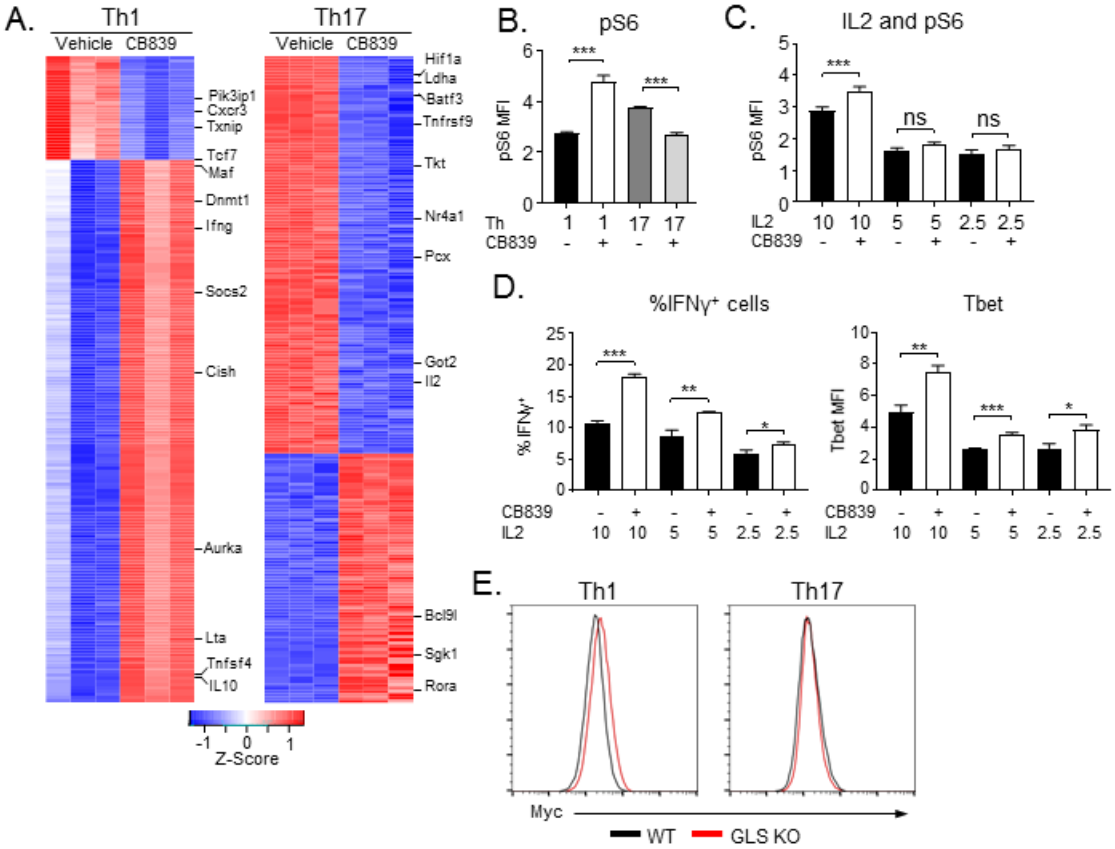

Figure 22: GLS inhibition promotes upregulation of mTOR signaling and is reliant on IL-2.

(A) Top 200 modified genes from RNA-Seq compared to vehicle (Log2Fold > 0.5, $p < 0.05$) in Th1 (left) and Th17 (right) (n = 3 replicates/group). (B and C) Phospho-S6 expression on day 5 in Th1 and Th17 conditions as indicated with or without CB839 or IL2 at concentrations shown (ng/mL) at day 3 (*** $p < 0.001$, student's t test, n = 3 replicates). (D) Left: Percent IFNγ+ producers in Th1 skewing conditions treated with or without CB839 and indicated levels of IL-2 (ng/mL). Right: Tbet protein expression as in left. (*** $p < 0.001$, student's t-test). (E) Myc protein expression in WT and GLS KO CD4+ T cells in Th1 and Th17 skewing conditions (representative of n = 3 replicates).

Importantly, while GLS-inhibition in the presence of IL2 led to enhanced differentiation and a hypomethylated state, T cells hypermethylated H3K27 upon treatment with CB839 in the absence of IL2 (Figure 23A). The role of mTORC1 signaling in GLS-mediated regulation of Th1 cells was directly tested by treatment of cells on day three after activation with rapamycin. While rapamycin treatment at this time had no effect on control Th1 cells, it reduced phospho-S6 and cytokine production in CB839-treated Th1 cells (Figure 23B, C). A similar mechanism may occur for regulation of Th0 and CTL, as GLS-inhibition also led to enhanced phospho-S6 for these cells in the presence of IL2 (Figure 23D).

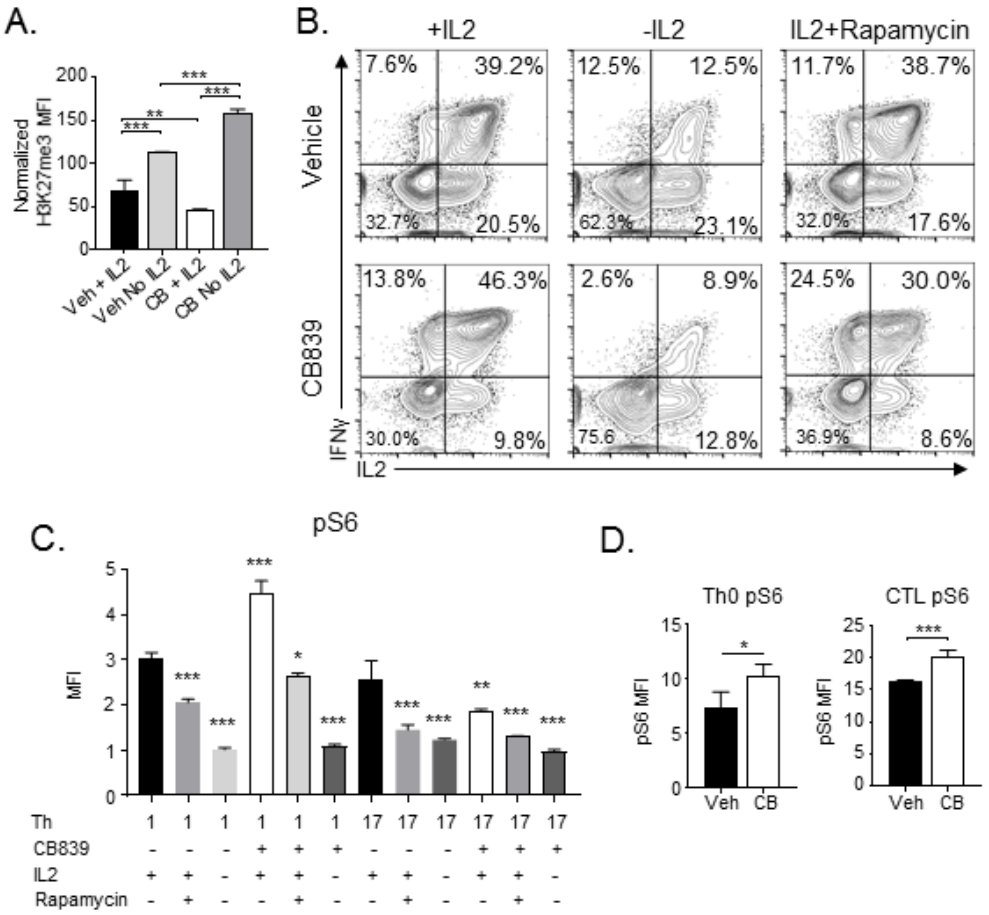

Figure 23: CB839 effects on Th1 cells is dependent on Il2 and mTORC1 signaling.

(A) MFI of H3K27me3 normalized to total H3 of CD4+ T cells in Th1 skewing conditions with indicated IL2 with or without CB839 (*** $p < 0.001$, one-way ANOVA, n = 3 replicates/group). (B) Cytokine production in Th1 skewing conditions in the presence of vehicle (top) or CB839 (bottom) after five days, under no IL2 conditions or with IL2 + mTOR inhibitor rapamycin added on day 3. (C and D) phospho-S6 protein expression measured by flow cytometry (C) in IL2 and IL2 depleted conditions with or without rapamycin (** $p < 0.01$, one-way ANOVA compared to vehicle of each group, n = 3 replicates/group) or (D) pS6 expression in Th0 (left) and CD8+ CTL cells (right) (*** $p < 0.001$ student's t-test, n = 3 replicates/group).

Several regulators of mTORC1 signaling were altered by GLS-inhibition in Th1 cells by RNA-Seq, including *Pik3ip1*, *Akt*, *Tsc2*, *Sestrin2*, and *Castor1* (Figure 24A). Of these, *Pik3ip1*, which has been shown to suppress PI3K and mTORC1 in T cells (DeFrances et al., 2012b; Wei et al., 2016), was most strongly downregulated in Th1 cells by GLS inhibition. Restoring PIK3IP1 in CB839-treated Th1 cells by retroviral transduction was sufficient to reduce phospho-S6 and cytokine secretion (Figure 24B, 24C). Conversely, CRISPR genetic deletion of *Pik3ip1* (Figure 24D) in primary T cells led to increased phospho-S6 and IFNγ production (Figure 24E).

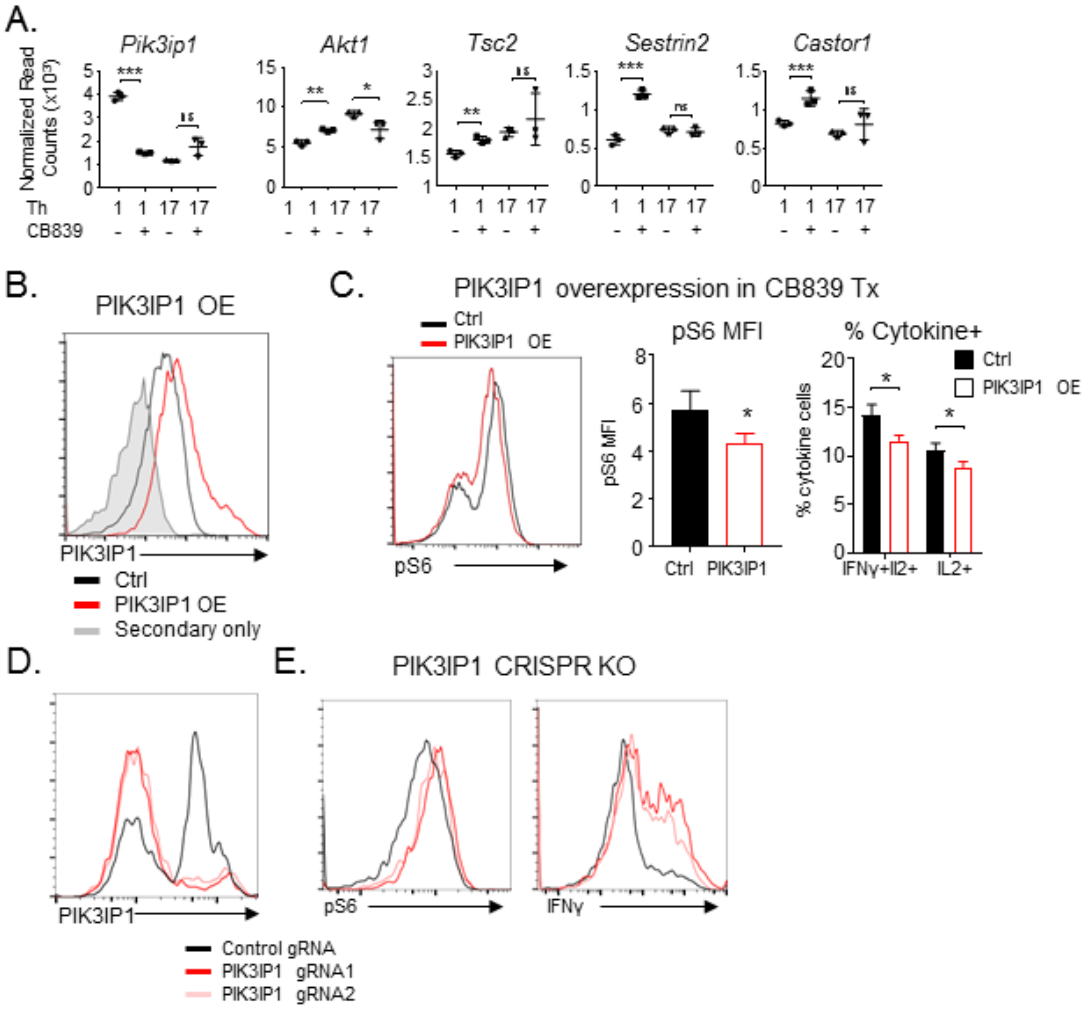

Figure 24: PIK3IP1 is a new target for Th1 effector function and cytokine secretion.

(A) Normalized message counts from RNA-Seq run on skewed Th1 and Th17 cells with or without CB839, highlighting PI3K/Akt/mTOR pathway targets (*** $p < 0.001$, p values obtained from defSeq2 program). (B) PIK3IP1 protein expression by flow after 6 days with PIK3IP1 overexpression plasmid in Th1 cells treated with CB839. (C) Phospho-S6 expression (left) by flow, average of three replicates (middle), and percent cytokine producers in PIK3IP1 overexpression as in (B). (D) PIK3IP1 protein expression in CAS9-expressing CD4+ T cells in Th1 skewing conditions with guide RNAs targeting PIK3IP1 (CRISPR KO). (E) p-S6 and IFNγ expression in Th1 cells from (D).

PIK3IP1 is a transmembrane protein and treatment of stimulated T cells with anti-PIK3IP1 antibody directed against the extracellular domain suppressed phospho-S6 (Figure 25A) and T cell activation as evidenced by downregulation of CD25, CD44, and CD62L (Figure 25B, C). Together, these data suggest that PIK3IP1 levels can contribute to mTORC1 activity and effector function in Th1 cells while Th17 cells are dependent on GLS-mediated regulation of cellular redox state.

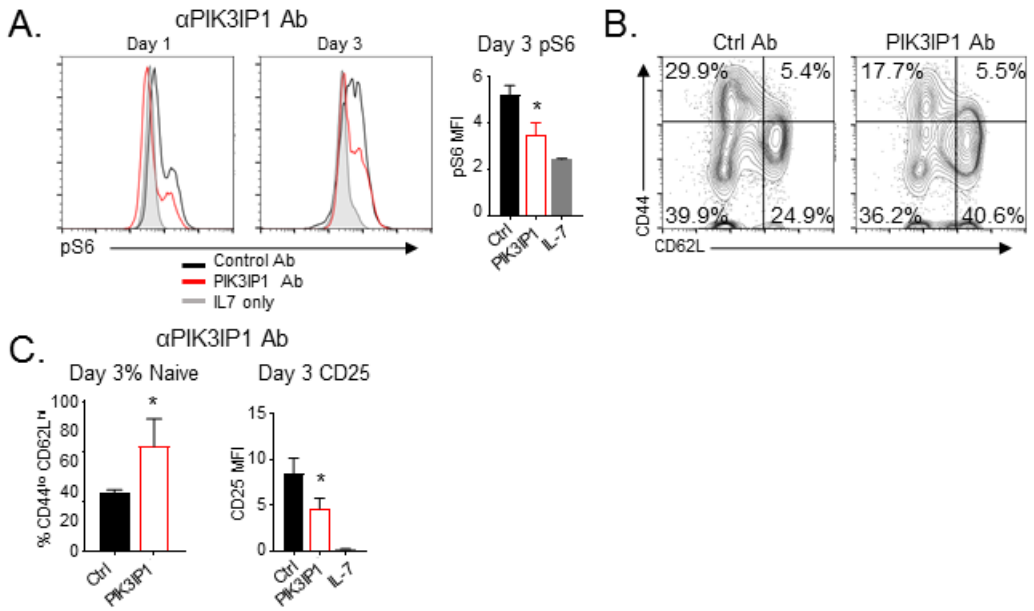

Figure 25: PIK3IP1 is targetable with an activating antibody.

(A-C) Wild type CD4+ T cells activated and treated with PIK3IP1 antibody or IgG control antibody over 3 days. (A) Protein expression of phospho-S6 (left), and average MFI of pS6 (right, one-way ANOVA). (B) Protein expression of activation markers of control- or PIK3IP1 antibody-treated T cells upon stimulation. (C) Percent naïve cells ($CD44^{low}$ $CD62L^{hi}$) in control or PIK3IP1 antibody-treated activated T cells (left) and CD25 expression (right) (* $p < 0.05$, student's t-test, n = 3 replicates/group).

3.2.6 GLS Regulates In Vivo for Inflammatory Effector T Cell Responses

We next tested if Th17 cells require GLS to elicit inflammation *in vivo*. Allogenic bone marrow was transplanted alone or with control and $GLS^{fl/fl}$CD4-Cre^{+} T cells to induce a model of IL17-dependent chronic Graft-vs-Host Disease (cGvHD). Recipient mice were weighed regularly and GLS-deficient allogenic T cells led to less weight loss than control T cells (Figure 26A). cGvHD is a multi-organ disease (Panoskaltsis-Mortari et al., 2007) and mouse models of cGvHD include lung inflammation. Histological examination showed that GLS-deficient T cells reduced lung immune infiltrate and clinical inflammation score (Figure 26B, C) and caused significantly less airway functional impairment than control T cells (Figure 26D). Immunologically, GLS deficiency reduced IL17 producing CD4 cells, with a trend towards reduced IFNγ (Figure 26E).

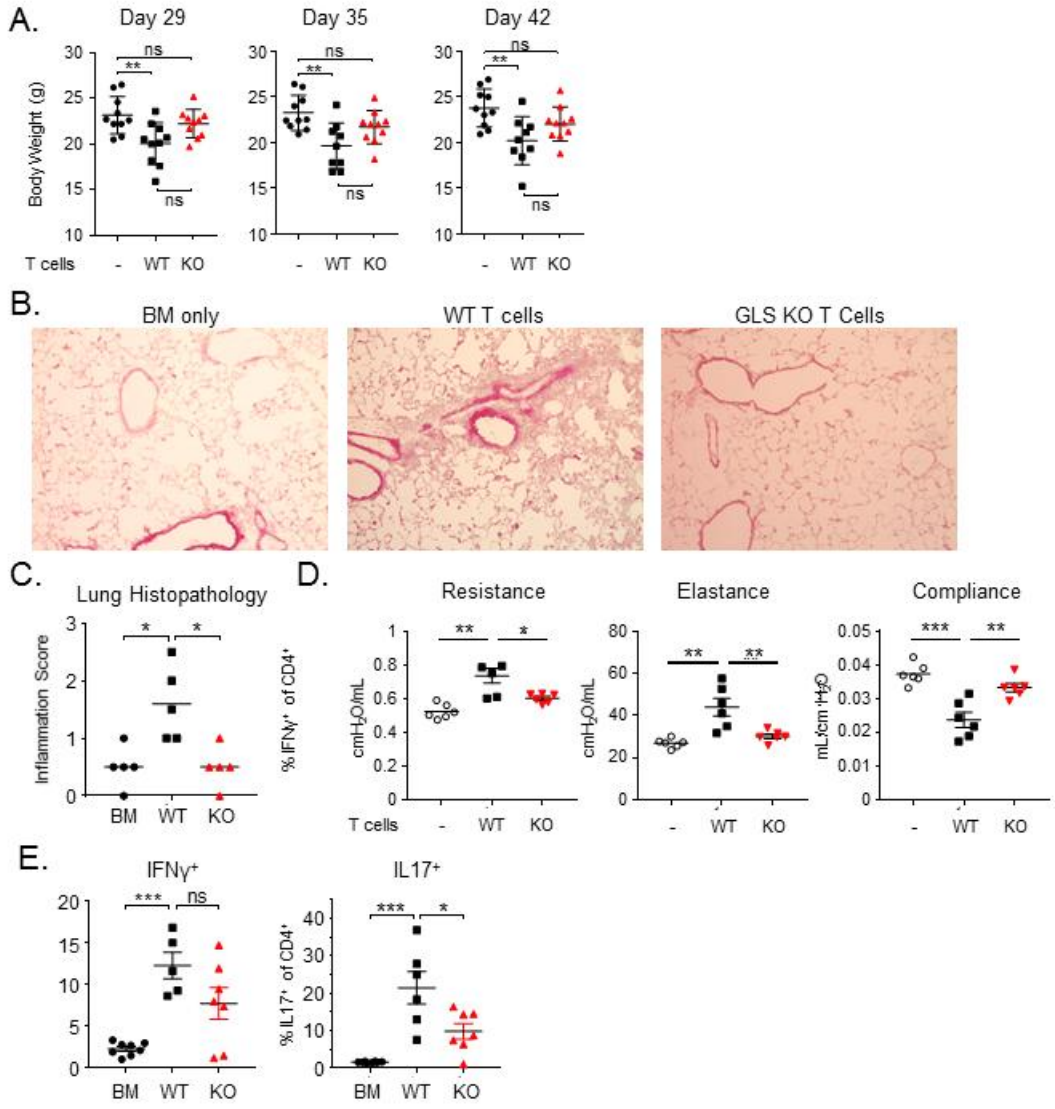

Figure 26: GLS KO T cells are unable to enact inflammatory response in graft versus host disease lung setting.

(A-E) GLS KO or WT T cells were adoptively transferred to recipient mice as a model of cGVHD in C57BL6 animals. (A) Bodyweights of recipient mice injected with T cell depleted bone marrow and either WT CD4+ or GLS KO CD4+ T cells from spleen. n = 9 animals/group (** $p < 0.01$, one-way ANOVA). (B) Hematoxylin and eosin stained lung sections focusing on bronchioles. (C) Average histopathological scores from sections from (A) (unpaired T test). (D) Lung physiology measurements (read out of Bronchiole

Obliterans) from (A) (*** $p < 0.001$, one-way ANOVA). (E) Percent cytokine producers from peripheral lymph node cells stimulated with PMA/ionomycin for 5 hours from GvHD mice (BM: n = 8, WT n = 5, KO n = 7, unpaired T test).

GLS was also critical in an independent model of Th17-mediated lung inflammation, in which control and GLS-deficient animals sensitized and challenged in the airway with House Dust Mite antigen and LPS failed to accumulate CD4 T cells and produce inflammatory cytokine in the lung (Figure 27A). Inflammatory bowel disease (IBD) also involves Th17 cells and we found that while adoptive transfer of control T cells led to weight loss and inflammation, mice that received GLS-deficient T cells maintained weight (Figure 27B). Despite partial protection from disease, a greater percentage of GLS-deficient T cells in the mesenteric lymph nodes produced IFNγ, consistent with a preferential Th1 response (Figure 27C).

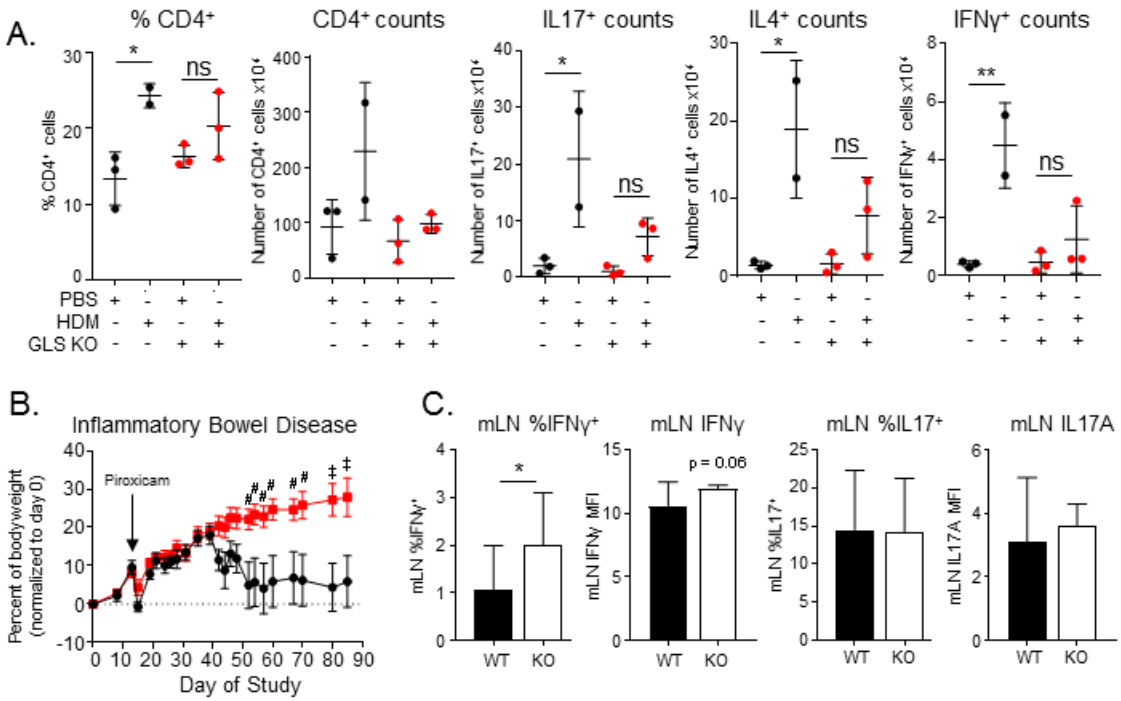

Figure 27: GLS KO T cells fail to induce inflammation in airway model of asthma or murine colitis.

(A) Percent of CD4+ T cells (left), CD4+ counts, IL17+ counts, IL4+, and IFNγ+ counts in WT and GLS KO mice immunized with PBS or house dust mite antigen (HDM) over 14 days (* $p < 0.05$, student's t test). (B) Bodyweights from T cell adoptive transfer Inflammatory Bowel Disease (IBD) model in which RAG1 KO mice injected with WT and GLS KO naïve CD4+ T cells and induced for IBD with piroxicam (# $p < 0.05$, ‡ $p < 0.01$, two-way ANOVA, WT n = 6, GLS KO n = 8, data presented as mean ± Standard Error (SEM). (C) Percent IFNγ+, IFNy MFI, or percent IL17+, and IL17A MFI in mesenteric lymph nodes collected from RAG1 KO mice injected with wild type or GLS KO naïve CD4 T cells in IBD (* $p < 0.05$, student's t test).

The role of GLS-deficiency to enhance Th1 and CTL function was next tested *in vivo*. Control and GLS$^{fl/fl}$CD4-Cre T cells were evaluated in a murine Chimeric Antigen Receptor (CAR) model for the ability to eliminate endogenous target B cells and persist

in vivo. T cells were *in vitro* transduced with CAR-T expression vectors either lacking a cytoplasmic tail (Δ) or with a CD3ζ-CD28 (28-ζ) intracellular tail and adoptively transferred into animals conditioned with cyclophosphamide. Fourteen days after T cell transfer, endogenous CD19-expressing B cells were significantly reduced by both control and GLS$^{fl/fl}$CD4-Cre CAR-T cells (Figure 28A). After 28 days, however, B cells had accumulated in recipients of GLS$^{fl/fl}$CD4-Cre CAR-T cells and were fully recovered in lymph nodes by day 42 (Figure 28A, B). Consistent with upregulation of inhibitory receptors upon activation, GLS-deficient T cells appeared unable to sustain an effector response in the absence of GLS activity *in vivo*.

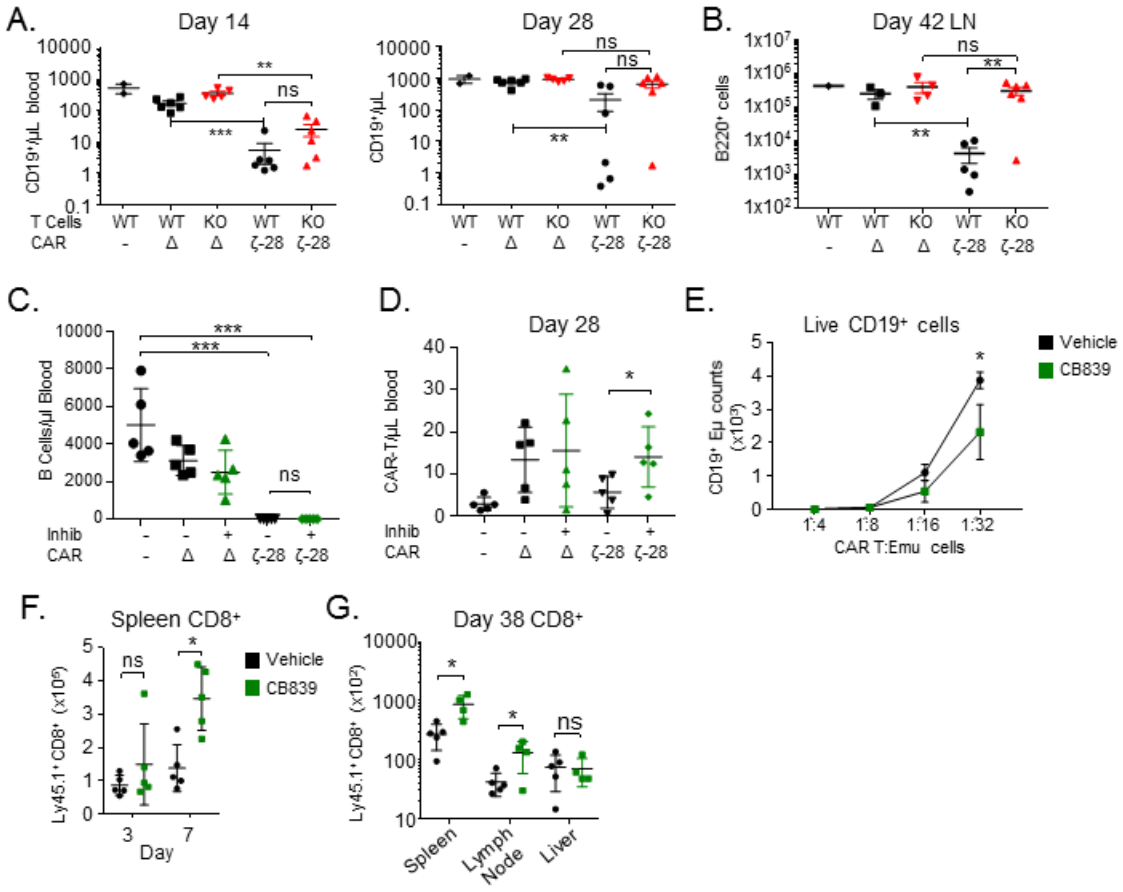

Figure 28: GLS KO T cells cannot sustain *in vivo* inflammatory responses, but temporary inhibition of GLS with inhibitor can promote B cell killing and increase T cell numbers.

(A and B) T cells from WT and GLS KO infected to express CAR T cell constructs and injected into recipient mice. CAR- (no infection), Δ = m19-delta-ζ, 28-ζ = m19-28-ζ. (E) CD19+ B cells per µL of blood at day 14 (left) and Day 28 (right). (B) Same as in A, but at day 42 (one-way ANOVA). (C) Frequency of CD19+ B cells in blood 4 weeks after injection of T cells activated and infected with CAR T cell construct 28-ζ or control delta-ζ with or without GLS inhibitor (*** $p < 0.001$, one-way ANOVA). (D) CAR-T cell numbers on day 28 following transfer of CAR-T cells treated with vehicle or CB839 prior to transfer to recipient mice (WT no CAR: n = 2 animals, all others n = 5-6 animals, one-way ANOVA). (E) Numbers of CD19+ Eµ-Myc lymphoma cells after 48 hours culture with indicated ratios of CAR-T cells treated with or without CB839 transduction of CAR

construct (student's t-test). (F) Counts of total CD8+ cells in response to hgp10025-33-expressing vaccinia virus collected from tail vein after indicated time (two-way ANOVA). (G) Counts of total CD8+ T cells in spleen (left) and lymph node (right) after 38 days and re-challenge with hgp10025-33-expressing vaccinia virus (Vehicle n = 5 animals, GLS inhibitor n = 4 animals, two-way ANOVA).

Because GLS-inhibition altered chromatin accessibility in Th1 cells *in vitro*, it was possible that transient treatment with CB839 could induce long lasting effect. T cells were treated with vehicle or CB839 during *in vitro* transduction to express CARs and tested for subsequent *in vivo* function. Vehicle and CB839-treated CAR T cells were equally capable of eliminating $CD19^+$ targets *in vivo* (Figure 28C). Importantly, *in vitro* CB839-treated 28-ζ CAR-T cells accumulated *in vivo* to a greater extent than untreated CAR-T cells (Figure 28D) and showed greater ability to eliminate B cell leukemia cells *in vitro* (Figure 28E). This increased ability of Th1 and CD8 effector T cells to proliferate or persist following transient GLS inhibition was not specific to CAR T cells. CD8 T cells bearing a Pmel-specific TCR transgene treated with CB839 *in vitro* prior to adoptive transfer also accumulated to greater numbers *in vivo* by day 7 when challenged with an antigen-expressing vaccinia virus (Figure 28F) and increased cell numbers persisted for greater than 5 weeks (Figure 28G). Thus, chronic or complete GLS deficiency impairs T cell responses *in vivo*, while transient *in vitro* inhibition may enhance subsequent Th1 and CD8 CTL effector function and long-lasting cell numbers *in vivo*.

3.3 Discussion

T cell activation and specification into functional subsets requires increased biosynthesis and establishment of the appropriate gene expression program. Importantly, the metabolic programs and requirements of each subset are distinct and Th1, Th17, and Treg have critical metabolic differences that influence their differentiation and fate. While glucose metabolism has been extensively studied, here we show that glutamine metabolism and GLS activity regulated T cell activation and promotes Th17 while impairing Th1 differentiation and effector function.

Glutamine and generation of α-KG through GLS and glutaminolysis can play a key role to maintain levels of TCA intermediates that support oxidative phosphorylation and TCA flux. Indeed, acute GLS inhibition lowered T cell respiration and abundance of TCA intermediates while increasing glucose contribution to these pathways. As T cells differentiate into effector populations, however, this association becomes context dependent as IL2 can promote a spontaneous Th1-like phenotype in CD4 T cells and enhance CD8 CTL effector function. Th17 cells, however, remain dependent on these pathways. For Th1 and cytotoxic CD8 T cells to adapt to GLS-deficiency, an alternate anaplerotic source is essential. This may be mediated through Pyruvate Carboxylase generation of oxaloacetate from glycolysis-derived pyruvate, as can occur in glutamine-independent cancers (Cheng et al., 2011).

While GLS acts on glutamine to facilitate the first event of glutaminolysis, modulation of glutamine metabolism at different steps can lead to strikingly different phenotypes. The absence of glutamine prevented cytokine production and proliferation of both Th1 and Th17 cells and instead promoting Treg generation. Deficiency of the glutamine transporter ASCT2 did not suppress proliferation but did impair both Th1 and Th17 T cell specification while enhancing Treg generation (Nakaya et al., 2014). Suppression of GOT1, which converts aspartate and α-KG to glutamate and oxaloacetate, impaired Th17 with increased Treg differentiation (Xu et al., 2017). GLS-deficiency differs still to selectively promote Th1 and impair Th17 differentiation while not affecting Treg. Subset-specific protein expression and levels of different metabolites in glutamine-related pathways may mediate distinct responses to glutamine metabolism. ASCT2 is one of multiple glutamine transporters to control intracellular glutamine levels and may interact with the CARMA1 complex upon T cell activation to regulate NF-κB signaling (Nakaya et al., 2014). GOT1 deficiency may restrict glutamate production from aspartate while leaving glutamine conversion to glutamate and α-KG intact. GLS deficiency, in contrast, allows glutamine uptake but leads to both glutamate and aspartate deficiencies and increased ROS. Given the interconnections and importance of each metabolite in glutamine metabolic pathways, it is likely that inhibition of this network of metabolites leads to context specific outcomes.

Modulation of glutamine-dependent metabolites may influence T cells through alteration of epigenetic marks and chromatin accessibility. Increased cytosolic acetyl-CoA levels can modulate histone acetylation and can regulate IFNγ expression (Peng et al., 2016) and α-KG can play an important role in histone and DNA methylation. Individual histone marks have distinct regulatory roles and while we found changes in consistent changes in global H3K4 and H3K27 trimethylation that can differentially influence gene expression, it is likely that other marks also affect chromatin status as a whole to determine gene expression. Changes in the abundance of α-KG, TCA cycle intermediates, and 2-HG likely contribute to altered chromatin state and gene expression. The initial hypermethylation phenotype continued in Th17 and reversed by IL2 in Th1 cells, suggesting that IL2-induced signals and Th1 differentiation ultimately dominate the overall chromatin accessibility and gene expression patterns. ROS also promoted increased histone methylation in GLS-inhibited Th17 cells and influenced cytokine production by Th1 cells, although the mechanisms are unclear. One protein that may play a central role in GLS-regulation of chromatin is CTCF, which was shown to regulate IL-2 dependent gene programming in T cells in response to α-KG (Chisolm et al., 2017). While *Ctcf* mRNA levels were not strongly affected in this study by either Th1 or Th17 GLS deficient T cells, CTCF consensus binding sequences were significantly enriched in chromatin sites identified in ATAC-seq studies for both up and down-

regulated genes. The shared occurrence of CTCF binding sites may represent an initial α-KG dependent response and lead to more open or closed chromatin based on other DNA binding factors and transcription factor expression differences in Th1 and Th17 cells.

Opposing effects of GLS inhibition on mTORC1 signaling in Th1 and Th17 and the ability of mTORC1 to promote a glycolytic and effector differentiation program suggest that this pathway plays a key role to mediate the effects of GLS on T cell fate. IL2 was essential to stimulate mTORC1 activity that enhanced differentiation of GLS-deficient Th1 cells. GLS-inhibition induced several changes in IL2 and mTORC1 signaling that may contribute to the differential response of Th1 and Th17. In addition to increased Sestrin2 and Castor1 that are involved in amino acid sensing (Chantranupong et al.; Wolfson and Sabatini) and Akt1, PIK3IP1 was sharply downregulated in GLS deficient Th1 cells. PIK3IP1 is a transmembrane protein and was expressed at low levels in Th17 cells. PIK3IP1 is inhibitory to the mTOR signaling pathway by binding PI3K p110 and inhibiting PI3K activity. It has been shown to suppress liver carcinomas (He et al., 2008) and also to inhibit T cell activation (DeFrances et al., 2012a; Wei et al., 2016). Manipulation of PIK3IP1 expression and deletion here demonstrates this PI3K-regulatory protein may contribute to GLS inhibition to modulate mTORC1 signaling in Th1 cells. Conversely, Th17 cells are described to respond poorly to IL2 (Quintana et al.,

2012), and reduced IL2 response or altered PI3K/Akt/mTORC1 activating signal may also impair differentiation in GLS-deficient Th17 cells.

Targeting GLS may selectively impair Th17 cells while having potential to enhance Th1 responses in vivo. Th17 cells were exquisitely sensitive to generation of ROS, as addition of the glutathione mimetic n-acetylcysteine rectified Th17 IL-17 production and RORγt levels. This also correlated with rectification of H3K27 trimethylation, indicating that ROS may significant effects on Th17 differentiation and epigenetic programming. Th17 cells were GLS-dependent and failed to induce lung inflammation in either cGvHD or acute airway inflammation models and GLS-deficiency protected against inflammatory bowel disease. In addition, inhibition of GLS was recently shown to suppress a model of rheumatoid arthritis (Takahashi et al., 2017), although mechanisms were uncertain. Th1 cells were also impaired in these models, potentially due to the lower levels of inflammation or the eventual impairment of Th1 cells due to induction of inhibitory receptors. Similarly, GLS-deficient CAR-T cells were initially competent to eliminate B cell targets in vivo but failed over time. Transient in vitro GLS inhibition, however, enhanced effector activity and allowed CAR T cells and anti-viral T cells to accumulate to greater numbers in vivo. This effect is likely due to GLS-inhibition induced changes to chromatin accessibility and sensitization to cytokine

signals that promote sustained function in a setting where T cells are capable of performing glutaminolysis.

The subset specific integration of glucose and glutamine metabolism may now offer new opportunities to modulate immunity. The enhancement of mTORC1 signaling in Th1 demonstrates that this metabolic pathway both promotes Th17 and suppresses Th1 responses. Previous work showed that Th1 and Th17 differentiation are both inhibited by elimination of Rheb, an mTOR target modulator protein required for mTORC1 activation (Delgoffe et al., 2011). However, we show here a more complicated model of mTOR regulation between Th1 and Th17 cells that depends on IL-2 and epigenetic changes of DNA. GLS may provide a target to treat inflammation *in vivo* with continuous inhibition. Conversely, based on the CD8+ CTL data, transient inhibition may program T cells for enhanced IFNγ-specific effector responses and promote survival. GLS is a promising candidate to inhibit cancer cell metabolism and may synergize with anti-cancer immune therapies. In these cases, it may be important to consider transient or episodic GLS inhibition to reprogram T cells for enhanced effector function.

4. Metabolic flexibility of Th1 and Th17 cells

4.1 Introduction

In response to activation signals through the TCR, T cells increase glycolytic and glutaminolytic machinery to meet demand. Recently, metabolic reprogramming of naïve T cells to rapidly dividing Teff cells was shown to directly modulate activity (Carr et al., 2010; Macintyre et al., 2014). While Teff cells have similar jobs to promote inflammatory responses to immune insults, metabolic programming varies amongst different subsets (Michalek et al., 2011).

Metabolic flexibility is prevalent on an organismal level. Mammals are particularly good at maintaining blood glucose levels and fatty acids as energy sources, even in anorexic conditions (Lohuis et al., 2007; Spiegelman and Flier, 2001). This is coordinated by several organ systems, including the liver, hypothalamus, adipose tissue, and pancreas. Hormone signaling allows for system-wide changes in gluconeogenesis performed by the liver and lipolysis in fat, balancing energy use and biosynthesis of precursors. These respond to glucagon and insulin produced by the pancreas (Duncan et al., 2007). Muscles in humans can use several biosynthetic processes to generate ATP for movement: creatine phosphate, glycogen, and glucose. This metabolic flexibility works on a large-scale organism such as humans but it stands to reason that lymphocytes may also need to be metabolically flexible. Teff cells switch from quiescent, oxidative

metabolism primarily in the mitochondria to a catabolic glycolytic metabolism in response to TCR stimulation (Buck et al., 2015). Importantly, however, they also migrate into areas that may be nutrient limited. In sites on inflammation and in tumors, for example, glucose and glutamine may be limited by high uptake from other cells in the surrounding tissue (Chang et al.). In some tumor microenvironments, lactate levels are high and glucose levels low. Treg can use lactate as a source of fuel but Teff cannot, promoting Treg suppression of immune responses (Angelin et al., 2017). The ability to shift metabolic responses in the surrounding environment could lead to immune dysregulation, especially in nutrient limiting conditions.

Cancer cells also engage in significant metabolic activity in order to rapidly divide. In renal cell carcinoma, for instance, loss of SETD2 enhances HIF1 expression to induce glycolytic metabolism (Keefe et al., 2013). Glycolysis generates pyruvate from glucose to feed into the TCA but is also pushed into lactate production by lactate dehydrogenase. This happens in the presence of oxygen, despite oxidative metabolism producing much more ATP per mol of glucose than glycolysis (known as the Warburg Effect). While causal reasons are still under investigation, several possibilities exist. Glucose-6-phosphate derived from hexokinase can be shunted into the Pentose Phosphate Pathway to generate nucleotides for DNA and RNA synthesis (Vander Heiden et al., 2009). Availability of NAD+/H, NADP/H, and FAD+/H_2 are necessary in

providing reducing equivalents for glycolytic and mitochondrial metabolism. For example, reductive carboxylation of α-KG was found to be important when mitochondria were dysfunctional, leading to restoration of citrate and generation of lipids for biosynthesis (Mullen et al., 2014). T cells similarly respond to activation signals to promote metabolic flux through glycolytic and glutaminolytic pathways. Biosynthetic precursors for nucleotides, lipids, redox reactions, and ATP generation are all necessary for T cell function. Based on signaling and metabolic demand, T cells may have specific metabolic needs that can be harnessed to promote or inhibit T cell subsets. Expression of HIF1α, for example, modulates the differentiation of naïve T cells to Th17 cells by allowing methylation of the Foxp3 locus (Shi et al., 2011). Deletion of the primary T cell glucose transporter Glut1 prevent Teff responses but spared Treg suppression (Macintyre et al., 2014). Alternative biosynthetic sources such as amino acids and fatty acids could be utilized by T cells in response to metabolic stressors in inflammatory and cancer disease states.

Here, we show several different pathways that alter T cell differentiation and function. Pharmacological inhibition of several major pathways, including glycolysis and glutaminolysis, under different conditions yielded changes to T cell specification. GLS-inhibited Th1 cells produced more cytokine, recovered proliferation, and differentiated better than control cells. Inhibition of the ASCT2 transporter by a small

molecule prevented Th17 differentiation and IL-17A producing cells, but spared Th2. We also show that Th1 cells treated with GLS inhibitor CB839 upregulate aspartate transport and alanine uptake, potentially pointing to a metabolic adaptation that improves Th1 responses, which were not present in Th17 cells. Further, inhibition of glycolysis by 2-deoxyglucose (2-DG) did not affect Th1 cytokine production, but inhibition of glycolysis and glutaminolysis together abrogated IFNγ producing Th1 cells. This occurred without preventing expression of IL-2. Interestingly, Th17 cells in the presence of 1 mM 2-DG strongly reduced IL-17-producing cells, but also generated a 4-fold increase of IFNγ cells that were not IL-17+. This points to Th1 cells being more metabolically flexible than Th17 cells and may indicate new metabolic avenues of treatment for autoimmune disorders specific to Th17 or Th1 cells.

4.2 Results

4.2.1 Inhibition of the glutamine transporter ASCT2 by V-9302 is deleterious to Th17 differentiation *in vitro*

Whole-body deletion of the glutamine transporter ASCT2 led to decreased Th1 and Th17 effector function without affecting proliferation (Nakaya et al., 2014). However, this could have multiple effects, as ASCT2 may be required for appropriate T cell signaling and development. Additionally, the SLC1A5 (ASCT2) protein could have structural roles that would be difficult to separate from its transporter role. The small

molecule inhibitor V-9302 is a selective and specific inhibitor of ASCT2 that prevented growth of tumor cells (Schulte et al., 2018). A pro-B cell line was dosed with a range of V-9302 over 36 hours to test cell growth. No difference was seen after 24 hours. At 5 and 10 μM, V-9302 inhibited FL5.12 cell growth (Figure 29A). In naïve T cells skewed to Th1, Th2, and Th17 subsets, 10 μM V-9302 reduced viability in Th17 cells and the number of cells in Th1 and Th17. Th2 cells appeared to be unaffected by ASCT 2 inhibition by viability or cellularity (Figure 29B). CB839, which is an inhibitor of the first enzymatic step of glutamine catabolism, reduced viability in Th2 and Th17 cells and reduced the number of cells in Th1, Th2, and Th17 skewing conditions.

Because differentiation of T cells is important in their function, we next tested whether subset-specific transcription factors were modified by V-9302. After five days in differentiation media, Th1 cells treated with V-9302 slightly increased Tbet while there was no effect on Gata3 in Th2. However, V-9302 significantly reduced RORγt expression in Th17 skewing conditions (Figure 29C). This matches responses to CB839 (Figure 14C and 14G). Importantly, V-9302 reduced cytokine production in Th17 cells (Figure 29D). This indicates that Th17 cells are particularly affected by inhibition of glutamine uptake, which is similar to CB839 dosing (Figure 14A), but only partially recapitulates ASCT2 knockout (Nakaya et al., 2014). This suggests that inhibition of ASCT2 transporter may have significant deleterious effects on Th17 but may not impact Th2 cells at all. Th2 cells

are known to be very glycolytic *in vitro* (Michalek et al., 2011) and may indicate almost no reliance on ASCT2 for glutamine transport or that Th2 cells express other transporters to make up for the loss of SLC1A5.

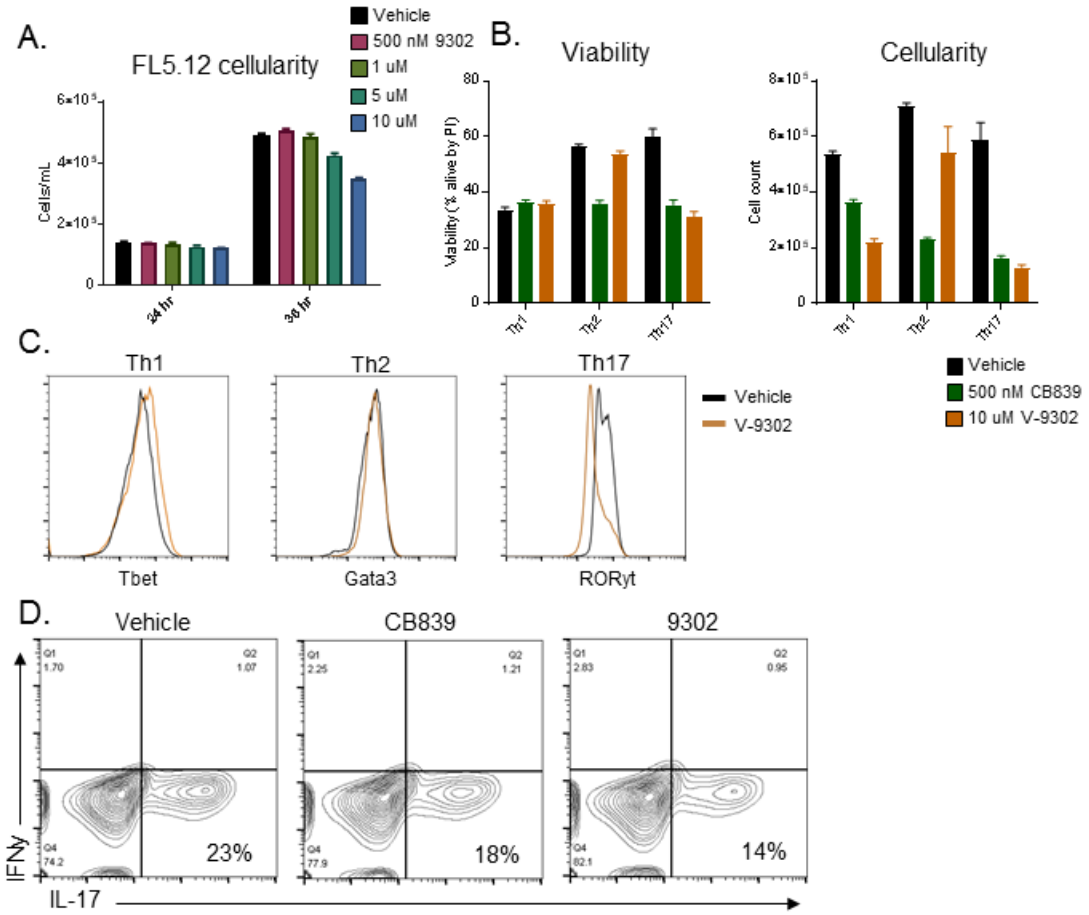

Figure 29: ASCT2 inhibitor V-9302 reduces viability of Th17 cells and cell numbers.

A) Cellularity of FL5.12 cells after 24 and 36 hours of V-9302 at various concentrations. B) Cell viability (left) and cell number/mL (right) of Th1, Th2, and Th17 skewed T cells after 5 days of culture. C) Transcription factor FACs plots in Th1, Th2, and Th17 cells

with or without V-9302 after 5 days. D) IFNy and IL-17 production in Th17 skewed T cells in the presence of vehicle, GLS1 inhibitor CB839, or V-9302.

4.2.2 Th1 effector cells rely on glycolysis to promote effector responses during GLS inhibition.

T cells use multiple sources of fuel for metabolic responses to activation. Teff cells are known generally to be glycolytic, whereas Treg utilize oxidative metabolism (Michalek et al., 2011). GLS deficient T cells upregulate glucose uptake compared to control (Figure 16D). The primary glucose transporter, Glut1, is upregulated in Th1 cells when GLS is inhibited with CB839. The other primary Glut transporters in T cells, Glut3 and Glut6, are somewhat downregulated. In comparison, GLS-deficient Th17 cells downregulate Glut1 and Glut6 transporters (Figure 30A). Together with glucose uptake data, this indicates glucose regulation could be a mechanism by which Th1 cells respond to GLS inhibition. To test whether T cells required glucose uptake and glycolysis for survival in the presence of GLS inhibitor CB839, Th1 skewed T cells were treated with CB839 and the hexokinase inhibitor 2-deoxyglucose (2-DG), which is a competitive glucose inhibitor. At 1 mM, 2-deoxyglucose did not affect Th1 IFNγ or IL-2 producers. However, in combination with CB839, 1 mM 2-deoxyglucose strongly reduced the IFNy+ and IFNy+Il2+ producer populations compared to vehicle or CB839 alone (Figure 30B and 30C).

Th17 cells rely on glucose uptake as addition of 1 mM 2-DG prevented IL-17 production in Th17 skewing conditions. However, just like Th1 cells, the combination of CB839 + 2-DG further reduced IL-17 production (Figure 30E and 30F). All treatments equally prevented induction of transcription factor required for Th17 differentiation RORγt (Figure 30G). Surprisingly, 1 mM 2-DG by itself promoted IFNγ-only producers in Th17 skewing conditions without inducing IL-17+IFNγ+, suggesting that glycolysis helps to specify differentiation of Th1 and Th17 cells. This did not occur in combination with CB839 (Figure 30H). In literature, glycolysis promotes IFNγ production (Chang et al., 2013) so it is somewhat perplexing that inhibition of glycolysis would promote IFNγ in Th17 skewed T cells. Taken together, these data show that Th1 cells may be more metabolically flexible when one pathway is inhibited, whereas Th17 cells are more stringently reliant on both glycolysis and glutaminolysis.

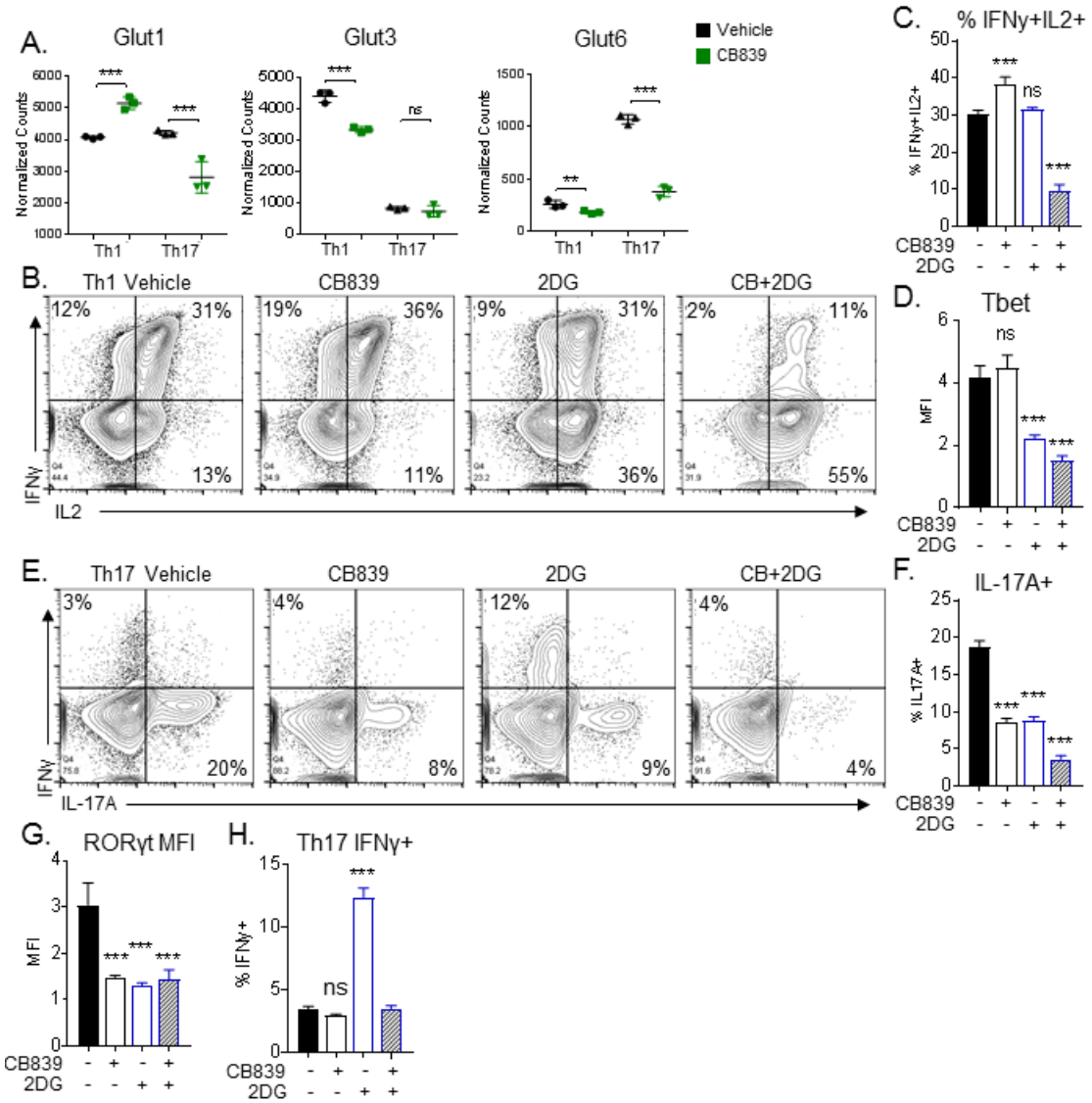

Figure 30: Th1 cells rely on glycolysis when glutaminolysis is inhibited.

(A) RNA expression by RNA-Seq of glucose transporters Glut1, Glut3, and Glut6 in Th1 and Th17 cells with or without CB839. (B-D) CD4+ T cells in Th1 skewing media. (B) FACs plots showing cytokine producers with or without CB839, 2-DG, or combination CB839 + 2-DG at 1 mM. (C) Average of n = 3 replicates of %IFNγ+IL2+ producers from (B). (D) Tbet expression in Th1 cells as in (B) (left) and average Tbet MFI of n = 3 replicates (right). (E-H) CD4+ T cells in Th17 skewing media. (E) FACs plots showing cytokine producers after five days culture as in (B) but with Th17 cells. (F) Percent IL-

17A producing Th17 cells from (E) averaged from n = 3 replicates/group. (G) Median fluorescence intensity of RORγt in Th17-skewed T cells as in (E). (G) Percent IFNγ+ Th17 cells as in (E).

4.2.3 Glutamic-Pyruvate Transaminase 2 (GPT2) may promote Th1 adaptation to GLS inhibition

The primary source of glutamate in T cells comes from GLS but can be generated via asparagine synthetase (ASNS), which requires aspartate, glutamine, and ATP to generate glutamate. Glutamate is also generated by GOT, which converts a-KG to glutamate using aspartate and generating oxaloacetate. Both ASNS and GOT require aspartate as the nitrogen donor but ASNS uses glutamine as the carbon backbone to generate glutamate rather than α-KG. From RNA-Seq data, GLS-deficient Th1 and Th17 cells both upregulated the surface aspartate transporter *Slc25a12* but did not upregulate the mitochondrial aspartate transporter *Slc25a13* (Figure 31A). *Got1* expression is low in T cells (Figure 8C) but another isoform, *Got2*, is high expression by RNA and differentially regulated in Th1 and Th17 cells (Figure 31B). Th1 cells increased RNA expression of *Got2*, whereas Th17 cells decreased. *Asns* was not changed in Th1 cells but was again downregulated by Th17 cells (Figure 31C). Despite the upregulation in transporter for aspartate, both Th1 and Th17 treated with CB839 had decreased intracellular aspartate levels. Lower intracellular aspartate is indicative of either decreased uptake, or increased use of aspartate. In vitro concentrations of aspartic acid

may be limiting, as they are 150 μM in RPMI media, which is approximately 10-fold less than glutamine levels (2 mM). Importantly, however, GOT2 requires a-KG to generate glutamate and vice-versa. Both a-KG and glutamate have reduced availability in GLS-deficient T cells.

Glutamic-pyruvic transaminase (GPT) has been shown to be important in tumorigenesis and mitochondrial stress (Coloff et al., 2016). Inhibition of GLS reduces available glutamate and α-KG in both Th1 and Th17 cells (Figure 16A and 18A). *Gpt1* has low expression in T cells but *Gpt2* is highly expressed and increases expression in Th1 cells upon GLS inhibition (Figure 31D). To test whether alanine was being consumed by Th1 and Th17 cells, CD4+ T cells were skewed to these subsets with or without CB839. Supernatant was collected after five days and alanine levels were quantified by Nuclear Magnetic Resonance (NMR). Th1 cells and Th17 cells tend to secrete alanine into the media, but upon GLS inhibition, alanine uptake increased strongly in Th1 cells but only modestly in Th17 cells (Figure 31E). Alanine is not added to RPMI media during formulation, so we tested RPMI complete media which contains fetal bovine serum. On average, NMR analysis revealed alanine levels in RPMI containing serum was around 130 μM from multiple types of sera (Figure 31F). This is similar to the level of aspartic acid, which may become limiting during high metabolic activity. Indeed, Th1 and Th17 cells treated with GLS inhibitor CB839 had reduced

intracellular alanine compared to controls (Figure 31G). Further, CD4+ T cells activated on αCD3/CD28 over 3 days had decreased glucose carbons being shunted to alanine compared to control, suggesting other sources of alanine – such as alanine uptake (Figure 5A). To test whether increasing levels of alanine allowed for increased responses to CB839 by replenishing glutamate levels, Th1 cells were skewed over 5 days in the presence of CB839, 1 mM alanine, CB839 + 0.25 mM alanine, or CB839 + 1 mM alanine. At day 5, no significant changes in cell number was observed with added alanine to CB839 groups (Figure 31I). At day 5, Tbet levels were slightly reduced in Th1 cells dosed with 1 mM alanine alone. In combination with CB839, however, 0.25 mM alanine enhanced Tbet expression (Figure 31J). This leads us to conclude that alanine may not be limiting in this setting, though it may have some role in differentiation. Both GOT2 and GPT2 rely on levels of a-KG and glutamate which are both reduced in GLS-deficient Th1 cells. Therefore, these results may suggest that availability of glutamate and a-KG dominate the adaptive response to glutaminolysis inhibition.

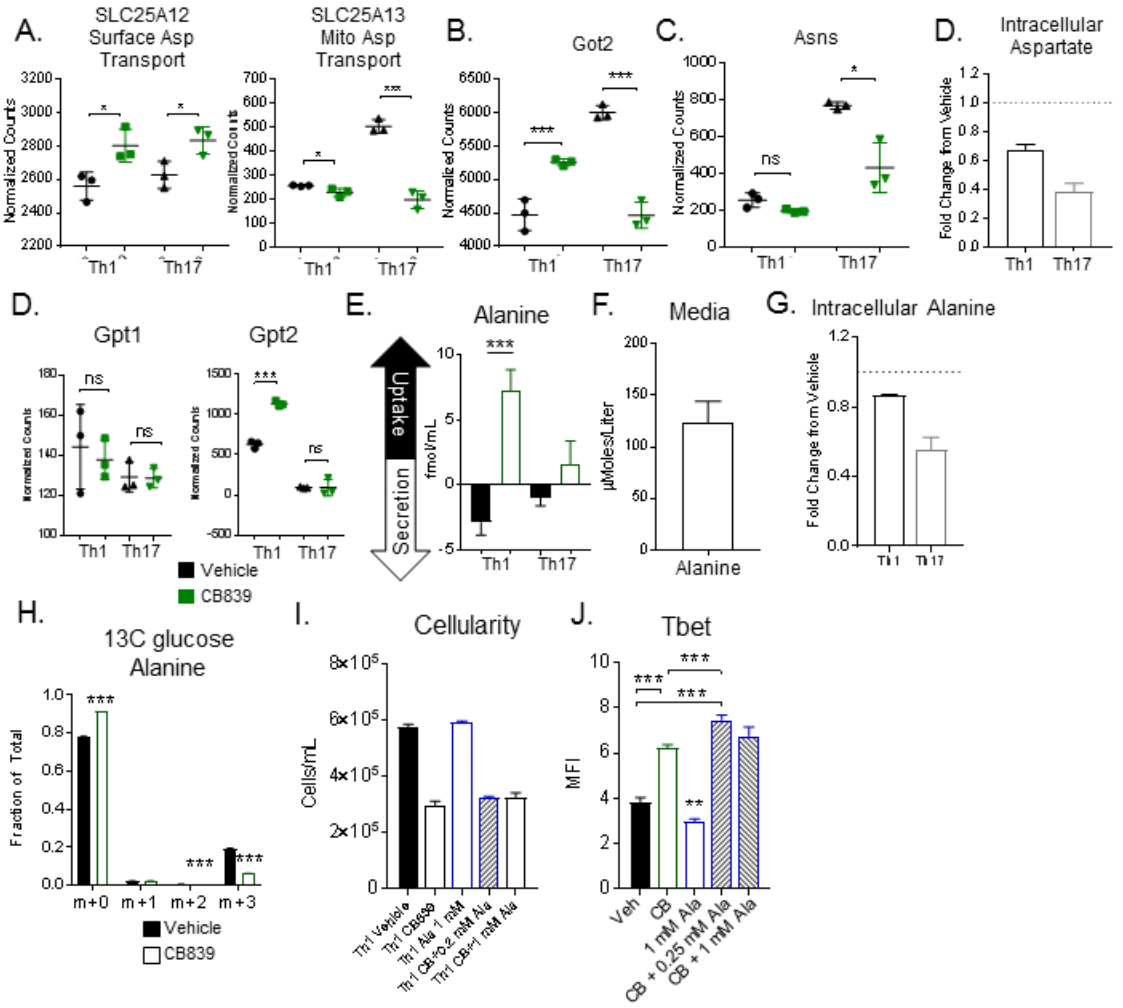

Figure 31: GOT2 and GPT2 are differentially regulated in Th1 and Th17 cells treated with CB839, pointing to aspartate and alanine as limiting metabolic points.

A) Aspartate transporter on cell surface (left) and mitochondria (right) expression by RNA-Seq. B) Got2 expression as in A. C) Asns expression as in (A). (D) Intracellular aspartate metabolite levels in Th1 and Th17 cells treated with CB839. Dotted line is vehicle levels. D) GPT1 (left) and GPT2 (right) RNA expression as in A. E) Alanine uptake in Th1 and Th17 cells treated with CB839. F) Alanine concentration in RPMI media used for in vitro experiments by Nuclear Magnetic Resonance (NMR). (H) Alanine carbons derived from 13C glucose tracing. (I) Cell count of CD4+ T cells in Th1 skewing media for 5 days with added alanine (Ala) alone or in combination with CB839. (J) Protein expression of Tbet as in (I).

4.3 Discussion

Metabolic flexibility helps organisms and cells respond to a constantly changing environment. Multiple sources of energy like glucose, fatty acids, and amino acids would clearly be useful to actively proliferating cells but may come with liabilities that prevent T cell function or enhance function too much. Inhibited T cell responses would lead to poor control of immune insults and enhanced responses would tend toward auto-immune or pro-inflammatory responses. The perfect balance, therefore, would be important to maintain while still being able to adjust for changing conditions external to the cell.

Inhibition of the glutamine transporter ASCT2 prevented Th17 cell differentiation and cytokine production yet enhanced slightly Th1 differentiation. This matched similar responses to inhibition of GLS. However, Nakaya and colleagues showed that both Th1 and Th17 cells were inhibited by full-body knockout of *Asct2*. This could mean one of four things: 1) ASCT2 has an important role outside of glutamine transport which is not recapitulated during inhibition, 2) Glutamine transport by ASCT2 may have some developmental role in other cells that support T cells, 3) Knockout of the protein is more complete than inhibition by the drug, or finally 4) Knockout of the protein allowed for T cells to adapt early on to make up for the loss of ASCT2. If 4) is true, then there will be differences between chronic and acute inhibition of ASCT2.

ASCT2 interacting proteins could be looked at by immunoprecipitation and pulldown of SLC1A5-interacting proteins. It is possible that binding partners may allow for more than just glutamine transport, which may explain the differences. Developmentally, the only way to rule out supporting role of ASCT2 would be to test other cell types that express the transporter. The liver may be an important place for glutamine uptake, as glutamine is important for supporting gluconeogenesis. ASCT2 knockout animals may be more susceptible to hypoglycemia if the liver cannot uptake glutamine appropriately.

Previous studies on glycolysis in T cells showed that deletion of the glucose transporter Glut1 prevented Teff activation and was protective in inflammatory mouse model of colitis (Macintyre et al., 2014). Moreover, inhibiting glycolysis with the glucose competitive inhibitor 2-DG enhanced CD8+ memory formation, which, when adoptively transferred to mice, had higher proliferation, persistence, and cancer killing (Sukumar et al., 2013). Here we showed that 2-DG has no effect on Th1 cytokine production *in vitro*, despite lower cell numbers at later time points. However, 2-DG in combination with CB839, Th1 cells rapidly lost IFNγ producers without preventing IL-2. As memory T cells have a higher potential for proliferation and cytokine production during secondary challenges, it would be interesting to verify whether 2DG or combination 2DG and CB839 enhance memory populations and recall responses in vivo. Additionally, 1 mM 2-DG enhanced IFNγ producers in Th17 skewing conditions. This result in Th17 cells has

not been reported in literature, but glycolysis has been shown to be required for IFNγ production in Th1 cells. 2-DG has additional effects on cells beyond inhibiting glycolysis, including activation of AMPK signaling pathways and induction of autophagy. Because AMPK signaling alters metabolic programming, the role of AMPK in Th17 differentiation and cytokine production should be explored. A recent study on the balance of Th17 and Treg showed that AICAR, an activator of AMPK, prevented Th17 differentiation and induced Treg via enhanced fatty acid oxidation (Gualdoni et al., 2016). It is possible that IFNγ production is not directly related to glycolysis, but available acetyl-CoA (Peng et al., 2016). Activation of AMPK to promote fatty acid oxidation could enhance acetyl-CoA levels which allows for changes in differentiation, even in Th17-skewing media. Thus, it will be important not only to look at memory formation in the presence of 2-DG, but also adaptive mechanisms to alter differentiation in T cell subsets.

We also showed increased aspartate and alanine uptake in CD4 T cell subsets treated with CB839. Multiple transaminases use aspartate and alanine, such as GOT2 and GPT2. We show that these enzymes are differentially regulated in Th1 and Th17 cells which may point to their involvement in Th1 adaptation to GLS inhibition. However, addition of alanine did not significantly alter Th1 function. We have not tested whether complete removal of aspartate or alanine would prevent Th1 responses

to GLS inhibition. Dialyzed serum has significantly reduced fatty acids and amino acids. Using dialyzed serum, we could test whether availability of these two amino acids supports Th1 adaptations. Unfortunately, dialyzed serum is not well-tolerated by T cells and may introduce more variables into the experiments.

While alanine may not be limiting *in vitro*, it will be important to test whether GPT2 and GOT2 expression affects the adaptive response. If knockout of these transaminases prevents Th1 adaptive response, we can then try and overexpress these transaminases in Th17 cells, which have low RNA expression. Aspartate transporter SLC25A12 was increased in Th17 cells as well which may allow Th17 cells to respond to GLS inhibition by increasing glycolysis to generate a-KG and promote transamination to glutamate. The results of these studies here show additional glutaminolytic pathways that can alter T cell function. It expands upon the known roles of glycolysis inhibition by 2-deoxyglucose and identifies acute glutamine uptake via ASCT2 as a potential Th17 therapeutic in inflammatory settings.

5. Conclusions

The work shown here expands upon the role of glutaminase and glutaminolysis in T cells. The primary conclusions of this work are 1) T cells rely on glutaminase to feed carbons into the TCA cycle, and when GLS inhibited, CD8+ T cells enhance effector function. 2) Glutaminase inhibition defaults mouse T cells to a Th1-like programming and enhances effector responses, potentially through epigenetic enzyme JMJD3 while inhibiting Th17 via reactive oxygen species. This is intriguing because it shows that we can target different subsets of effector T cells for therapy. 3) *In vivo* inflammatory and Chimeric Antigen Receptor (CAR) T cell responses in GLS KO T cells were blunted, indicating that permanent loss of GLS is deleterious. Contrasting this, in the same CAR T cell and vaccinia virus models (CTL and Th1-specific responses, respectively), temporary inhibition using the GLS inhibitor CB839 promoted T cell survival and proliferation. 4) Th1 cells adapt to metabolic inhibition of glycolysis and glutaminolysis whereas Th17 cells do not. Th1 cells could generate cytokines and survive despite inhibition of glutamine transport, glycolysis, or GLS. Th17 cells had the opposite response, with reduced differentiation and cytokine production. This may lead to new therapies to enhance Th1 viral responses or prevent IFNγ production in a two-pronged metabolic approach.

5.1 Glutaminase inhibition leads to enhanced effector function after initial inhibition in CD4+ and CD8+ T cells.

Based on T effector cell requirements to proliferate and grow, it seems counterintuitive that inhibition of glutaminase would tend to promote T cell activity. T cells rely on glycolysis and glutaminolysis to function effectively *in vivo*. However, the data described here does not contradict these claims. Instead, what we find is that glutaminase may act cell-autonomously to partially dampen the effector cell responses to prevent over-activation and induction of exhausted cell phenotype. The interplay between alternative sources of carbons and ATP can have profound effects on T cell function. Indeed, Treg are known to be insensitive to glucose uptake inhibition by 2-deoxyglucose and were still functional despite loss of glucose transporter Glut1. However, Teff responses were dependent on Glut1 and prevented effector cytokine production and differentiation (Macintyre et al., 2014). We show here that when glutaminase (GLS) is inhibited by CB839, activated T cells rely on transport of pyruvate into the mitochondria to maintain oxidative phosphorylation. This leads to glucose uptake, and in Th0 settings, where cells were activated without additional cytokine generation, GLS inhibition enhanced IFNγ production and differentiation to a more effector state. This meshes nicely with literature showing that enhanced glucose flux also increases IFNγ in T cells. However, GLS inhibition also induced surface markers of exhaustion such as Lag3 and PD-1, which, when bound to their cognate proteins, can

modulate T cells into an anergic and exhausted state. It may be that glutaminolytic machinery provides biosynthetic intermediates necessary for T cell growth and activation, which allows cells to use glucose at a moderate level for ATP to prevent early exhaustion. For example, Siska and colleagues showed that tumor infiltrating lymphocytes (TILs) in renal cell carcinoma had reduced glucose uptake, increased mitochondrial mass, and were in an anergic state (Siska et al., 2017). It is unclear whether the cells were initially hyper-activated (increasing glucose use) and then became anergic, or whether the tumor microenvironment prevented upregulation of key metabolic signaling pathways (via checkpoint proteins such as PD-1).

Interestingly, the tumor microenvironment can also have profound effects on T cells. Renal cell carcinoma is known to uptake glucose and produce large amounts of lactate. Lactate, a primary end metabolite of glycolysis in tumor cells (Romero-Garcia et al., 2016) and in T cells (Macintyre et al., 2014), can have significant effects on immune cell infiltration. Treg cells were shown to use lactate as a source of carbons when glucose availability is low (Angelin et al., 2017). Lactic acid itself prevented inflammatory responses of LPS-induced genes in humans (Peter et al., 2015). In the case of tumor cells or the surrounding environment being conducive to inducing anergy, GLS deficient CD4 and CD8+ T cells may be particularly sensitive to additional nutrient starvation or checkpoint inhibition. However, in many cases, the push and pull between proliferation,

cytokine production, memory formation, and T cell exhaustion all form an appropriate T cell response during immune insult.

To test whether the exhaustion response in glutaminase-inhibited CD8+ CTLs are truly more sensitive to checkpoint inhibition, several experiments will need to be tested. First, ectopic expression of the cognate ligand for PD-1, PDL-1, could be induced in xenograft tumors to see if GLS-KO CTLs are more sensitive to inhibition – thus allowing cancer cells to grow over wild type. To test for the direct interaction, an anti-PD-1 antibody could be dosed at the same time to disrupt PD-1:PDL-1 interaction. If GLS-deficient CD8 cells can induce tumor cell lysis and prevent tumor growth in the presence of anti-PD-1 antibody better than wild type control, we would conclude that glutaminase enhances effector responses but also makes them more susceptible to exhaustion. Given the role that both CD4+ T cells (Linnemann et al., 2014) and CD8+ T cells have on tumor elimination, it will be very important to elucidate whether inhibition of GLS truly enhances tumor killing *in vivo*.

5.2 Glutaminolysis promotes Th17 via ROS but inhibits Th1 effector function in an mTORC1 dependent fashion

Modulating glutaminolysis at different enzymatic steps has varied effects on T cell differentiation and function. Inhibition of GOT1, the transaminase responsible for generation of α-KG and aspartate from oxaloacetate and glutamate, lowered 2-

hydroxyglutarate production and promoted Foxp3+ Treg differentiation while reducing Th17 (Xu et al., 2017). Deletion of the primary glutamine transporter ASCT2 prevented activation of both Th1 and Th17 cells and reduced mTOR activation but did not reduce proliferation (Nakaya et al., 2014). Here we show that inhibition at the level of GLS prevented Th17 differentiation and proliferation, but counter-intuitively promoted Th1 effector phenotypes. Despite early reductions in proliferation in both Th1 and Th17 cells, Th1 cells eventually overcame the GLS inhibition, likely through promoting glucose uptake and epigenetic modifications. These Th1 responses were dependent on IL-2, which has been shown to regulate α-KG -dependent gene signatures (Chisolm et al., 2017). Additionally, Th1 cells treated with CB839 were exquisitely sensitive to inhibition of mTOR by rapamycin. We suggest, but do not prove specifically here, that altered gene signatures in Th1 cells in the presence of IL-2 allows these cells to adapt. To test whether IL-2 has a transcriptional activity promoting mTOR dependency, T cells treated with CB839 with or without IL2, in the presence or absence of rapamycin could be differentiated into Th1 cells. RNA Seq could then be performed and gene-set enrichment analysis run to identify pathways dependent both on IL-2 and rapamycin.

T cell reprogramming after activation through the TCR is modulated by PI3K and mTOR signaling. We show in this work that PIK3IP1, a surface membrane protein with a p85-like subunit to bind PI3K, has modulatory effects on Th1 cells. By CRISPR

knockout we see increased IFNγ cytokine production, while overexpression of PIK3IP1 reduces it. We also show that an antibody targeting PIK3IP1 reduces mTORC1 activation and enhances the naïve portion of T cells in response to αCD3/CD28 stimulation. While the *in vitro* results are very promising, a key point to address is whether this has *in vivo* efficacy. This inhibition of mTOR and reduction in cytokines could be useful in inflammatory settings related to IFNγ production. We have yet to show a role in Th17 cells, however, their expression of PIK3IP1 by RNA is quite low, and so we would not expect responses there. Primarily, though we have shown a correlation between PIK3IP1 expression and Th1 cell function, we do not know the mechanism behind these modulatory effects. PI3K signaling pathways can be addressed via western blot. Additionally, mutations in the p85 region of the PIK3IP1 protein could be generated that prevent binding of PI3K and reduce inhibition. Finally, because TBET drives both Th1 and CD8+ CTL transcriptional programming, it will be important to test whether CD8+ T cells also have modified mTORC and PI3K signaling.

Glutamate is the primary amino acid downregulated by GLS inhibition. However, there are several different transaminases that can generate glutamate in the absence of GLS activity. For example, GOT can generate glutamate from α-KG, consuming aspartate and generating oxaloacetate. The aspartate transporter SLC25A12 is upregulated in both Th1 and Th17 cells and aspartate levels are low in both cell types.

It is possible that GOT activity is ongoing in both Th1 and Th17 cells, however we do not have direct evidence that it is specifically regulating the Th1 and Th17 phenotypes. GPT, also known as alanine transaminase, can catalyze glutamate from alanine and α-KG. From RNA-Seq data, we show that GPT2 is differentially regulated in Th1 and Th17 cells. GPT2 was found to couple glycolytic metabolism with glutamine to feed the TCA cycle in colon cancer cells and knockdown of GPT2 prevented tumor proliferation (Smith et al., 2016). *Gpt2* is upregulated in Th1 (Figure 31D) and it is possible that GPT2 is a key metabolic target of IL-2 signaling that promotes Th1 differentiation during GLS inhibition. As shown in data section 4, alanine uptake in Th1 cells is strongly increased versus control which also points to alanine as substrate for adapting metabolism. *Gpt1* is not well expressed by RNA. Adding alanine to GLS-deficient Th1 cells did not strongly modify differentiation (Figure 31I and 31J) which could mean that alanine is not limiting in RPMI media. Unfortunately, removing alanine from serum would require dialyzed serum, which is not tolerated by T cells well. To get at whether GPT2 is regulating Th1 differentiation, CRISPR will be used to knockout GPT2 in murine T cells treated with CB839. This will help determine whether adaptation to GLS inhibition by GPT2 promotes effector T cell responses and enhances IFNγ and TBET. To test whether GPT2 directly promotes T cell differentiation, overexpression of GPT2 by retrovirus could be used in naïve T cells activated on αCD3/CD28. Overexpression of GPT2 may drive IFNy

production by itself, and we will test whether overexpression will allow Th17 cells to adapt to GLS inhibition and promote IL-17 cytokine production.

Th17 cells were, in contrast, adversely affected by ROS generation which could be rescued by n-acetylcysteine (NAc). Strangely, despite increases in cellular ROS in both Th1 and Th17 cells, Th1 cells were not rescued by addition of NAc. Th1 cells also had increased mitochondrial ROS levels in response to GLS inhibition, which did not occur in Th17 cells (Figure 19E). It may be that mitochondrial ROS elimination by superoxide dismutases is enhanced in Th1 cells compared to Th17. This can be tested by western blot to probe for SOD1 and SOD2 in Th1 and Th17 cells to determine whether there is increased protein in mitochondria responsible for eliminating ROS. Alternatively, GSHR is responsible for glutathione recycling from oxidized GSSG to its active, reduced form GSH. Th17 cells are particularly sensitive to ROS levels (Gerriets et al., 2015) and our data are suggestive that *de novo* synthesis of GSH is impaired upon GLS inhibition (Figure 9B). To test whether GSH recycling is important for Th1 response to GLS inhibition, we can knock down *Gshr* using CRISPR/Cas9 in Th1 cells in the presence of CB839, which will reduce the available recycling component and render Th1 cells vulnerable to ROS levels.

5.3 Inflammatory responses in vivo *require GLS and temporary inhibition of GLS promotes T cell survival and proliferation.*

The conclusions of enhanced effector Th1 and reduced Th17 cells in vitro and in vivo were based entirely on murine models of inflammation and cancer. An important consideration in these conclusions are that murine T cells and immune systems, while similar to human, do not recapitulate human disease perfectly. Indeed, in some cases, murine mouse models have been notoriously poor at predicting preventative or therapeutic medicine in clinical trials (Webb, 2014). However, memory T cells in both human and mouse have been shown to increase T cell responses in acute viral responses (Wherry and Ahmed, 2004). More recently, memory formation in cancer-specific CD4 and CD8+ T cells has become an important target of therapy (Sukumar et al., 2013). Memory T cells utilize oxidative metabolism compared to effector T cells, increased AMPK signaling (van der Windt et al., 2012), and a heightened ability to respond to immune challenges.

CB839 treatment enhanced *in vivo* cell numbers in vaccinia virus and CAR T cell models compared to control (Figure 28D and 28F). Discerning whether this is due to increased memory formation, survival, or enhanced proliferation will yield interesting biological and clinical questions. For example, if memory T cell formation is enhanced in CAR T cells treated with CB839 *ex vivo*, this may indicate significant clinical benefit to immune surveillance against B cell leukemias. However, if proliferation is merely

enhanced, that would suggest that the T cells are just increasing effector function and in fact may lead to reduced clinical significance as Teff populations do not survive long-term. To test whether CB839-treated CAR T cells enhance memory formation, we can use flow cytometry techniques to phenotype the adoptively transferred CAR T cells up to two months after initial transfer. We will look at markers of memory in mice, including longevity of CAR T, CD62L and CD44 expression, and AMPK-targeted signaling at both early and late time points. Proliferation will be assessed by staining CAR T cells with proliferative dye Cell-Trace Violet (CTV) before adoptive transfer. At early time points, up to a week after transfer, CTV is used. Another marker of proliferation is Ki67, which can be used longer-term than CTV (Gerriets et al., 2016). We show evidence of increased Ki67 in CD8+ CTLs treated with CB839 (Figure 13H). Because T cell numbers could be a result of reduced apoptotic cells, cleaved Caspase3 and expression of BCL-2 family proteins can be assessed by flow cytometry at the same time. Further, re-introduction of B cell leukemia cells after initial B cell loss would provide a functional readout of T cell memory formation, as memory cells confer immunity against re-challenge.

CB839 is already being dosed in clinical trials for cancer indications. However, primary readouts do not include immune cell phenotyping. Because clinical trials are expensive and time consuming, the first step to determine human efficacy will be to

recreate some of the *in vitro* evidence of GLS reliance in CD4 and CD8+ T cells isolated from healthy human donors. Skewing of human T cells into Th1, Th17, and Treg subsets has become viable in the past few years (Burgler et al., 2009; McGeachy and Cua, 2008). Cytokines required for this differentiation do not entirely match murine. Indeed, the role of TGFβ in human T cell differentiation is much less clear than in mice, as it was found to inhibit Th17 development in humans (Acosta-Rodriguez et al., 2007). These differing cytokine milieu profiles could alter responses to downstream activation and mTOR signaling, which we show here to be important in T cell responses to GLS inhibition. The goal of *in vitro* human T cell experiments would be to test whether differentiation and activation matches the responses seen in mice. These results would then inform the forthcoming clinical trials. The most exciting possibility is that CAR T cells generated in the presence of GLS inhibitor CB839 could enhance CAR T cell function and survival in B cell leukemia patients. This may allow for cost savings, as well, as fewer CAR T cells would be required to infuse.

One of the problems inherent in human testing is variation amongst the population. Gene status, immune system health, etc., can all affect how T cells respond to manipulations. Murine models are genetically identical and we can control the environment much more accurately. Therefore, it will be important to test larger numbers of human donors both *in vitro* and *in vivo*.

The mechanism behind increased survival and proliferation has yet to be mechanistically shown. Though this work suggests epigenetic factors based on α-KG levels could be the answer, they have not been directly tested. TET2 loss in a murine model of viral infection promoted memory CD8+ T cell formation and better viral recall response (Carty et al., 2018). And recently, a patient report showed that accidental inactivation of TET2, a DNA methyltransferase, promoted CAR T cell activation that became the dominant clonotype in a B cell leukemic response. Lentiviral insertion of the CAR T construct is random and happened to insert into the TET2 locus. Importantly, the TET2 disruption promoted a central memory phenotype in these CAR T cells in humans (Fraietta et al., 2018). This rare event lends credence to the idea that epigenetic manipulation of CAR T cells could have therapeutic benefit to patients.

The JMJD3 inhibitor, GSKJ4, was used here to show that CB839 dosing phenocopies JMJD3 inhibition in T cells. There are many methyltransferases and demethylases, so to test whether JMJD3 is indeed the target, we will use the CRISPR/CAS9 system to delete JMJD3 in Th1 cells and see if it copies the JMJD3 inhibitor and CB839 dosing. However, this does not precisely target the reason why α-KG levels enhance proliferation and survival. JMJD3 may bind specific sites regulating cell cycle (CDKs) or survival genes (Bcl-2, Bax, etc) to demethylate. Chromatin IP (ChIP) Seq for JMJD3 can be performed on human T cells treated with CB839, both in standard

activation on aCD3/CD28 and in the CAR T cell model. This will pinpoint DNA sites bound by JMJD3 specific to GLS inhibition. Bisulfite sequencing can then be used to measure the methylation status of target gene loci (Hodges et al., 2009).

Metabolic machinery have roles outside of their known enzymatic activity. GAPDH, for example, can bind mRNA and affect transcription of target proteins, like IFNγ production in T cells (Chang et al., 2013). While this particular mechanism is still being debated (Peng et al., 2016), it is possible that GLS may also bind and affect mRNA. ChIP-Seq for GLS could yield a new activity for glutaminase. As the enzymatically active GLS is a homo-tetramer, the inactive dimer form may moonlight in separate biologic activities. The chemical class derived from BPTES all disrupt the homo-tetramer formation (Thangavelu et al., 2014). In this case, we can easily inhibit tetramer formation of GLS using CB839 or BPTES, and ChIP GLS in both active and inactive states.

5.4 Th1 cells are more metabolically flexible than Th17 cells

2-deoxyglucose dosing in Th1 and Th17 cells reduces proliferation and effector differentiation (Gerriets et al., 2015). We show here that counter to what is published, glycolysis-inhibited Th1 cells seem to generate cytokines just as well as control, despite reduced proliferation. It was only in combination with CB839 that IFNγ production dropped. It is possible that AMPK activation by 2-DG has a role to play in this as the AMPK-activating aspect of 2-DG in T cells has not been shown. To test whether AMPK

is necessary for the 2-DG response, AMPK knockout T cells could be skewed to Th1 in the presence of CB839, 2-DG, and combination CB839+2-DG. Without AMPK to induce fatty acid oxidation, Th1 cells may not be able to continue in the face of glycolytic inhibition.

Both GOT2 and ASNS utilize aspartate to generate glutamate. A potential problem with knocking out GOT2 or ASNS separately could be that either enzyme would still potentially make up for the loss of the other. This functional redundancy could muddy the interpretation of the data if it is unsuccessful. However, one could potentially knockout both GOT2 and ASNS together, as they likely do act in some way to restore glutamate levels. In this case, only the conversion to glutamate from GPT2 and GOT2 would be contributing to glutamate levels. However, based on metabolite levels *in vitro*, the primary enzyme responsible for glutamine to glutamate conversion is GLS.

If aspartate or alanine are responsible for metabolic adaptation in Th1 cells, it would be important to understand where the nitrogen and carbon groups are coming from. GPT2 generates pyruvate from alanine and α-KG, which could be further metabolized by PDH to enter the TCA cycle, or it could be shunted into the cytosol for conversion to lactate by LDH. Aspartate, on the other hand, could be used to generate oxaloacetate and glutamate via GOT. This can be directly tested by 13C-labeled aspartate or alanine to trace carbons by metabolomics. However, the GOT2 and GPT2

reactions are likely futile in low intracellular glutamate and α-kG levels. They both rely on α-KG or glutamate availability. We showed that add-back of dimethyl alpha ketoglutarate (DMaKG) rectified Th1 responses. The GOT2 or GPT2 reactions could also be important in the response of GLS-inhibited Th1 cells to DMaKG, beyond the epigenetic component as described (Figure 18C and 18D). If knockout of GOT2 in CB839-treated Th1 cells prevents rectification with addition of DMaKG, we would conclude that GOT2 is active only when a-KG is available to regenerate glutamate in GLS-deficient T cells. Conversely, if there is no change in the rectification during GOT2 knockout, we would conclude that a-KG acts primarily as either biosynthetic intermediate for the TCA or to inhibit epigenetic enzymes.

The biological basis for cell-autonomous adaptive metabolism could be that in tumor environments or inflammatory sites, cells that can still enact host defenses in the face of nutrient shortages would be beneficial. However, why Th1 cells would be more able to adjust for changing nutrient availability than Th17 remains unknown. It is possible that IL-2 allows for alterations in accessible DNA in Th1, thus ability to transcribe and translate new metabolic machinery. It will be important to dissect further the role of IL-2 and mTORC1 in the future. We show that without IL-2, Th1 cell adaptation is the same, or worse than, GLS-deficient Th17 cells. One way to test this would be to look at transcription in GLS-deficient or control Th1 cells treated with or

without IL-2 by RNA-Seq. This may point to particular programs promoted by IL-2 that allow for survival that do not get induced when IL-2 is absent. These particular genes could then be targeted for inhibition or knockout in Th1 cells. This could be compared to other cell types, such as cancer cell lines, that are known to be insensitive to GLS inhibition. In some cell lines, pyruvate carboxylase is important in these cell lines, and so pyruvate carboxylase (PCX) could be deleted in GLS-deficient Th1 cells. If this prevents Th1 effector responses, we could conclude that PCX is necessary for metabolic adaptation in Th1 cells.

5.5 Concluding Remarks

The work here describes the role of the metabolic enzyme glutaminase (GLS) in activated or differentiated T cells. It expands on the notion that metabolic perturbations can induce functional outcomes, and that metabolic upregulation is not just a mass action response to growth signals in proliferating cells. Previous work has shown that the glucose transporter, Glut1, is imperative for effector T cell responses, as T cells without Glut1 cannot upregulate glycolysis and fail to induce inflammatory responses *in vivo*. While inhibition of glutamine transport ASCT2 also prevented CD4+ T cell effector function, this work shows that inhibition of glutaminolysis at different steps in the pathway yields considerably different responses in T cells. Significantly, GLS inhibition led to enhanced Th1 differentiation and function but inhibited Th17, indicating that GLS

functions to promote Th17 cells but put the brakes on Tbet-driven Th1 and CTLs. Th1 and CTL cells adapted to glutaminolysis inhibition by upregulating glucose uptake, enhancing cytokine production and differentiation. Th17, in contrast, failed to adapt and reduced proliferation and cytokine production. We have teased apart the notion that glycolysis and glutaminolysis go hand-in-hand; Th1 cells can increase glycolysis in response to inhibition of a major TCA carbon source, whereas Th17 cannot. Th1 metabolic flexibility may be driven by IL-2 programming, in which mTORC1 nutrient sensing is particularly well-tuned and allows adaptive metabolic responses. Th17 cells do not respond similarly to IL-2, and this may lead Th17 cells into requiring both glycolysis and glutaminolysis to function.

Beyond GLS, much is still unknown about how ASNS, GLUDs, GOTs, and GPTs affect T cell activity. GOT1 knockout modified Treg/Th17 balance but no data about Th1 or Th2 cells was reported (Xu et al., 2017). Interestingly, the argument proposed by Xu and colleagues is that increased 2-HG promotes Th17. Here, we show that despite increased 2-HG in both Th1 and Th17 cells treated with CB839, induction of Treg did not occur. Clearly, there is much we don't know about the glutamine catabolic pathways. These pathways can be quickly interrogated by CRISPR knockout screens, in which these other transaminases and glutaminolytic enzymes can be removed and functional T

cell responses tested. There may be even more subset-specific metabolic liabilities to explore in the realm of treating human inflammatory disease and cancer.

Metabolism is well known to be important for cell survival and energy generation, and recently it has become clear that metabolism plays an active role in cell growth and activation signals rather than a passive player in cell dynamics. Metabolic adaptation may be just as important in a constantly changing microenvironment as responses to activation signals, and indeed metabolism may be constantly communicating when and how to enact host defenses in inflammatory and cancer settings.

References

Abu Aboud, O., Habib, S.L., Trott, J., Stewart, B., Liang, S., Chaudhari, A.J., Sutcliffe, J., and Weiss, R.H. (2017). Glutamine Addiction in Kidney Cancer Suppresses Oxidative Stress and Can Be Exploited for Real-Time Imaging. Cancer Research *77*, 6746.
Acosta-Rodriguez, E.V., Napolitani, G., Lanzavecchia, A., and Sallusto, F. (2007). Interleukins 1β and 6 but not transforming growth factor-β are essential for the differentiation of interleukin 17–producing human T helper cells. Nature Immunology *8*, 942.

Acuto, O., and Michel, F. (2003). CD28-mediated co-stimulation: a quantitative support for TCR signalling. Nature Reviews Immunology *3*, 939.

Afkarian, M., Sedy, J.R., Yang, J., Jacobson, N.G., Cereb, N., Yang, S.Y., Murphy, T.L., and Murphy, K.M. (2002). T-bet is a STAT1-induced regulator of IL-12R expression in naïve CD4+ T cells. Nature Immunology *3*, 549.

Ahmadzadeh, M., Johnson, L.A., Heemskerk, B., Wunderlich, J.R., Dudley, M.E., White, D.E., and Rosenberg, S.A. (2009). Tumor antigen–specific CD8 T cells infiltrating the tumor express high levels of PD-1 and are functionally impaired. Blood *114*, 1537-1544.

Aledo, J.C., Gomez-Fabre, P.M., Olalla, L., and Marquez, J. (2000). Identification of two human glutaminase loci and tissue-specific expression of the two related genes. Mammalian genome : official journal of the International Mammalian Genome Society *11*, 1107-1110.

Allison, J.P., McIntyre, B.W., and Bloch, D. (1982). Tumor-specific antigen of murine T-lymphoma defined with monoclonal antibody. The Journal of Immunology *129*, 2293.

Angelin, A., Gil-de-Gómez, L., Dahiya, S., Jiao, J., Guo, L., Levine, M.H., Wang, Z., Quinn, W.J., Kopinski, P.K., Wang, L., *et al.* (2017). Foxp3 Reprograms T Cell Metabolism to Function in Low-Glucose, High-Lactate Environments. Cell Metabolism *25*, 1282-1293.e1287.

Araki, K., Turner, A.P., Shaffer, V.O., Gangappa, S., Keller, S.A., Bachmann, M.F., Larsen, C.P., and Ahmed, R. (2009). mTOR regulates memory CD8 T-cell differentiation. Nature *460*, 108.

Augustine, J.J., Bodziak, K.A., and Hricik, D.E. (2007). Use of Sirolimus in Solid Organ Transplantation. Drugs *67*, 369-391.

Bahrami, S., and Drabløs, F. (2016). Gene regulation in the immediate-early response process. Advances in Biological Regulation *62*, 37-49.

Banerjee, A., Gordon, S.M., Intlekofer, A.M., Paley, M.A., Mooney, E.C., Lindsten, T., Wherry, E.J., and Reiner, S.L. (2010). The Transcription Factor Eomesodermin Enables CD8(+) T Cells to Compete for the Memory Cell Niche. Journal of immunology (Baltimore, Md : 1950) *185*, 4988-4992.

Bedard, K., and Krause, K.-H. (2007). The NOX Family of ROS-Generating NADPH Oxidases: Physiology and Pathophysiology. Physiological reviews *87*, 245-313.

Beier, U.H., Angelin, A., Akimova, T., Wang, L., Liu, Y., Xiao, H., Koike, M.A., Hancock, S.A., Bhatti, T.R., Han, R., *et al.* (2015). Essential role of mitochondrial energy metabolism in Foxp3^{+} T-regulatory cell function and allograft survival. FASEB journal : official publication of the Federation of American Societies for Experimental Biology *29*, 2315-2326.

Belikov, A.V., Schraven, B., and Simeoni, L. (2015). T cells and reactive oxygen species. Journal of Biomedical Science *22*, 85.

Bennett, C.L., Christie, J., Ramsdell, F., Brunkow, M.E., Ferguson, P.J., Whitesell, L., Kelly, T.E., Saulsbury, F.T., Chance, P.F., and Ochs, H.D. (2001). The immune dysregulation, polyendocrinopathy, enteropathy, X-linked syndrome (IPEX) is caused by mutations of FOXP3. Nat Genet *27*, 20-21.

Berg, D.J., Zhang, J., Weinstock, J.V., Ismail, H.F., Earle, K.A., Alila, H., Pamukcu, R., Moore, S., and Lynch, R.G. (2002). Rapid development of colitis in NSAID-treated IL-10–deficient mice. Gastroenterology *123*, 1527-1542.

Birsoy, K., Wang, T., Chen, Walter W., Freinkman, E., Abu-Remaileh, M., and Sabatini, David M. (2015). An Essential Role of the Mitochondrial Electron Transport Chain in Cell Proliferation Is to Enable Aspartate Synthesis. Cell *162*, 540-551.

Blagih, J., Coulombe, F., Vincent, E.E., Dupuy, F., Galicia-Vazquez, G., Yurchenko, E., Raissi, T.C., van der Windt, G.J., Viollet, B., Pearce, E.L., *et al.* (2015). The energy sensor AMPK regulates T cell metabolic adaptation and effector responses in vivo. Immunity *42*, 41-54.

Blazar, B.R., Taylor, P.A., McElmurry, R., Tian, L., Panoskaltsis-Mortari, A., Lam, S., Lees, C., Waldschmidt, T., and Vallera, D.A. (1998). Engraftment of Severe Combined Immune Deficient Mice Receiving Allogeneic Bone Marrow Via In Utero or Postnatal Transfer. Blood *92*, 3949-3959.

Boyman, O., and Sprent, J. (2012). The role of interleukin-2 during homeostasis and activation of the immune system. Nat Rev Immunol *12*, 180-190.

Brand, S. (2009). Crohn's disease: Th1, Th17 or both? The change of a paradigm: new immunological and genetic insights implicate Th17 cells in the pathogenesis of Crohn's disease. Gut *58*, 1152-1167.

Buck, M.D., O'Sullivan, D., and Pearce, E.L. (2015). T cell metabolism drives immunity. The Journal of Experimental Medicine *212*, 1345-1360.

Buenrostro, J.D., Giresi, P.G., Zaba, L.C., Chang, H.Y., and Greenleaf, W.J. (2013). Transposition of native chromatin for fast and sensitive epigenomic profiling of open chromatin, DNA-binding proteins and nucleosome position. Nat Meth *10*, 1213-1218.

Burgler, S., Ouaked, N., Bassin, C., Basinski, T.M., Mantel, P.-Y., Siegmund, K., Meyer, N., Akdis, C.A., and Schmidt-Weber, C.B. (2009). Differentiation and functional analysis of human TH17 cells. Journal of Allergy and Clinical Immunology *123*, 588-595.e587.

Carr, E.L., Kelman, A., Wu, G.S., Gopaul, R., Senkevitch, E., Aghvanyan, A., Turay, A.M., and Frauwirth, K.A. (2010). Glutamine uptake and metabolism are coordinately regulated by ERK/MAPK during T lymphocyte activation. J Immunol *185*, 1037-1044.

Carty, S.A., Gohil, M., Banks, L.B., Cotton, R.M., Johnson, M.E., Stelekati, E., Wells, A.D., Wherry, E.J., Koretzky, G.A., and Jordan, M.S. (2018). The Loss of TET2 Promotes CD8⁺ T Cell Memory Differentiation. The Journal of Immunology *200*, 82.

Cemerski, S., Cantagrel, A., van Meerwijk, J.P.M., and Romagnoli, P. (2002). Reactive Oxygen Species Differentially Affect T Cell Receptor-signaling Pathways*. Journal of Biological Chemistry *277*, 19585-19593.

Cerione, J.W.E., and Richard, A. (2010). Glutaminase: A Hot Spot For Regulation Of Cancer Cell Metabolism? Oncotarget *1*.

Cham, C.M., and Gajewski, T.F. (2005). Glucose availability regulates IFN-gamma production and p70S6 kinase activation in CD8(+) effector T cells. Journal of Immunology *174*, 4670-4677.

Chang, C.-H., Qiu, J., O'Sullivan, D., Buck, Michael D., Noguchi, T., Curtis, Jonathan D., Chen, Q., Gindin, M., Gubin, Matthew M., van der Windt, Gerritje J.W., *et al.* Metabolic Competition in the Tumor Microenvironment Is a Driver of Cancer Progression. Cell *162*, 1229-1241.

Chang, C.H., Curtis, J.D., Maggi, L.B., Jr., Faubert, B., Villarino, A.V., O'Sullivan, D., Huang, S.C., van der Windt, G.J., Blagih, J., Qiu, J., *et al.* (2013). Posttranscriptional control of T cell effector function by aerobic glycolysis. Cell *153*, 1239-1251.

Chantranupong, L., Scaria, Sonia M., Saxton, Robert A., Gygi, Melanie P., Shen, K., Wyant, Gregory A., Wang, T., Harper, J.W., Gygi, Steven P., and Sabatini, David M. (2016). The CASTOR Proteins Are Arginine Sensors for the mTORC1 Pathway. Cell *165*, 153-164.

Chantranupong, L., Wolfson, Rachel L., Orozco, Jose M., Saxton, Robert A., Scaria, Sonia M., Bar-Peled, L., Spooner, E., Isasa, M., Gygi, Steven P., and Sabatini, David M. The Sestrins Interact with GATOR2 to Negatively Regulate the Amino-Acid-Sensing Pathway Upstream of mTORC1. Cell Reports *9*, 1-8.

Chassaing, B., Aitken, J.D., Malleshappa, M., and Vijay-Kumar, M. (2014). Dextran Sulfate Sodium (DSS)-Induced Colitis in Mice. Current protocols in immunology / edited by John E Coligan [et al] *104*, Unit-15.25.

Cheng, R.J.D. (2009). Q's next: the diverse functions of glutamine in metabolism, cell biology and cancer. Oncogene *29*, 313-324.

Cheng, T., Sudderth, J., Yang, C., Mullen, A.R., Jin, E.S., Matés, J.M., and DeBerardinis, R.J. (2011). Pyruvate carboxylase is required for glutamine-independent growth of tumor cells. Proc Natl Acad Sci U S A *108*, 8674-8679.

Chesler, D.A., and Reiss, C.S. (2002). The role of IFN-γ in immune responses to viral infections of the central nervous system. Cytokine & Growth Factor Reviews *13*, 441-454.

Chi, H. (2012). Regulation and function of mTOR signalling in T cell fate decisions. Nat Rev Immunol *12*, 325-338.

Chisolm, D.A., Savic, D., Moore, A.J., Ballesteros-Tato, A., Leon, B., Crossman, D.K., Murre, C., Myers, R.M., and Weinmann, A.S. (2017). CCCTC-Binding Factor Translates Interleukin 2- and alpha-Ketoglutarate-Sensitive Metabolic Changes in T Cells into Context-Dependent Gene Programs. Immunity *47*, 251-267 e257.

Coloff, Jonathan L., Murphy, J.P., Braun, Craig R., Harris, Isaac S., Shelton, Laura M., Kami, K., Gygi, Steven P., Selfors, Laura M., and Brugge, Joan S. (2016). Differential Glutamate Metabolism in Proliferating and Quiescent Mammary Epithelial Cells. Cell Metabolism *23*, 867-880.

Cooper, M.D., and Alder, M.N. (2006). The Evolution of Adaptive Immune Systems. Cell *124*, 815-822.

Curthoys, N.P., and Watford, M. (1995). Regulation of glutaminase activity and glutamine metabolism. Annu Rev Nutr *15*, 133-159.

Dang, Eric V., Barbi, J., Yang, H.-Y., Jinasena, D., Yu, H., Zheng, Y., Bordman, Z., Fu, J., Kim, Y., Yen, H.-R., *et al.* (2011). Control of TH17/Treg Balance by Hypoxia-Inducible Factor 1. Cell *146*, 772-784.

Davila, M.L., Kloss, C.C., Gunset, G., and Sadelain, M. (2013). CD19 CAR-Targeted T Cells Induce Long-Term Remission and B Cell Aplasia in an Immunocompetent Mouse Model of B Cell Acute Lymphoblastic Leukemia. PLOS ONE *8*, e61338.

DeBerardinis, R.J., Lum, J.J., Hatzivassiliou, G., and Thompson, C.B. (2008). The biology of cancer: metabolic reprogramming fuels cell growth and proliferation. Cell Metab *7*, 11-20.

DeFrances, M.C., Debelius, D.R., Cheng, J., and Kane, L.P. (2012a). Inhibition of T-cell activation by PIK3IP1. Eur J Immunol *42*, 2754-2759.

DeFrances, M.C., Debelius, D.R., Cheng, J., and Kane, L.P. (2012b). Inhibition of T-Cell Activation by PIK3IP1. European journal of immunology *42*, 2754-2759.

Delgoffe, G.M., Kole, T.P., Zheng, Y., Zarek, P.E., Matthews, K.L., Xiao, B., Worley, P.F., Kozma, S.C., and Powell, J.D. (2009). The mTOR kinase differentially regulates effector and regulatory T cell lineage commitment. Immunity *30*, 832-844.

Delgoffe, G.M., Pollizzi, K.N., Waickman, A.T., Heikamp, E., Meyers, D.J., Horton, M.R., Xiao, B., Worley, P.F., and Powell, J.D. (2011). The kinase mTOR regulates the

differentiation of helper T cells through the selective activation of signaling by mTORC1 and mTORC2. Nat Immunol *12*, 295-303.

Duncan, R.E., Ahmadian, M., Jaworski, K., Sarkadi-Nagy, E., and Sul, H.S. (2007). Regulation of lipolysis in adipocytes. Annual review of nutrition *27*, 79-101.

Eissenberg, J.C., and Shilatifard, A. (2010). Histone H3 Lysine 4 (H3K4) Methylation in Development and Differentiation. Developmental biology *339*, 240-249.

Elgogary, A., Xu, Q., Poore, B., Alt, J., Zimmermann, S.C., Zhao, L., Fu, J., Chen, B., Xia, S., Liu, Y., *et al.* (2016). Combination therapy with BPTES nanoparticles and metformin targets the metabolic heterogeneity of pancreatic cancer. Proceedings of the National Academy of Sciences *113*, E5328.

Espinosa-Diez, C., Miguel, V., Mennerich, D., Kietzmann, T., Sánchez-Pérez, P., Cadenas, S., and Lamas, S. (2015). Antioxidant responses and cellular adjustments to oxidative stress. Redox Biology *6*, 183-197.

Estenne, M., and Hertz, M.I. (2002). Bronchiolitis Obliterans after Human Lung Transplantation. American Journal of Respiratory and Critical Care Medicine *166*, 440-444.

Fathman, C.G., and Lineberry, N.B. (2007). Molecular mechanisms of CD4+ T-cell anergy. Nature Reviews Immunology *7*, 599.

Finkelman, F.D., Shea-Donohue, T., Goldhill, J., Sullivan, C.A., Morris, S.C., Madden, K.B., Gause, W.C., and Urban, J.F. (1997). CYTOKINE REGULATION OF HOST DEFENSE AGAINST PARASITIC GASTROINTESTINAL NEMATODES:Lessons from Studies with Rodent Models*. Annual Review of Immunology *15*, 505-533.

Floess, S., Freyer, J., Siewert, C., Baron, U., Olek, S., Polansky, J., Schlawe, K., Chang, H.-D., Bopp, T., Schmitt, E., *et al.* (2007). Epigenetic Control of the <italic>foxp3</italic> Locus in Regulatory T Cells. PLoS Biol *5*, e38.

Fraietta, J.A., Nobles, C.L., Sammons, M.A., Lundh, S., Carty, S.A., Reich, T.J., Cogdill, A.P., Morrissette, J.J.D., DeNizio, J.E., Reddy, S., *et al.* (2018). Disruption of TET2 promotes the therapeutic efficacy of CD19-targeted T cells. Nature *558*, 307-312.

Franz, D.N., Leonard, J., Tudor, C., Chuck, G., Care, M., Sethuraman, G., Dinopoulos, A., Thomas, G., and Crone, K.R. (2006). Rapamycin causes regression of astrocytomas in tuberous sclerosis complex. Annals of Neurology *59*, 490-498.

Galvez, J. (2014). Role of Th17 Cells in the Pathogenesis of Human IBD. ISRN Inflamm *2014*, 928461.

Gao, P., Tchernyshyov, I., Chang, T.-C., Lee, Y.-S., and Kita, K. (2009). c-Myc suppression of miR-23a/b enhances mitochondrial glutaminase expression and glutamine metabolism. Nature *458*, 762-765.

Gerriets, V.A., Kishton, R.J., Johnson, M.O., Cohen, S., Siska, P.J., Nichols, A.G., Warmoes, M.O., de Cubas, A.A., MacIver, N.J., Locasale, J.W., *et al.* (2016). Foxp3 and Toll-like receptor signaling balance Treg cell anabolic metabolism for suppression. Nature Immunology *17*, 1459.

Gerriets, V.A., Kishton, R.J., Nichols, A.G., Macintyre, A.N., Inoue, M., Ilkayeva, O., Winter, P.S., Liu, X., Priyadharshini, B., Slawinska, M.E., *et al.* (2015). Metabolic programming and PDHK1 control CD4+ T cell subsets and inflammation. J Clin Invest *125*, 194-207.

Gualdoni, G.A., Mayer, K.A., Göschl, L., Boucheron, N., Ellmeier, W., and Zlabinger, G.J. (2016). The AMP analog AICAR modulates the Treg/Th17 axis through enhancement of fatty acid oxidation. The FASEB Journal *30*, 3800-3809.

Harris, T.J., Grosso, J.F., Yen, H.-R., Xin, H., Kortylewski, M., Albesiano, E., Hipkiss, E.L., Getnet, D., Goldberg, M.V., Maris, C.H., *et al.* (2007). Cutting Edge: An In Vivo Requirement for STAT3 Signaling in T_H17 Development and T_H17-Dependent Autoimmunity. The Journal of Immunology *179*, 4313-4317.

Harty, J.T., Tvinnereim, A.R., and White, D.W. (2000). CD8+ T Cell Effector Mechanisms in Resistance to Infection. Annual Review of Immunology *18*, 275-308.

Haskins, K., Kubo, R., White, J., Pigeon, M., Kappler, J., and Marrack, P. (1983). The major histocompatibility complex-restricted antigen receptor on T cells. I. Isolation with a monoclonal antibody. The Journal of Experimental Medicine *157*, 1149.

He, X., Zhu, Z., Johnson, C., Stoops, J., Eaker, A.E., Bowen, W., and DeFrances, M.C. (2008). PIK3IP1, a Negative Regulator of PI3K, Suppresses the Development of Hepatocellular Carcinoma. Cancer Research *68*, 5591-5598.

Heinz, S., Benner, C., Spann, N., Bertolino, E., Lin, Y.C., Laslo, P., Cheng, J.X., Murre, C., Singh, H., and Glass, C.K. (2010). Simple Combinations of Lineage-Determining Transcription Factors Prime cis-Regulatory Elements Required for Macrophage and B Cell Identities. Molecular cell *38*, 576-589.

Herry, I., Neukirch, C., Debray, M.-P., Mignon, F., and Crestani, B. (2007). Dramatic effect of sirolimus on renal angiomyolipomas in a patient with tuberous sclerosis complex. European Journal of Internal Medicine *18*, 76-77.

Hidalgo, M., Buckner, J.C., Erlichman, C., Pollack, M.S., Boni, J.P., Dukart, G., Marshall, B., Speicher, L., Moore, L., and Rowinsky, E.K. (2006). A Phase I and Pharmacokinetic Study of Temsirolimus (CCI-779) Administered Intravenously Daily for 5 Days Every 2 Weeks to Patients with Advanced Cancer. Clinical Cancer Research *12*, 5755.

Hildeman, D.A., Mitchell, T., Teague, T.K., Henson, P., Day, B.J., Kappler, J., and Marrack, P.C. (1999). Reactive Oxygen Species Regulate Activation-Induced T Cell Apoptosis. Immunity *10*, 735-744.

Ho, P.-C., Bihuniak, Jessica D., Macintyre, Andrew N., Staron, M., Liu, X., Amezquita, R., Tsui, Y.-C., Cui, G., Micevic, G., Perales, Jose C., *et al.* (2015). Phosphoenolpyruvate Is a Metabolic Checkpoint of Anti-tumor T Cell Responses. Cell *162*, 1217-1228.

Hodges, E., Smith, A.D., Kendall, J., Xuan, Z., Ravi, K., Rooks, M., Zhang, M.Q., Ye, K., Bhattacharjee, A., Brizuela, L., *et al.* (2009). High definition profiling of mammalian DNA methylation by array capture and single molecule bisulfite sequencing. Genome Research *19*, 1593-1605.

Howie, D., Cobbold, S.P., Adams, E., Ten Bokum, A., Necula, A.S., Zhang, W., Huang, H., Roberts, D.J., Thomas, B., Hester, S.S., *et al.* Foxp3 drives oxidative phosphorylation and protection from lipotoxicity. In JCI Insight.

Hsieh, C., Macatonia, S., Tripp, C., Wolf, S., O'Garra, A., and Murphy, K. (1993). Development of TH1 CD4+ T cells through IL-12 produced by Listeria-induced macrophages. Science *260*, 547-549.

Jacobs, S.R., Herman, C.E., MacIver, N.J., Wofford, J.A., Wieman, H.L., Hammen, J.J., and Rathmell, J.C. (2008). Glucose Uptake Is Limiting in T Cell Activation and Requires CD28-Mediated Akt-Dependent and Independent Pathways. Journal of immunology (Baltimore, Md : 1950) *180*, 4476-4486.

Jacobs, S.R., Michalek, R.D., and Rathmell, J.C. (2010). IL-7 Is Essential for Homeostatic Control of T Cell Metabolism In Vivo. Journal of immunology (Baltimore, Md : 1950) *184*, 3461-3469.

Jewell, J.L., Kim, Y.C., Russell, R.C., Yu, F.-X., Park, H.W., Plouffe, S.W., Tagliabracci, V.S., and Guan, K.-L. (2015). Differential regulation of mTORC1 by leucine and glutamine. Science *347*, 194.

Jiao, L., and Liu, X. (2015). Structural basis of histone H3K27 trimethylation by an active polycomb repressive complex 2. Science (New York, NY) *350*, aac4383-aac4383.

Jones, W., and Bianchi, K. (2015). Aerobic Glycolysis: Beyond Proliferation. Frontiers in Immunology *6*, 227.

Katt, W.P., Lukey, M.J., and Cerione, R.A. (2017). A tale of two glutaminases: homologous enzymes with distinct roles in tumorigenesis. Future Medicinal Chemistry *9*, 223-243.

Keefe, S.M., Nathanson, K.L., and Kimryn Rathmell, W. (2013). The Molecular Biology of Renal Cell Carcinoma. Seminars in Oncology *40*, 421-428.

Kennedy, R., Mayo Vaccine Research Group, M.C.C.o.M.R.M.N.U.S.A., Celis, E., Immunology Program, H.L.M.C.C., and Research institute, U.o.S.F.T.F.L.U.S.A. (2018). Multiple roles for CD4+ T cells in anti-tumor immune responses. Immunological Reviews *222*, 129-144.

Kim, J., Kundu, M., Viollet, B., and Guan, K.-L. (2011). AMPK and mTOR regulate autophagy through direct phosphorylation of Ulk1. Nature cell biology *13*, 132-141.

Klysz, D., Tai, X., Robert, P.A., Craveiro, M., Cretenet, G., Oburoglu, L., Mongellaz, C., Floess, S., Fritz, V., Matias, M.I., *et al.* (2015). Glutamine-dependent alpha-ketoglutarate production regulates the balance between T helper 1 cell and regulatory T cell generation. Sci Signal *8*, ra97.

Knox, J.J., Cosma, G.L., Betts, M.R., and McLane, L.M. (2014). Characterization of T-Bet and Eomes in Peripheral Human Immune Cells. Frontiers in Immunology *5*, 217.

Kohli, R.M., and Zhang, Y. (2013). TET enzymes, TDG and the dynamics of DNA demethylation. Nature *502*, 472.

Kovacevic, Z., and McGivan, J.D. (1983). Mitochondrial metabolism of glutamine and glutamate and its physiological significance. Physiological reviews *63*, 547-605.

Kruidenier, L., Chung, C.-w., Cheng, Z., Liddle, J., Che, K., Joberty, G., Bantscheff, M., Bountra, C., Bridges, A., Diallo, H., *et al.* (2012). A selective jumonji H3K27 demethylase inhibitor modulates the proinflammatory macrophage response. Nature *488*, 404-408.

Laplante, M., and Sabatini, D.M. (2012). mTOR signaling in growth control and disease. Cell *149*, 274-293.

Lee, C.-F., Lo, Y.-C., Cheng, C.-H., Furtmüller, Georg J., Oh, B., Andrade-Oliveira, V., Thomas, Ajit G., Bowman, Caitlyn E., Slusher, Barbara S., Wolfgang, Michael J., *et al.* (2015). Preventing Allograft Rejection by Targeting Immune Metabolism. Cell Reports *13*, 760-770.

Lee, Y.K., Turner, H., Maynard, C.L., Oliver, J.R., Chen, D., Elson, C.O., and Weaver, C.T. (2009). Late Developmental Plasticity in the T Helper 17 Lineage. Immunity *30*, 92-107.

Li, G., Park, K., and Davila, M.L. (2017). Gammaretroviral Production and T Cell Transduction to Genetically Retarget Primary T Cells Against Cancer. In T-Cell Differentiation: Methods and Protocols, E. Lugli, ed. (New York, NY: Springer New York), pp. 111-118.

Li, H., Handsaker, B., Wysoker, A., Fennell, T., Ruan, J., Homer, N., Marth, G., Abecasis, G., Durbin, R., and Genome Project Data Processing, S. (2009). The Sequence Alignment/Map format and SAMtools. Bioinformatics *25*, 2078-2079.

Li, Y., and Seto, E. (2016). HDACs and HDAC Inhibitors in Cancer Development and Therapy. Cold Spring Harbor perspectives in medicine *6*, a026831.

Lian, G., Gnanaprakasam, J.N.R., Wang, T., Wu, R., Chen, X., Liu, L., Shen, Y., Yang, M., Yang, J., Chen, Y., *et al.* (2018). Glutathione de novo synthesis but not recycling process

coordinates with glutamine catabolism to control redox homeostasis and directs murine T cell differentiation. eLife *7*, e36158.

Liao, Y., Smyth, G.K., and Shi, W. (2014). featureCounts: an efficient general purpose program for assigning sequence reads to genomic features. Bioinformatics *30*, 923-930.

Ling, P., Gately, M.K., Gubler, U., Stern, A.S., Lin, P., Hollfelder, K., Su, C., Pan, Y.C., and Hakimi, J. (1995). Human IL-12 p40 homodimer binds to the IL-12 receptor but does not mediate biologic activity. The Journal of Immunology *154*, 116-127.

Linnemann, C., van Buuren, M.M., Bies, L., Verdegaal, E.M.E., Schotte, R., Calis, J.J.A., Behjati, S., Velds, A., Hilkmann, H., Atmioui, D.e., *et al.* (2014). High-throughput epitope discovery reveals frequent recognition of neo-antigens by CD4+ T cells in human melanoma. Nature Medicine *21*, 81.

Lobo, C., Ruiz-Bellido, M.A., Aledo, J.C., Marquez, J., Nunez De Castro, I., and Alonso, F.J. (2000). Inhibition of glutaminase expression by antisense mRNA decreases growth and tumourigenicity of tumour cells. Biochem J *348 Pt 2*, 257-261.

Locasale, J.W., and Cantley, L.C. (2011). Metabolic flux and the regulation of mammalian cell growth. Cell Metab *14*, 443-451.

Lock, C., Hermans, G., Pedotti, R., Brendolan, A., Schadt, E., Garren, H., Langer-Gould, A., Strober, S., Cannella, B., Allard, J., *et al.* (2002). Gene-microarray analysis of multiple sclerosis lesions yields new targets validated in autoimmune encephalomyelitis. Nature Medicine *8*, 500.

Lohuis, T.D., Harlow, H.J., and Beck, T.D.I. (2007). Hibernating black bears (Ursus americanus) experience skeletal muscle protein balance during winter anorexia. Comparative Biochemistry and Physiology Part B: Biochemistry and Molecular Biology *147*, 20-28.

Love, M.I., Huber, W., and Anders, S. (2014). Moderated estimation of fold change and dispersion for RNA-seq data with DESeq2. Genome Biology *15*, 550.

Lukey, M.J., Greene, K.S., Erickson, J.W., Wilson, K.F., and Cerione, R.A. (2016). The oncogenic transcription factor c-Jun regulates glutaminase expression and sensitizes cells to glutaminase-targeted therapy. Nature Communications *7*, 11321.

MacDonald, K.P.A., Blazar, B.R., and Hill, G.R. (2017). Cytokine mediators of chronic graft-versus-host disease. The Journal of Clinical Investigation *127*, 2452-2463.

Macintyre, A.N., Gerriets, V.A., Nichols, A.G., Michalek, R.D., Rudolph, M.C., Deoliveira, D., Anderson, S.M., Abel, E.D., Chen, B.J., Hale, L.P., *et al.* (2014). The glucose transporter Glut1 is selectively essential for CD4 T cell activation and effector function. Cell Metab *20*, 61-72.

MacIver, N.J., Michalek, R.D., and Rathmell, J.C. (2013). Metabolic regulation of T lymphocytes. Annu Rev Immunol *31*, 259-283.

Mak, T.W., Grusdat, M., Duncan, G.S., Dostert, C., Nonnenmacher, Y., Cox, M., Binsfeld, C., Hao, Z., Brüstle, A., Itsumi, M., *et al.* (2017). Glutathione Primes T Cell Metabolism for Inflammation. Immunity *46*, 1089-1090.

Mariette, X., Cazals-Hatem, D., Warszawki, J., Liote, F., Balandraud, N., and Sibilia, J. (2002). Lymphomas in rheumatoid arthritis patients treated with methotrexate: a 3-year prospective study in France. Blood *99*, 3909.

Martini, M., De Santis, M.C., Braccini, L., Gulluni, F., and Hirsch, E. (2014). PI3K/AKT signaling pathway and cancer: an updated review. Annals of Medicine *46*, 372-383.

Matusevicius, D., Kivisäkk, P., He, B., Kostulas, N., Özenci, V., Fredrikson, S., and Link, H. (1999). Interleukin-17 mRNA expression in blood and CSF mononuclear cells is augmented in multiple sclerosis. Multiple Sclerosis Journal *5*, 101-104.

McGeachy, M.J., and Cua, D.J. (2008). Th17 Cell Differentiation: The Long and Winding Road. Immunity *28*, 445-453.

Medzhitov, R., and Janeway, C.A., Jr. (1997). Innate Immunity: The Virtues of a Nonclonal System of Recognition. Cell *91*, 295-298.

Michalek, R.D., Gerriets, V.A., Jacobs, S.R., Macintyre, A.N., MacIver, N.J., Mason, E.F., Sullivan, S.A., Nichols, A.G., and Rathmell, J.C. (2011). Cutting edge: distinct glycolytic and lipid oxidative metabolic programs are essential for effector and regulatory CD4+ T cell subsets. J Immunol *186*, 3299-3303.

Miller, D.M., Thomas, S.D., Islam, A., Muench, D., and Sedoris, K. (2012). c-Myc and Cancer Metabolism. Clinical cancer research : an official journal of the American Association for Cancer Research *18*, 5546-5553.

Moon, J.J., Chu, H.H., Pepper, M., McSorley, S.J., Jameson, S.C., Kedl, Ross M., and Jenkins, M.K. (2007). Naive CD4+ T Cell Frequency Varies for Different Epitopes and Predicts Repertoire Diversity and Response Magnitude. Immunity *27*, 203-213.

Mottet, C., Uhlig, H.H., and Powrie, F. (2003). Cutting Edge: Cure of Colitis by CD4⁺CD25⁺ Regulatory T Cells. The Journal of Immunology *170*, 3939.

Mudge, J.M., and Harrow, J. (2015). Creating reference gene annotation for the mouse C57BL6/J genome assembly. Mammalian Genome *26*, 366-378.

Mullen, Andrew R., Hu, Z., Shi, X., Jiang, L., Boroughs, Lindsey K., Kovacs, Z., Boriack, R., Rakheja, D., Sullivan, Lucas B., Linehan, W.M., *et al.* (2014). Oxidation of Alpha-Ketoglutarate Is Required for Reductive Carboxylation in Cancer Cells with Mitochondrial Defects. Cell Reports *7*, 1679-1690.

Murphy, Michael P. (2009). How mitochondria produce reactive oxygen species. Biochemical Journal *417*, 1-13.

Nakajima, H., and Kunimoto, H. (2014). TET2 as an epigenetic master regulator for normal and malignant hematopoiesis. Cancer Science *105*, 1093-1099.

Nakaya, M., Xiao, Y., Zhou, X., Chang, J.H., Chang, M., Cheng, X., Blonska, M., Lin, X., and Sun, S.C. (2014). Inflammatory T cell responses rely on amino acid transporter ASCT2 facilitation of glutamine uptake and mTORC1 kinase activation. Immunity *40*, 692-705.

Neurath, M.F., Hildner, K., Becker, C., Schlaak, J.F., Barbulescu, K., Germann, T., Schmitt, E., Schirmacher, P., Haralambous, S., Pasparakis, M., *et al.* (1999). Methotrexate specifically modulates cytokine production by T cells and macrophages in murine collagen-induced arthritis (CIA): a mechanism for methotrexate-mediated immunosuppression. Clinical and Experimental Immunology *115*, 42-55.

Nishikomori, R., Usui, T., Wu, C.-Y., Morinobu, A., O'Shea, J.J., and Strober, W. (2002). Activated STAT4 Has an Essential Role in Th1 Differentiation and Proliferation That Is Independent of Its Role in the Maintenance of IL-12Rβ2 Chain Expression and Signaling. The Journal of Immunology *169*, 4388-4398.

Norde, W.J., Maas, F., Hobo, W., Korman, A., Quigley, M., Kester, M.G., Hebeda, K., Falkenburg, J.H., Schaap, N., de Witte, T.M., *et al.* (2011). PD-1/PD-L1 interactions

contribute to functional T-cell impairment in patients who relapse with cancer after allogeneic stem cell transplantation. Cancer Res *71*, 5111-5122.

O'Connor, W., Kamanaka, M., Booth, C.J., Town, T., Nakae, S., Iwakura, Y., Kolls, J.K., and Flavell, R.A. (2009). A protective function for interleukin 17A in T cell–mediated intestinal inflammation. Nature immunology *10*, 603-609.

Ott, P.A., Hodi, F.S., and Robert, C. (2013). CTLA-4 and PD-1/PD-L1 Blockade: New Immunotherapeutic Modalities with Durable Clinical Benefit in Melanoma Patients. Clinical Cancer Research *19*, 5300-5309.

Ouyang, W., Kolls, J.K., and Zheng, Y. (2008). The Biological Functions of T Helper 17 Cell Effector Cytokines in Inflammation. Immunity *28*, 454-467.

Panoskaltsis-Mortari, A., Tram, K.V., Price, A.P., Wendt, C.H., and Blazar, B.R. (2007). A new murine model for bronchiolitis obliterans post-bone marrow transplant. Am J Respir Crit Care Med *176*, 713-723.

Park, M.-J., Lee, S.-Y., Moon, S.-J., Son, H.-J., Lee, S.-H., Kim, E.-K., Byun, J.-K., Shin, D.Y., Park, S.-H., Yang, C.-W., *et al.* (2016). Metformin attenuates graft-versus-host disease via restricting mammalian target of rapamycin/signal transducer and activator of transcription 3 and promoting adenosine monophosphate–activated protein kinase-autophagy for the balance between T helper 17 and Tregs. Translational Research *173*, 115-130.

Parry, R.V., Chemnitz, J.M., Frauwirth, K.A., Lanfranco, A.R., Braunstein, I., Kobayashi, S.V., Linsley, P.S., Thompson, C.B., and Riley, J.L. (2005). CTLA-4 and PD-1 Receptors Inhibit T-Cell Activation by Distinct Mechanisms. Molecular and Cellular Biology *25*, 9543.

Patsoukis, N., Bardhan, K., Chatterjee, P., Sari, D., Liu, B., Bell, L.N., Karoly, E.D., Freeman, G.J., Petkova, V., Seth, P., *et al.* (2015). PD-1 alters T-cell metabolic reprogramming by inhibiting glycolysis and promoting lipolysis and fatty acid oxidation. Nat Commun *6*.

Pearce, E.L., Walsh, M.C., Cejas, P.J., Harms, G.M., Shen, H., Wang, L.-S., Jones, R.G., and Choi, Y. (2009). Enhancing CD8 T Cell Memory by Modulating Fatty Acid Metabolism. Nature *460*, 103-107.

Peng, M., Yin, N., Chhangawala, S., Xu, K., Leslie, C.S., and Li, M.O. (2016). Aerobic glycolysis promotes T helper 1 cell differentiation through an epigenetic mechanism. Science *354*, 481-484.

Peter, K., Rehli, M., Singer, K., Renner-Sattler, K., and Kreutz, M. (2015). Lactic acid delays the inflammatory response of human monocytes. Biochemical and Biophysical Research Communications *457*, 412-418.

Procaccini, C., De Rosa, V., Galgani, M., Abanni, L., Cali, G., Porcellini, A., Carbone, F., Fontana, S., Horvath, T.L., La Cava, A., *et al.* (2010). An oscillatory switch in mTOR kinase activity sets regulatory T cell responsiveness. Immunity *33*, 929-941.

Quintana, F.J., Jin, H., Burns, E.J., Nadeau, M., Yeste, A., Kumar, D., Rangachari, M., Zhu, C., Xiao, S., Seavitt, J., *et al.* (2012). Aiolos promotes TH17 differentiation by directly silencing Il2 expression. Nature Immunology *13*, 770.

Ramadoss, S., Chen, X., and Wang, C.-Y. (2012). Histone Demethylase KDM6B Promotes Epithelial-Mesenchymal Transition. Journal of Biological Chemistry *287*, 44508-44517.

Rashida Gnanaprakasam, J.N., Wu, R., and Wang, R. (2018). Metabolic Reprogramming in Modulating T Cell Reactive Oxygen Species Generation and Antioxidant Capacity. Frontiers in Immunology *9*, 1075.

Reid, M.A., Dai, Z., and Locasale, J.W. (2017). The impact of cellular metabolism on chromatin dynamics and epigenetics. Nature Cell Biology *19*, 1298.

Romero-Garcia, S., Moreno-Altamirano, M.M.B., Prado-Garcia, H., and Sánchez-García, F.J. (2016). Lactate Contribution to the Tumor Microenvironment: Mechanisms, Effects on Immune Cells and Therapeutic Relevance. Frontiers in Immunology *7*, 52.

Ropero, S., and Esteller, M. (2007). The role of histone deacetylases (HDACs) in human cancer. Molecular Oncology *1*, 19-25.

Rose, N.R., McDonough, M.A., King, O.N.F., Kawamura, A., and Schofield, C.J. (2011). Inhibition of 2-oxoglutarate dependent oxygenases. Chemical Society Reviews *40*, 4364-4397.

Ruella, M., Xu, J., Barrett, D.M., Fraietta, J.A., Reich, T.J., Ambrose, D.E., Klichinsky, M., Shestova, O., Patel, P.R., Kulikovskaya, I., *et al.* (2018). Induction of resistance to chimeric

antigen receptor T cell therapy by transduction of a single leukemic B cell. Nature Medicine *24*, 1499-1503.

Saxton, R.A., Knockenhauer, K.E., Wolfson, R.L., Chantranupong, L., Pacold, M.E., Wang, T., Schwartz, T.U., and Sabatini, D.M. (2016). Structural basis for leucine sensing by the Sestrin2-mTORC1 pathway. Science *351*, 53.

Schulte, M.L., Fu, A., Zhao, P., Li, J., Geng, L., Smith, S.T., Kondo, J., Coffey, R.J., Johnson, M.O., Rathmell, J.C., *et al.* (2018). Pharmacological blockade of ASCT2-dependent glutamine transport leads to antitumor efficacy in preclinical models. Nature Medicine *24*, 194.

Semenza, G.L. (2007). Hypoxia-Inducible Factor 1 (HIF-1) Pathway. Science's STKE *2007*, cm8.

Sena, Laura A., Li, S., Jairaman, A., Prakriya, M., Ezponda, T., Hildeman, David A., Wang, C.-R., Schumacker, Paul T., Licht, Jonathan D., Perlman, H., *et al.* (2013). Mitochondria Are Required for Antigen-Specific T Cell Activation through Reactive Oxygen Species Signaling. Immunity *38*, 225-236.

Sheppard, K.-A., Fitz, L.J., Lee, J.M., Benander, C., George, J.A., Wooters, J., Qiu, Y., Jussif, J.M., Carter, L.L., Wood, C.R., *et al.* (2004). PD-1 inhibits T-cell receptor induced phosphorylation of the ZAP70/CD3ζ signalosome and downstream signaling to PKCθ. FEBS Letters *574*, 37-41.

Shi, L.Z., Wang, R., Huang, G., Vogel, P., Neale, G., Green, D.R., and Chi, H. (2011). HIF1α–dependent glycolytic pathway orchestrates a metabolic checkpoint for the differentiation of T(H)17 and T(reg) cells. The Journal of Experimental Medicine *208*, 1367-1376.

Shresta, S., Pham, C.T.N., Thomas, D.A., Graubert, T.A., and Ley, T.J. (1998). How do cytotoxic lymphocytes kill their targets? Current opinion in immunology *10*, 581-587.

Sinclair, L.V., Rolf, J., Emslie, E., Shi, Y.B., Taylor, P.M., and Cantrell, D.A. (2013). Control of amino-acid transport by antigen receptors coordinates the metabolic reprogramming essential for T cell differentiation. Nat Immunol *14*, 500-508.

Siska, P.J., Beckermann, K.E., Mason, F.M., Andrejeva, G., Greenplate, A.R., Sendor, A.B., Chiang, Y.-C.J., Corona, A.L., Gemta, L.F., Vincent, B.G., *et al.* (2017). Mitochondrial

dysregulation and glycolytic insufficiency functionally impair CD8 T cells infiltrating human renal cell carcinoma. JCI Insight *2*.

Siska, P.J., Kim, B., Ji, X., Hoeksema, M.D., Massion, P.P., Beckermann, K.E., Wu, J., Chi, J.-T., Hong, J., and Rathmell, J.C. (2016). Fluorescence-based measurement of cystine uptake through xCT shows requirement for ROS detoxification in activated lymphocytes. Journal of Immunological Methods *438*, 51-58.

Smith-Garvin, J.E., Koretzky, G.A., and Jordan, M.S. (2009). T Cell Activation. Annual review of immunology *27*, 591-619.

Smith, B., Schafer, Xenia L., Ambeskovic, A., Spencer, Cody M., Land, H., and Munger, J. (2016). Addiction to Coupling of the Warburg Effect with Glutamine Catabolism in Cancer Cells. Cell Reports *17*, 821-836.

Spiegelman, B.M., and Flier, J.S. (2001). Obesity and the regulation of energy balance. Cell *104*, 531-543.

Strober, W., and Fuss, I.J. (2011). Proinflammatory Cytokines in the Pathogenesis of Inflammatory Bowel Diseases. Gastroenterology *140*, 1756-1767.e1751.

Sukumar, M., Liu, J., Ji, Y., Subramanian, M., Crompton, J.G., Yu, Z., Roychoudhuri, R., Palmer, D.C., Muranski, P., Karoly, E.D., *et al.* (2013). Inhibiting glycolytic metabolism enhances CD8(+) T cell memory and antitumor function. The Journal of Clinical Investigation *123*, 4479-4488.

Szabo, S.J., Kim, S.T., Costa, G.L., Zhang, X., Fathman, C.G., and Glimcher, L.H. (2000). A Novel Transcription Factor, T-bet, Directs Th1 Lineage Commitment. Cell *100*, 655-669.

Tajan, M., Hock, A.K., Blagih, J., Robertson, N.A., Labuschagne, C.F., Kruiswijk, F., Humpton, T.J., Adams, P.D., and Vousden, K.H. (2018). A Role for p53 in the Adaptation to Glutamine Starvation through the Expression of SLC1A3. Cell Metabolism.

Tee, A.R., Manning, B.D., Roux, P.P., Cantley, L.C., and Blenis, J. (2003). Tuberous Sclerosis Complex Gene Products, Tuberin and Hamartin, Control mTOR Signaling by Acting as a GTPase-Activating Protein Complex toward Rheb. Current Biology *13*, 1259-1268.

Thangavelu, K., Chong, Q.Y., Low, B.C., and Sivaraman, J. (2014). Structural basis for the active site inhibition mechanism of human kidney-type glutaminase (KGA). Sci Rep *4*, 3827.

Tumeh, P.C., Harview, C.L., Yearley, J.H., Shintaku, I.P., Taylor, E.J.M., Robert, L., Chmielowski, B., Spasic, M., Henry, G., Ciobanu, V., *et al.* (2014). PD-1 blockade induces responses by inhibiting adaptive immune resistance. Nature *515*, 568-571.

Tyagi, R.K., Azrad, A., Degani, H., and Salomon, Y. (1996). Simultaneous extraction of cellular lipids and water-soluble metabolites: Evaluation by NMR spectroscopy. Magnetic Resonance in Medicine *35*, 194-200.

Umeki, S., Kusunoki, Y., Cologne, J.B., Iwamoto, K.S., Hirai, Y., Seyama, T., Ohama, K., and Kyoizumi, S. (1998). Lifespan of human memory T-cells in the absence of T-cell receptor expression. Immunology Letters *62*, 99-104.

Urak, R., Walter, M., Lim, L., Wong, C.W., Budde, L.E., Thomas, S., Forman, S.J., and Wang, X. (2017). Ex vivo Akt inhibition promotes the generation of potent CD19CAR T cells for adoptive immunotherapy. Journal for ImmunoTherapy of Cancer *5*, 26.

van Geldermalsen, M., Wang, Q., Nagarajah, R., Marshall, A.D., Thoeng, A., Gao, D., Ritchie, W., Feng, Y., Bailey, C.G., Deng, N., *et al.* (2015). ASCT2/SLC1A5 controls glutamine uptake and tumour growth in triple-negative basal-like breast cancer. Oncogene *35*, 3201.

van Loosdregt, J., Vercoulen, Y., Guichelaar, T., Gent, Y.Y.J., Beekman, J.M., van Beekum, O., Brenkman, A.B., Hijnen, D.-J., Mutis, T., Kalkhoven, E., *et al.* (2010). Regulation of Treg functionality by acetylation-mediated Foxp3 protein stabilization. Blood *115*, 965-974.

van der Windt, Gerritje J.W., Everts, B., Chang, C.-H., Curtis, Jonathan D., Freitas, Tori C., Amiel, E., Pearce, Edward J., and Pearce, Erika L. (2012). Mitochondrial Respiratory Capacity Is a Critical Regulator of CD8+ T Cell Memory Development. Immunity *36*, 68-78.

Vander Heiden, M.G., Cantley, L.C., and Thompson, C.B. (2009). Understanding the Warburg Effect: The Metabolic Requirements of Cell Proliferation. Science *324*, 1029-1033.

Waite, J.C., and Skokos, D. (2012). Th17 Response and Inflammatory Autoimmune Diseases. International Journal of Inflammation *2012*, 819467.

Wander, S.A., Hennessy, B.T., and Slingerland, J.M. (2011). Next-generation mTOR inhibitors in clinical oncology: how pathway complexity informs therapeutic strategy. The Journal of Clinical Investigation *121*, 1231-1241.

Wang, J.B., Erickson, J.W., Fuji, R., Ramachandran, S., Gao, P., Dinavahi, R., Wilson, K.F., Ambrosio, A.L., Dias, S.M., Dang, C.V., *et al.* (2010). Targeting mitochondrial glutaminase activity inhibits oncogenic transformation. Cancer Cell *18*, 207-219.

Wang, L., Chang, J., Varghese, D., Dellinger, M., Kumar, S., Best, A.M., Ruiz, J., Bruick, R., Peña-Llopis, S., Xu, J., *et al.* (2013). A small molecule modulates Jumonji histone demethylase activity and selectively inhibits cancer growth. Nature Communications *4*, 2035.

Wang, R., Dillon, C.P., Shi, L.Z., Milasta, S., Carter, R., Finkelstein, D., McCormick, L.L., Fitzgerald, P., Chi, H., Munger, J., *et al.* (2011). The transcription factor Myc controls metabolic reprogramming upon T lymphocyte activation. Immunity *35*, 871-882.

Wang, T., Marquardt, C., and Foker, J. (1976). Aerobic glycolysis during lymphocyte proliferation. Nature *261*, 702.

Wang, X., and Sun, S.-Y. (2009). Enhancing mTOR-targeted cancer therapy. Expert opinion on therapeutic targets *13*, 1193-1203.

Weaver, C.T., Hatton, R.D., Mangan, P.R., and Harrington, L.E. (2007). IL-17 Family Cytokines and the Expanding Diversity of Effector T Cell Lineages. Annual Review of Immunology *25*, 821-852.

Webb, D.R. (2014). Animal models of human disease: Inflammation. Biochemical Pharmacology *87*, 121-130.

Wei, H., Geng, J., Shi, B., Liu, Z., Wang, Y.H., Stevens, A.C., Sprout, S.L., Yao, M., Wang, H., and Hu, H. (2016). Cutting Edge: Foxp1 Controls Naive CD8+ T Cell Quiescence by Simultaneously Repressing Key Pathways in Cellular Metabolism and Cell Cycle Progression. J Immunol *196*, 3537-3541.

Wei, Y., Liang, J., Zhang, R., Guo, Y., Shen, S., Su, L., Lin, X., Moran, S., Helland, Å., Bjaanæs, M.M., *et al.* (2018). Epigenetic modifications in KDM lysine demethylases associate with survival of early-stage NSCLC. Clinical Epigenetics *10*, 41.

Wherry, E.J., and Ahmed, R. (2004). Memory CD8 T-Cell Differentiation during Viral Infection. Journal of Virology *78*, 5535.

Wiersinga, W.J. (2011). Current insights in sepsis: from pathogenesis to new treatment targets. Current Opinion in Critical Care *17*, 480-486.

Wing, K., and Sakaguchi, S. (2010). Regulatory T cells exert checks and balances on self tolerance and autoimmunity. Nat Immunol *11*, 7-13.

Wise, D.R., and Thompson, C.B. (2010). Glutamine addiction: a new therapeutic target in cancer. Trends Biochem Sci *35*, 427-433.

Wolfe, F., and Michaud, K. (2004). Lymphoma in rheumatoid arthritis: The effect of methotrexate and anti–tumor necrosis factor therapy in 18,572 patients. Arthritis & Rheumatism *50*, 1740-1751.

Wolfson, R.L., and Sabatini, D.M. The Dawn of the Age of Amino Acid Sensors for the mTORC1 Pathway. Cell Metabolism *26*, 301-309.

Xu, T., Stewart, K.M., Wang, X., Liu, K., Xie, M., Kyu Ryu, J., Li, K., Ma, T., Wang, H., Ni, L., *et al.* (2017). Metabolic control of TH17 and induced Treg cell balance by an epigenetic mechanism. Nature *548*, 228-233.

Xu, X., Araki, K., Li, S., Han, J.-H., Ye, L., Tan, W.G., Konieczny, B.T., Bruinsma, M.W., Martinez, J., Pearce, E.L., *et al.* (2014). Autophagy is essential for effector CD8+ T cell survival and memory formation. Nature Immunology *15*, 1152.

Y, H.Y., Lin, L.J., Zheng, C.Q., Jin, Y., and Lin (2012). Cytokine expression and the role of Th17 cells in a mouse model of colitis. - PubMed - NCBI. Molecular Medicine Reports *6*, 1438-1442.

Yang, J., Sundrud, M.S., Skepner, J., and Yamagata, T. (2014). Targeting Th17 cells in autoimmune diseases. Trends in Pharmacological Sciences *35*, 493-500.

Yang, L., Venneti, S., and Nagrath, D. (2017). Glutaminolysis: A Hallmark of Cancer Metabolism. Annual Review of Biomedical Engineering *19*, 163-194.

Yin, Y., Choi, S.-C., Xu, Z., Perry, D.J., Seay, H., Croker, B.P., Sobel, E.S., Brusko, T.M., and Morel, L. (2015). Normalization of CD4⁺ T cell metabolism reverses lupus. Science Translational Medicine *7*, 274ra218-274ra218.

Yu, D., Shi, X., Meng, G., Chen, J., Yan, C., Jiang, Y., Wei, J., and Ding, Y. (2015). Kidney-type glutaminase (GLS1) is a biomarker for pathologic diagnosis and prognosis of hepatocellular carcinoma. Oncotarget *6*, 7619-7631.

Yuan, Q., Song, Y., Yang, C.H., Jan, L.Y., and Jan, Y.N. (2014). Female contact modulates male aggression via a sexually dimorphic GABAergic circuit in Drosophila. Nat Neurosci *17*, 81-88.

Zeng, H., Yang, K., Cloer, C., Neale, G., Vogel, P., and Chi, H. (2013). mTORC1 couples immune signals and metabolic programming to establish T(reg)-cell function. Nature *499*, 485-490.

Zhang, L., and Romero, P. (2018). Metabolic Control of CD8⁺ T Cell Fate Decisions and Antitumor Immunity. Trends in Molecular Medicine *24*, 30-48.

Zhang, W., Sloan-Lancaster, J., Kitchen, J., Trible, R.P., and Samelson, L.E. (1998). LAT: The ZAP-70 Tyrosine Kinase Substrate that Links T Cell Receptor to Cellular Activation. Cell *92*, 83-92.

Zhou, M., and Ouyang, W. (2003). The function role of GATA-3 in Th1 and Th2 differentiation. Immunologic Research *28*, 25-37.

Zoncu, R., Bar-Peled, L., Efeyan, A., Wang, S., Sancak, Y., and Sabatini, D.M. (2011). mTORC1 Senses Lysosomal Amino Acids Through an Inside-Out Mechanism That Requires the Vacuolar H⁺-ATPase. Science *334*, 678.

Biography

Marc O. Johnson attended Boston University in Boston, Massachusetts as a biology major with a specialization in neuroscience, where he graduated with honors. He worked for four years at Sirtris Pharmaceuticals in Cambridge, Massachusetts. In 2013, he was accepted to the Pharmacology and Cancer Biology (PCB) department at Duke University in Durham, North Carolina. Under the mentorship of Jeffrey C. Rathmell, Marc initiated his research on T cell metabolism and how glutaminase affects T cell function. In 2015, the Rathmell lab moved to Vanderbilt University in Nashville, Tennessee. Marc continued his graduate career at Vanderbilt while graduating from Duke University in the fall of 2018.